2012

Using "Designer" Nucleosomes to Study Enzymatic Crosstalk Between Histone Ubiquitylation and Histone Methyltransferases

Sarah J. Whitcomb

USING "DESIGNER" NUCLEOSOMES TO STUDY ENZYMATIC CROSSTALK BETWEEN HISTONE UBIQUITYLATION AND HISTONE METHYLTRANSFERASES

A Thesis Presented to the Faculty of

The Rockefeller University

in Partial Fulfillment of the Requirements for

the degree of Doctor of Philosophy

by

Sarah J. Whitcomb

June 2012

USING "DESIGNER" NUCLEOSOMES TO STUDY ENZYMATIC CROSSTALK BETWEEN HISTONE UBIQUITYLATION AND HISTONE METHYLTRANSFERASES

Sarah J. Whitcomb, Ph.D.

The Rockefeller University 2012

It is well established that chromatin is a destination and source for signal transduction affecting all types of DNA metabolism. Histone proteins in particular are extensively post-translationally modified (PTM), and many of these individual modifications have been studied in depth. I have been interested in how the complex repertoire of histone PTMs are co-regulated to generate combinations with meaningful physiological outcomes. One important mechanism is "crosstalk" between pre-existing histone PTMs and enzymes that add or remove subsequent modifications on chromatin. It has been previously shown that H3 lysine 4 methyltransferases involved in transcriptional activation are stimulated and repressed by H2Bub and H2Aub, respectively. Here, using chemically-defined "designer" mononucleosomes, I tested whether nucleosomal H2BK120ub and H2AK119ub influence the activity of a well-studied histone methyltransferases complex that is repressive to transcription, Polycomb Repressive Complex 2 (PRC2). I also built upon previous studies of direct enzymatic crosstalk between histone ubiquitylation and H3 lysine 79 methyltransferase, Dot1L, by

investigating the plasticity of ubiquitin position in stimulation of Dot1L methyltransferase activity. Finally, using designer mononucleosomes containing H3 phosphoserine mimetics, crosstalk studies with PRC2 methyltransferase uncovered a putative novel methyl/phos switch specific to the histone variant H3.3 These studies address the specificity of crosstalk between pre-existing post-translational modifications and subsequent methylation, and thereby strengthen our understanding of mechanisms to establish and maintain functional combinations of histone modifications in chromatin.

ACKNOWLEDGEMENTS

First of all, I want to acknowledge my PhD advisor, Dr. C. David Allis. Throughout my thesis, his love for chromatin was infectious, and his remarkable scientific career served as an inspiring example, particularly because he carries it with such humility. I would also like to express my gratitude for the freedom he gave me, his patience and generosity.

This thesis would not have been possible without the collaboration, consistent support, and commitment of Dr. Tom Muir and members of his laboratory, especially Drs. Robert McGinty, Champak Chatterjee, and Beat Fierz. Similarly, I want to express my gratitude to the current and past members of Dr. Allis's lab, for generously sharing their expertise with me as well as providing friendship. And I'd like to specifically thank our laboratory manager, Jamie Winshell, who keeps the lab work humming, despite needing to "save us from ourselves" nearly daily.

I want to thank my Faculty Advisory Committee, Drs. F. Nina Papavasiliou, Robert G. Roeder, and Sanford M. Simon, for their guidance throughout my thesis work. I would also like to acknowledge Dr. Yang Shi, of the Children's Hospital Boston, for serving as the external examiner for my thesis defense.

I am blessed to have an extremely supportive immediate family, extended family, and partner. Their unwavering faith in my capacity to solve and to persevere has been a great source of strength.

TABLE OF CONTENTS

LIST OF FIGURES

CHAPTER 1

CHAPTER 2

CHAPTER 3

CHAPTER 4

CHAPTER 5

CHAPTER 6

CHAPTER 1: INTRODUCTION

1.1 Chromatin is the physiologically relevant form of eukaryotic genomes

Approximately two meters of DNA need to fit into the nucleus of each human cell, requiring a compaction level of nearly 10,000 fold (Allis et al., 2007). Despite this extreme level of compaction (Figure 1.1A), the DNA must remain accessible to the molecular machinery for critical processes such as DNA replication, transcription, and DNA repair. Chromatin is evolution's solution to this so-called "packaging problem."

Chromatin is an extremely complex composite structure of genomic DNA, structural proteins, regulatory proteins, and non-coding RNA. Many aspects of chromatin structure are highly regulated and dynamic in nature, which allows chromatin to meet the seemingly antagonistic requirements for DNA compaction and accessibility.

The fundamental structural unit in chromatin is the nucleosome: 146 base pairs (bp) of DNA wrapped 1.65 times around an octamer of histone proteins, two each of histones H3, H4, H2A and H2B (Kornberg, 1974; Van Holde et al., 1980)(Figure 1.1). In a landmark paper, Luger, Richmond and colleagues determined the X-ray crystal structure of the nucleosome at 2.8 A resolution (Luger et al., 1997). This structure, and other more refined structures that followed (Davey et al., 2002; Schalch et al., 2005) (Figure 1.1B), has informed innumerable experiments conducted by chromatin biologists, including those presented in this thesis.

In vivo the nucleosome unit repeats throughout the genome every 160-240 bp (Van Holde, 1989). Nucleosomes arranged in series, and the linker DNA between them can, be visualized in electron micrographs of decondensed chromatin to reveal the so-called "beads on a string" structure of nucleosome arrays (Olins and Olins, 1974; Van

Holde, 1989). A variety of factors regulate progressive compaction of extended nucleosome arrays into higher and higher order structures, including histone N- and C-terminal "tails" which extend out from the core of the nucleosome particle, linker histone H1 association, and the recruitment of structural proteins (Hansen, 2002) (Figure 1.1A).

All DNA-templated processes in eukaryotes must navigate the complex chromatin landscape. Similarly, investigations of these processes must take chromatin as the physiological form of the genome into account.

1.1.1 Variation and complexity in chromatin

Chromatin is not only an elegant solution to the eukaryotic genome's packaging problem, but it is also at the heart of how these organisms index their genome to reflect cellular memory states and to appropriately respond to the current environment. The diversity of processes regulated by chromatin is mirrored by the immense structural and compositional complexity of chromatin itself. This structural diversity typically functions by modulating the accessibility of DNA or by recruiting various protein "effectors" to specific genomic loci. Evolution has generated a battery of mechanisms for regulated introduction of complexity into chromatin, and a few of these mechanisms will be highlighted below.

Historically chromatin was characterized as being either heterochromatic or euchromatic based on microscopic inspection of cytological DNA stains that differentiated based on local DNA density. Broadly, euchromatin is considered to be relatively permissive to transcription and its structure is decondensed, whereas heterochromatin is considered to be highly compacted and transcriptionally silent. The

regulated incorporation of specific non-histone proteins and non-coding RNA are critical to the establishment and maintenance of highly compacted chromatin regions (Allis et al., 2007).

Even mononucleosomes, the minimal repeating units of chromatin, are endowed with extensive variation. Canonical histones can be replaced with variant versions of these histones by specific ATP-dependent chromatin remodelers and chaperones. Although histone variants represent only a minor amount of the total histone pool, evidence suggests that they have important specialized functions in genome regulation (Banaszynski et al., 2010; Gamble and Kraus, 2010; Talbert and Henikoff, 2010; Verdaasdonk and Bloom, 2011). One of the most extensively studied types of variation in nucleosomes is introduced through enzymatic addition of post-translational modifications (PTMs) to histone proteins. This important mechanism for chromatin regulation is the topic of the remainder of this introduction.

All of the above processes to generate structural complexity in chromatin are dynamic on biological time scales. And most of them are reversible, allowing the same genome to function differently depending on the precise cellular, developmental, or environmental context.

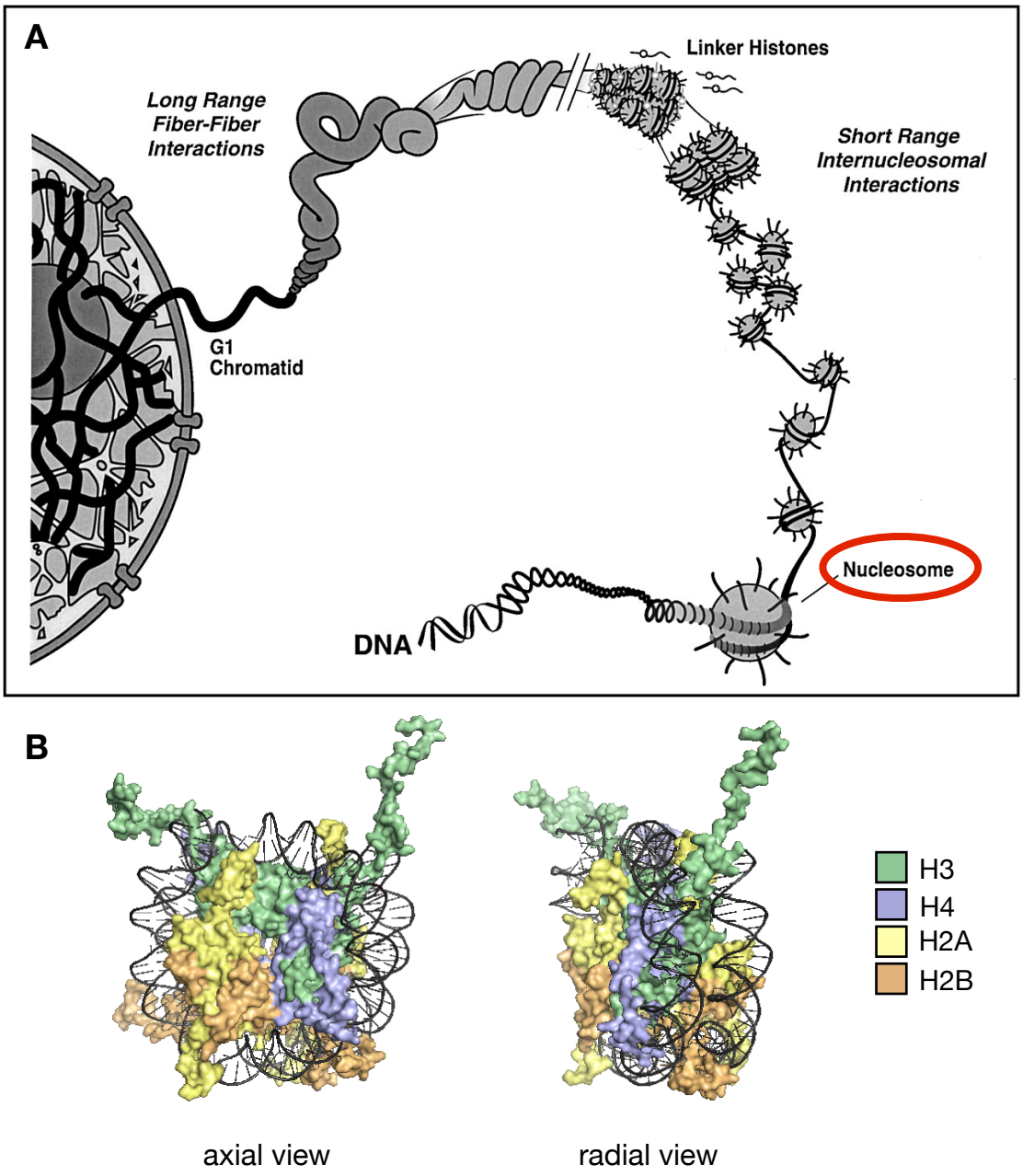

Figure 1.1 Nucleosomes are the fundamental repeating unit of chromatin.
A) schematic representation of progressive chromatin fiber compaction in eukaryotic nuclei, from extended nucleosome arrays into chromatin fibers. Adapted from Hansen et al. 2002. B) surface rendition of mononucleosome structure, Protein Data Bank code 1KX5. DNA is colored in black and the histones H3, H4, H2A, and H2B are colored green, lavender, yellow, and orange respectively.

1.2 Post-translational modification of histones

Post-translational modification of histone proteins takes many chemical forms, including methylation, acetylation, ubiquitylation, phosphorylation, citrullination, ADP-ribosylation, sumoylation, and biotinylation among others (Tan et al., 2011). Over the past 10 years the pace at which histone PTMs have been discovered, mapped and their functions explored has been remarkable.

1.2.1 General mechanisms of histone PTM function

In general, histone PTMs can be thought of as functioning in *cis* or in *trans* (Figure 1.2). Modifications that function in *cis* alter the biophysical properties of chromatin and directly influence chromatin structure. Those that function in *trans* modulate the association or activity of non-histone proteins on chromatin.

Lysine acetylation is a classic example of a histone PTM that can function in *cis*. Chromatin is a highly charged polymer as the DNA backbone is negatively charged and histone proteins are enriched in positively charged side-groups. The especially basic character of histone tails is understood to neutralize some of the negative charge on the DNA backbone, allowing for the high degree of chromatin compaction required to fit a large eukaryotic genome into a nucleus. Further, structural studies of nucleosomes revealed that the positively charged N-terminal tail of H4 interacts with an acidic surface on adjacent nucleosomes (Chodaparambil et al., 2007; Dorigo et al., 2003; Luger et al., 1997). However, acetylation of lysine residues neutralizes the positive charge on the lysine side chain. This change in the electrostatic properties of histone tails antagonizes chromatin fiber compaction (Tse et al., 1998). A particularly compelling example of

reduced chromatin compaction resulting from electrostatic effects has been demonstrated with nucleosome arrays reconstituted with either H4 acetylated on lysine 16 (H4K16Ac) or unmodified H4 (Robinson et al., 2008; Shogren-Knaak et al., 2006). Acetylation-mediated chromatin decompaction is likely to result in a chromatin template that is more permissive to transcription (Tse et al., 1998), providing an attractive molecular mechanism for the long-observed correlation between histone acetylation and transcription (Allfrey et al., 1964).

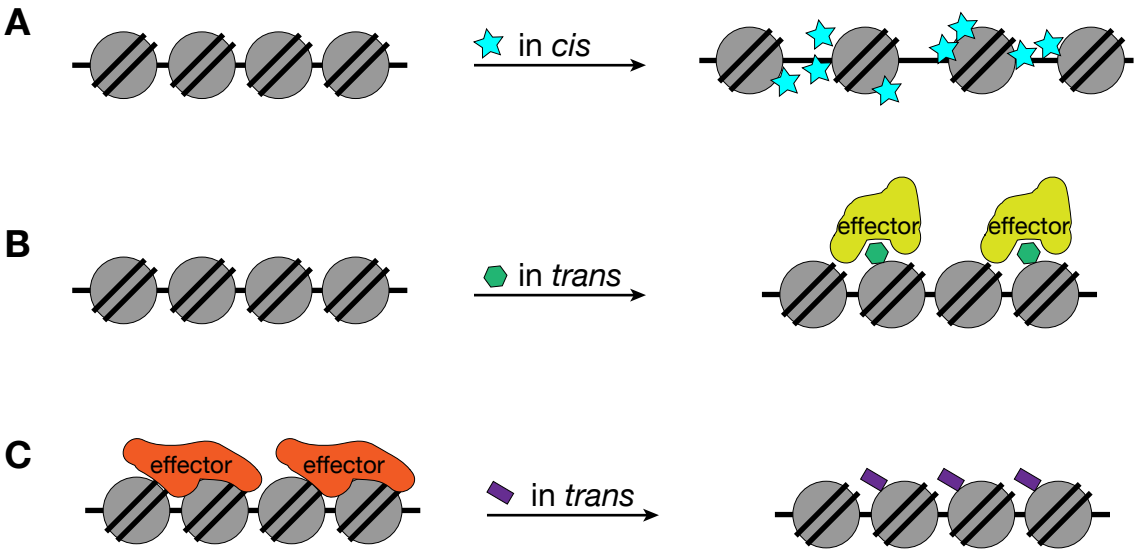

Figure 1.2 General mechanisms of histone PTM function. A) post-translational modifications that function in *cis* directly influence the propensity of the chromatin fiber to compact or decompact. Modifications that function in *trans* modulate either stabilize binding of non-histone effector proteins on chromatin (B) or inhibit their binding (C).

Relatively bulky PTMs like ubiquitylation and ADP-ribosylation have also been proposed to function in *cis*. Ubiquitylation of H2B on K120 (H2Bub) in particular was presumed to disrupt nucleosome stacking because of its location on the axial face of the nucleosome (Davey et al., 2002; Schalch et al., 2005). Very recently, that hypothesis was validated using nucleosome arrays reconstituted with H2Bub or unmodified octamers (Fierz et al., 2011). Additionally, H2Bub and H4K16Ac were found to function synergistically in preventing inter-array interactions, another aspect of chromatin compaction into higher-order structures (Fierz et al., 2011).

Lysine methylation is the one of the better-studied categories of histone PTMs to function in *trans*. The work of many groups has uncovered a handful of distinct methyl-lysine "reader" domains that are remarkably specific for particular methylation states (mono, di, trimethyl) and particular methylation sites in histone tails (Taverna et al., 2007). Perhaps the most famous example is chromodomain-mediated binding of Heterochromatin Protein 1 (HP1), to histone H3 via methylation on lysine 9 (H3K9me) (Bannister et al., 2001; Jacobs and Khorasanizadeh, 2002; Jacobs et al., 2001; Lachner et al., 2001; Nielsen et al., 2002). H3K9me and HP1 are necessary for proper heterochromatin maintenance from yeast to multicellular eukaryotes (Eissenberg et al., 1992; Lorentz et al., 1994), and HP1 can be described as an "effector" protein for H3K9 methylation-mediated heterochromatin formation. The regulation of the HP1/H3K9me interaction will be discussed further in Chapter 5.

PTMs can also disrupt binding surfaces non-histone proteins. For example, H4K16Ac prevents binding of the telomere-associated protein Silent Information Regulator 3 (Sir3) (Armache et al., 2011). In this way H4K16Ac blocks the

encroachment of heterochromatin into parts of the genome that need to retain euchromatic characteristics.

In addition to modulating the binding of effector proteins, histone PTMs can function in *trans* by allosterically altering the activity of enzymes that act upon chromatin. This direct enzymatic crosstalk will be the focus of the experiments presented in this thesis. More specifically, studies of how specific ubiquitylation marks on histones influence the activity of methyltransferase enzymes on nucleosomal substrates will be presented. The remainder of Chapter 1 will be dedicated to the relevant methyltransferases (PRC2 and Dot1L), the methylation marks they transduce (H3K27me2/3 and H3K79me2/3), and to the two most abundant histone ubiquitylation sites in mammals (H2AK119ub and H2BK120ub) (Figure 1.3).

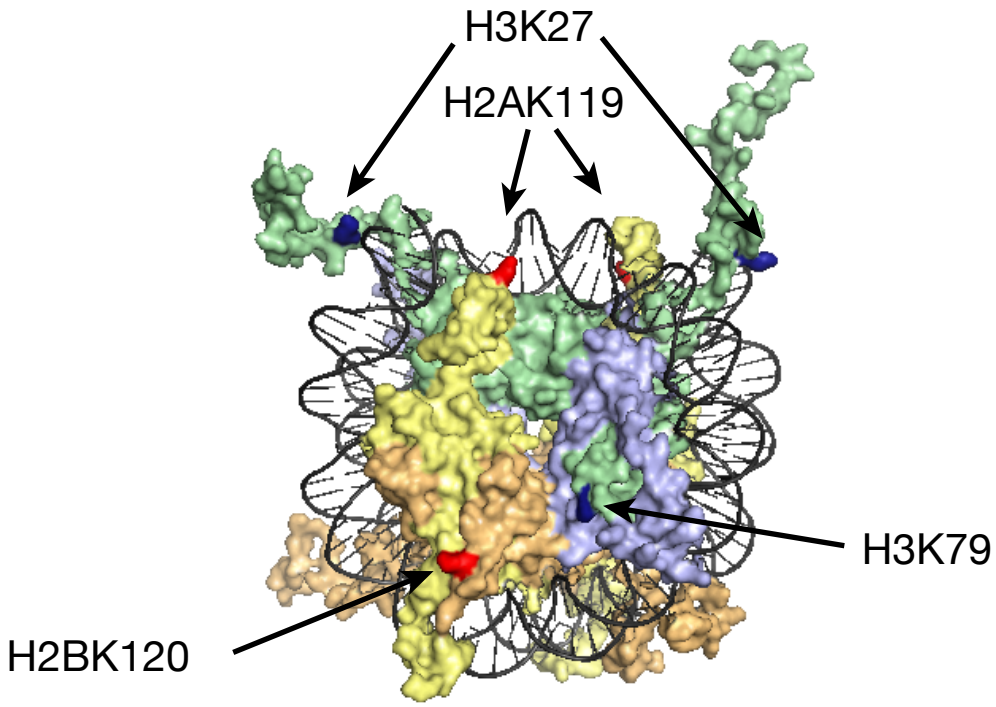

Figure 1.3 Nucleosome position of H3K27, H3K79, H2BK120, H2AK119.
Surface rendition of mononucleosome structure, Protein Data Bank code 1KX5. DNA is colored in black and the histones H3, H4, H2A, and H2B are colored green, lavender, yellow, and orange respectively. Ubiquitylated lysines are colored in red. Methylated lysines are colored in dark blue.

1.2.2 Histone methylation

Methylation is the covalent transfer of a methyl (-CH_3) group. The biological substrates for methylation are diverse, including lipids, small molecules, nucleic acids as well as proteins (Walsh, 2006). S-adenosylmethionine (SAM, AdoMet) is the methyl donor in these reactions. In proteins, methylation occurs on nucleophilic side chains, especially on nitrogens (N-methylation) and oxygens (O-methylation). Thus far, only N-methylation has been observed on histone proteins.

Methylation of arginines and lysines in histones has been extensively studied, and in many cases their regulation has a clear biological outcome and function (Allis et al.,

2007). Recently, N-methylation on proline 1 of *Drosophila* H2B was also reported (Villar-Garea et al., 2011). Arginines are methylated on their guanidino moiety and can receive up to two methyl groups. Lysines are methylated on their ε-amine and can accept up to three methyl groups (Figure 1.4). Methylation of arginine and lysine does not alter the cationic charge of the side chain but does result in increased hydrophobicity and bulk. These changes can have a large impact on how histone proteins interact with other components of chromatin, exemplified by the methylation state-specific recruitment/stabilization of histone methylation "readers" (Taverna et al., 2007).

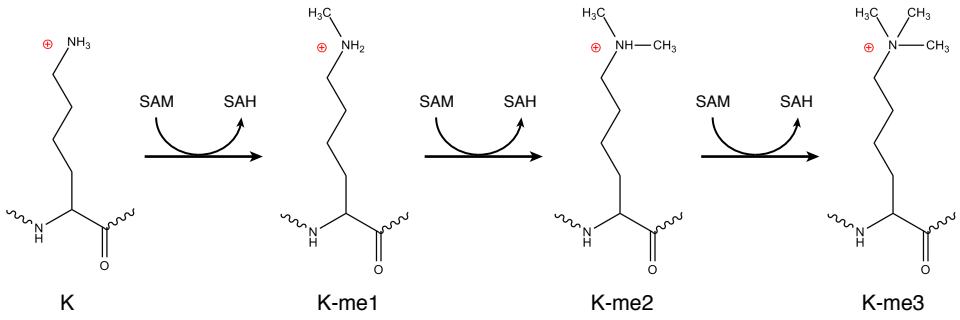

Figure 1.4 Methylation of lysine ε-NH_2. Adapted from Walsh, 2006. The lysine side chain (K) can accept up to three methyl groups, resulting in monomethyl-lysine (K-me1), dimethyl-lysine (K-me2), and trimethyl-lysine (K-me3). N-methyltransferases use S-adenosylmethionine (SAM) as the methyl donor for these reactions, which is converted into S-adenosylhomocysteine (SAH).

For lysine methyltransferases (MTases), the transformation from unmodified lysine to trimethylated lysine (me3) is believed to be due to kinetic processivity of the enzyme, with dimethylation and trimethylation reactions occurring before release of product from the monomethylation enzymatic cycle (Walsh, 2006). Although lysine side chains can accept up to three methyl groups, not all methyltransferase enzymes are

competent to catalyze the addition of three methyl groups on the same lysine. At least in some cases, the size of the lysine-binding pocket in the methyltransferase can limit which methylation states can be accepted as substrates (Zhang et al., 2003).

Of the many important histone methylation sites identified to date (Tan et al., 2011), this thesis will focus on two lysines in histone H3: K27, a classical histone "tail" PTM, and K79, a solvent exposed residue located in the folded core of H3 (Figure 1.3).

1.2.2.1 SET- mediated methylation of H3K27 by Polycomb Repressive Complex 2

The 130 amino acid SET domain was identified over 15 years ago as a shared motif between three chromatin associated MTases: SU(VAR)3-9, E(Z), and TRX (Tschiersch et al., 1994). Subsequent biochemical studies showed that the methyltransferase activity of these proteins resides in their SET domains. In addition to these founding *Drosophila* MTases, SET domains are found in all identified histone lysine MTases, (except Dot1, which will be discussed in Section 1.2.2.2).

SET domain containing MTases have also been found across much of the tree of life, from viruses and bacteria, to plants and animals (Qian and Zhou, 2006). Across all this evolutionary time, the motif critical for catalytic activity, HΦΦNHSC (where Φ is a hydrophobic residue) has been largely conserved (Rea et al., 2000). In addition to this catalytic motif, histone methyltransferases contain cysteine-rich domains flanking their SET domain, and these are also required for catalytic activity. However, plant *P. sativum* (pea) and *Arabidopsis* Rubisco MTases lack cysteine-rich regions but retain catalytic activity (Klein and Houtz, 1995; Rea et al., 2000), suggesting that these cysteine-rich regions are important for MTase activity on histones but not for activity per se.

SET domain histone MTases tend to be inactive on their own, but are active if found in the presence of their native or reconstituted complexes. Non-catalytic complex members are often rich in chromatin associated functional domain/motifs. It remains an active area of research to determine how complex members contribute to the catalytic activity of SET-domain MTases and how they affect substrate specificity. The SET domain containing MTase complex of particular relevance to this thesis is Polycomb Repressive Complex 2 (PRC2).

Members of the Polycomb group (PcG), including components of PRC2, were originally identified in *Drosophila melanogaster* as factors necessary to maintain cell-fate decisions through embryogenesis by repressing Hox genes in a body segment-specific manner (Kennison, 1995). Biochemical characterization of PcG proteins revealed that they are structurally and functionally diverse and form large multimeric complexes of two general types: Polycomb Repressive Complex 1 and 2 (PRC1, PRC2).

In fact, both complexes post-translationally modify histone tails, although the mechanistic details that may link these activities remain unclear. PRC1 monoubiquitylates H2AK119 (Wang et al., 2004), a modification that will be discussed in Section 1.2.3, and PRC2 is the methyltransferase complex for H3K27me2/3 (Cao et al., 2002). Ezh2 is the catalytic subunit of PRC2 and methylates H3 via its SET domain. One of the initial goals of my thesis work was to explore potential cross-talk relationships between H2Aub and H3K27me2/3.

SET-domain mediated MTase activity contained in the Ezh2 polypeptide is required to maintain repression of homeotic genes (Cao et al., 2002; Muller et al., 2002). These studies were among the first to directly link histone methylation with

developmentally-regulated gene expression programs. In addition to body patterning and cellular differentiation programs, Polycomb Repressive Complexes are important for other cellular memory processes such as stem cell maintenance (Boyer et al., 2006), X inactivation in female mammals (Heard, 2004), and vernalization in plants (Sung and Amasino, 2005).

1.2.2.2 Non-SET-mediated methylation of H3K79 by Dot1

Dot1 (disruptor of telomeric silencing-1) was first identified in a *S. cerevisiae* screen for genes that disrupt telomeric silencing when overexpressed (Singer et al., 1998). Approximately 5 years after its initial discovery, several groups independently discovered that yeast Dot1 (yDot1p) and the mammalian homolog Dot1L (Dot1-Like) are histone methyltransferases for H3K79 (Feng et al., 2002; Lacoste et al., 2002; Ng et al., 2002a; van Leeuwen et al., 2002). Knockouts of Dot1 in yeast (van Leeuwen et al., 2002), flies (Shanower et al., 2005), and mice (Jones et al., 2008) have no detectable H3K79 methylation, showing Dot1 to be the sole MTase for H3K79 in these organisms. Dot1 is unique among histone lysine MTases because its catalytic domain is evolutionarily unrelated to SET domains in all other identified histone lysine MTases. In fact, the catalytic domain of Dot1 family enzymes is structurally much more similar to arginine MTases than to histone lysine MTases like Ezh2.

Because over-expression in yeast resulted in de-repression of telomeric regions (Singer et al., 1998), it was first assumed that Dot1 was involved in heterochromatin formation. However, deletion of Dot1 also resulted in defective telomeric silencing (van Leeuwen et al., 2002). Further, H3K79 was found to be hypomethylated in

heterochromatic domains in yeast (van Leeuwen et al., 2002), and hypermethylated in euchromatic domains (Ng et al., 2003a), strongly arguing against a direct role for H3K79 methylation in heterochromatin formation.

Telomeric regions are enriched in Sir (silent information regulator) protein binding. However, in the absence of H3K79 methylation, Sir protein enrichment at telomeres is lost and their binding titrated out across much larger chromatin domains, thereby contributing to a breakdown of telomeric heterochromatin (Ng et al., 2002a; van Leeuwen et al., 2002). A mechanistic explanation for the redistribution of Sir proteins comes from the observation that methylation of H3K79 prevents Sir3 binding to chromatin (Altaf et al., 2007). This is an excellent example of a histone PTM acting in *cis* to prevent binding an effector protein (Chapter 1.2.1). Further, Dot1 and Sir3 were shown to compete for the same basic patch on the H4 tail for chromatin-association (Altaf et al., 2007), thereby contributing to mutually exclusive domains of Dot1/H3K79 methylated euchromatin and Sir bound heterochromatin. Taken together, these results lead to the current model whereby Dot1 and K79 methylation are involved in heterochromatinization indirectly by blocking the spread and "dilution" of heterochromatin-associated proteins into H3K79 methylated, euchromatic regions of the genome.

In higher eukaryotes, Dot1L activity is also linked to transcriptional regulation. In *Drosophila* and mammals, the level of H3K79 methylation correlates well with transcription level (Okada et al., 2005; Schubeler et al., 2004; Steger et al., 2008). In actively transcribed genes H3K79 methylation is enriched in the coding region (Kouskouti and Talianidis, 2005), suggesting a role for Dot1 and H3K79 methylation in transcriptional elongation. Indeed, H3K79 methylation requires components of the Paf1

complex (Krogan et al., 2003), which is associated with RNA Pol II during transcriptional elongation into gene coding regions. However, Paf1 is also required for ubiquitylation of H2B (H2Bub) in gene coding regions, and H2Bub strongly and directly stimulates Dot1 MTase activity on chromatin (Chapter 1.2.3.1). Therefore it seems likely that the requirement of the Paf1 complex for Dot1L MTase activity may be indirect, via H2Bub.

Dot1-mediated H3K79 methylation is known to function in *trans* in telomere maintenance by influencing the binding of effector proteins (see above). However, to date, H3K79 methylation is not known to influence the binding of proteins involved in transcriptional regulation. Of course, H3K79 methylation-state sensitive transcriptional effector proteins may be identified in the future. Interestingly, nucleosomes incorporated with H3K79me2 have a subtly different local surface contour and electrostatic surface potential than nucleosomes incorporated with unmodified H3 (Lu et al., 2008). How H3K79me2-mediated biophysical differences may affect dynamic processes such as transcription and are intriguing and challenging areas to pursue in Dot1-mediated H3K79me functional investigations.

1.2.3 Histone ubiquitylation

Ubiquitylation is the covalent addition of the relatively small protein ubiquitin to target proteins (Figure 1.5). Most eukaryotic proteins are ubiquitylated at some point in their life cycle, either to modulate the protein's localization, function or to promote degradation of the protein. Unlike protein methylation, which occurs in one step, ubiquitylation requires a three-step enzymatic cascade to effect the formation of an

isopeptide bond between the C-terminal glycine of ubiquitin and the ε-amino group of a target lysine side chain (Pickart, 2004) (Figure 1.5B). In the first step, the C-terminal carboxylate of ubiquitin is activated ("paid for") by ATP hydrolysis, for ligation by forming a thioester with a cysteine in an ubiquitin-activating enzyme (E1) (Figure 1.5C). The activated ubiquityl is then passed from the active site cysteine of E1 to the active site cysteine of an ubiquitin-conjugating enzyme (E2) in an energy-neutral thioester exchange (transthiolation) (Figure 1.5D). Finally, an ubiquitin-ligase (E3) facilitates the transfer of activated ubiquityl from the E2 to the lysine amino group on the target protein (Figure 1.5E). The majority of E3 ubiquitin-ligases contain a RING domain that contains both E2 binding and ubiquitin transfer activity (Deshaies and Joazeiro, 2009). Ubiquitylation-site specificity is determined by the E2/E3 pair, whose three-dimensional structures contain recognition elements to select protein lysine acceptors for ubiquitin. Given this, it is perhaps not surprising that humans have ~ 600 E3s, ~40 E2s, but only two E1 enzymes (Chen and Sun, 2009). Like many other PTMs, ubiquitylation is a reversible modification. The human proteome contains ~ 90 ubiquitin-specific isopeptidases, called deubiquitylating enzymes (DUBs)(Chen and Sun, 2009). As will be discussed below, cycles of ubiquitylation and deubiquitylation on the same histone lysine are implicated in transcriptional regulation.

Figure 1.5 Ubiquitylation enzymatic machinery. Adapted from Walsh, 2006. A) ribbon diagram of the 3-dimensional fold of ubiquitin, Protein Data Bank code 1UBQ. Ubiquitin is a relatively small protein of 76 amino acids, approximately 8.5 kDa. B) ubiquitylation of lysine ε-NH_2 requires the hydrolysis of ATP and the stepwise action of a ubiquitin-activating enzyme (E1), a ubiquitin-conjugating enzyme (E2), and a ubiquitin-ligase (E3). C) activation of ubiquitin for ligation. D) transfer of the activated ubiquityl from the active-site cysteine of E1 to the active-site cysteine of E2. E) E3 mediated transfer of ubiquityl from E2 to the lysine amino group in the target protein.

Figure 1.5

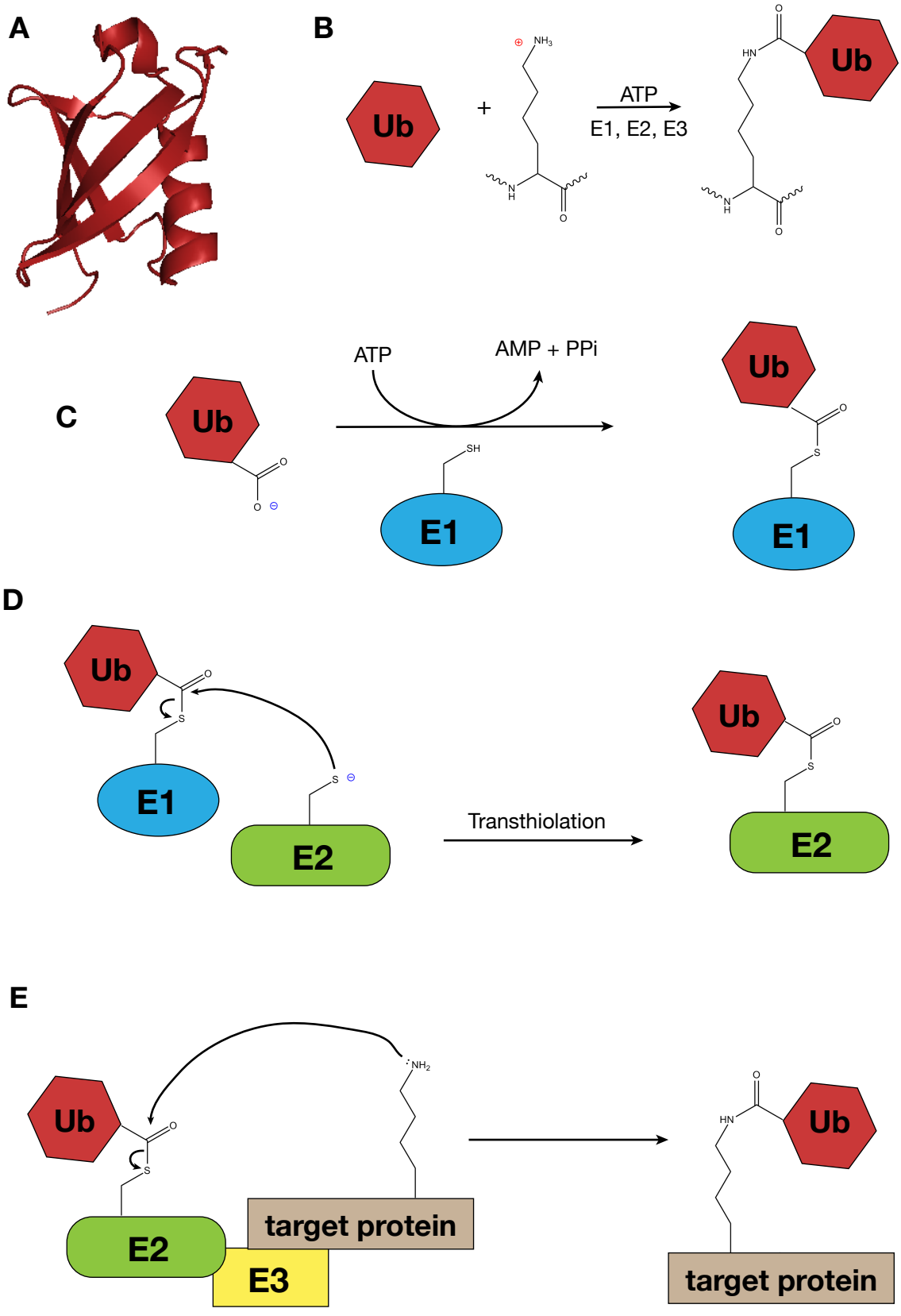
A
B
Ub
+
ATP
E1, E2, E3
Ub
C
Ub
ATP
AMP + PPi
SH
E1
Ub
E1
D
Ub
E1
E2
Transthiolation
Ub
E2
E
Ub
E2
E3
target protein
target protein

In addition to monoubiquitylation of target protein lysine side chains, lysines in ubiquitin itself can be ubiquitylated, resulting in the formation of ubiquitin chains linked by isopeptide bonds. It is becoming clear that chains of different architectures and of different lengths are interpreted differently by the cell and result in different outcomes for the ubiquitylated protein (Ikeda and Dikic, 2008).

Although best known as a proteomic degradation signal, ubiquitylation (especially monoubiquitylation) also functions as a reversible signal to regulate protein localization and activity (Chen and Sun, 2009; Schnell and Hicke, 2003). In addition to its well-described roles in vesicle trafficking and transmembrane receptor localization, monoubiquitylation is crucial for chromatin mediated processes such DNA damage response (DDR) (Al-Hakim et al., 2010) and transcriptional regulation (Weake and Workman, 2008).

In mammalian cells 5-15% of H2A is monoubiquitylated at lysine 119 (K119) (Goldknopf and Busch, 1977; West and Bonner, 1980) and approximately 1% of H2B is ubiquitylated at K120 (West and Bonner, 1980). Other less abundant ubiquitylation sites in mammalian histones include H2BK125 (Minsky and Oren, 2004), H2BK34 (Wu et al., 2011), and H4K91 (Yan et al., 2009).

There is no evidence I know of that ubiquitylated histones are degraded more rapidly than their non-ubiquitylated counterparts, supporting the notion that histone-monoubiquitylation plays a chromatin regulatory role rather than functions as a degradative signal. Although steady-state levels of histone-monoubiquitylation are high (especially H2Aub), the ubiquitin moieties themselves on histones are rapidly turned over (Seale, 1981; Wu et al., 1981). Histone ubiquitylation levels are therefore tunable by

modulating the activity of either E2/E3 pairs or DUBs for a particular ubiquitylation site, which will rapidly increase or decrease of the ubiquitylation level. How the dynamic nature of histone monoubiquitylation contributes to the chromatin regulatory functions of H2Aub and H2Bub is an active area of investigation.

Evidence acquired to date support histone ubiquitylation functioning both in *cis* and in *trans*. Relative to other histone PTMs, monoubiquitylation is quite bulky (*e.g.* ~200x larger than trimethylation), and consequently it has long been thought to influence chromatin structure in *cis* through steric effects (Robzyk et al., 2000). This hypothesis was supported by the observation that histone ubiquitylation is lost during the final stage of chromosome condensation during mitosis and reappears shortly after cytokinesis as chromosomes decondense (Mueller et al., 1985; Wu et al., 1981). A significantly more direct biophysical study of ubiquitylated nucleosomal array compaction will be discussed below (Fierz et al., 2011).

Like other histone PTMs, histone ubiquitylation may function in *trans* by recruiting or stabilizing the binding of an effector protein on chromatin, thereby translating the histone PTM into specific functional outcomes. The three-dimensional fold of ubiquitin is recognized by at least 20 structurally distinct ubiquitin binding domains (UBD), some of which are found in chromatin proteins involved in DNA damage response and transcriptional regulation (Chen and Sun, 2009). Typically, UBD-Ub binding is relatively weak, ranging from several micromolar to several millimolar, suggesting that additional contacts between the UBD containing protein and the ubiquitylated protein are important for sufficient affinity as well as specificity (Chen and Sun, 2009).

Histone ubiquitylation can also function by modulating the activity of other enzymes on chromatin, such as proteins that post-translationally modify histones. Several documented cases of crosstalk between histone ubiquitylation and histone methylation will be described below.

1.2.3.1 Functions of H2BK120ub

H2Bub was first strongly associated with active transcription in the ciliate *Tetrahymena thermophila* (Nickel et al., 1989). This organism physically partitions its genome into two distinct nuclei, one transcriptionally active and the other transcriptionally silent. After careful fractionation of these two types of nuclei, H2Bub was shown to be strongly enriched in the transcriptionally active macronucleus relative to the transcriptionally silent micronucleus (Nickel et al., 1989). Genetic studies in yeast also supported a role of H2Bub in transcriptional activation, especially the elongation step (Henry et al., 2003; Pavri et al., 2006; Tanny et al., 2007; Xiao et al., 2005). Genome-wide chromatin immunoprecipitation (ChIP) studies have mapped H2Bub levels and locations in human cells and found H2Bub in the coding regions of highly expressed genes (Minsky et al., 2008).

The E2/E3 pair for H2Bub is Rad6/Bre1 (Kim et al., 2009; Kim et al., 2005; Zhu et al., 2005). For proper chromatin recruitment, these polypeptides require association with the transcriptional elongation complex, Paf1 (Ng et al., 2003b; Wood et al., 2003), which is believed to carry the ubiquitylation machinery into the coding region of the gene. Importantly, this association establishes a physical link between the H2B ubiquitylation machinery and transcription machinery (Kim and Roeder, 2009).

However, in the past few years our understanding of the link between ubiquitylation of H2B and active transcription has grown more complicated. Intriguingly, optimal transcription, at least for some genes, requires cycles of ubiquitylation and deubiquitylation in gene bodies (Daniel et al., 2004; Henry et al., 2003; Wyce et al., 2007). Depletion of the E3 for H2BK120 and near abolishment of H2Bub does not significantly alter the expression level of most genes, and contrary to expectation, of those with altered expression, about equal numbers are activated and suppressed by the H2Bub E3 ligase RNF20/Bre1A (Batta et al., 2011; Shema et al., 2008). Further, although steady-state H2Bub level correlates genome-wide with expression level (Minsky et al., 2008), genes suppressed by RNF20 were found to be associated with higher levels of H2Bub than genes activated by RNF20 (Shema et al., 2008). In yeast as well there is at least one report linking H2Bub to transcriptional repression of euchromatic genes (Turner et al., 2002). These data raise the possibility that H2Bub may be involved in transcriptional repression in some chromatin contexts.

One possibility is that the position of H2Bub within a gene may influence how H2Bub is "read". Schulze and colleagues found H2Bub enrichment in gene bodies correlates with active transcription while enrichment at promoters is correlated with repression (Schulze et al., 2011). The authors combined multiple existing hypotheses for H2Bub function and proposed two roles dependent on genomic location: 1) H2Bub within the coding region positively regulates transcriptional elongation by promoting nucleosome reformation after RNA Pol II passes through (Fleming et al., 2008), while in contrast, 2) H2Bub in the promoter region negatively regulates transcription initiation by inhibition of nucleosome displacement (Chandrasekharan et al., 2009), which in turn

poses a physical barrier to the transcriptional machinery. Therefore at promoters H2Bub may participate in keeping lowly transcribed genes "off".

Due to ubiquitin's relative bulk and the location of the major H2B ubiquitylation site on the axial face of the nucleosome (Figure 1.3), H2Bub has long been proposed to facilitate transcription by serving as a wedge between adjacent nucleosomes and thereby preventing the formation of compacted chromatin structures (Robzyk et al., 2000; Sun and Allis, 2002). Further, determination of the tetranucleosome structure supported the notion that H2B ubiquitylation would be incompatible with compaction of nucleosome arrays (Schalch et al., 2005).

This "wedge" hypothesis was recently tested using chemically-defined nucleosomal arrays, *i.e.* "designer chromatin" (Section 1.2.4). At ion concentrations in the physiological range, nucleosome arrays assembled from unmodified octamers compact into helical structures of approximately 30 nm in diameter. However, arrays assembled from designer octamers containing H2Bub were relatively resistant to intra-array compaction and inter-array association (Fierz et al., 2011). Interestingly, the relative resistance to compaction of H2Bub arrays is not simply a function of ubiquitin's bulk. Hub1, an ubiquitin like protein of similar size and fold to ubiquitin does not prevent compaction in these assays (Fierz et al., 2011). This suggests that there is something about the precise fold of ubiquitin and its interaction with the nucleosomal surface that mediates the observed resistance to compaction of H2Bub nucleosomal arrays.

However, the most dramatic known effect of H2Bub in chromatin is its crosstalk with methylation of H3K4 and H3K79, both strongly implicated in transcriptional regulation. From yeast to humans, H2Bub is genetically upstream of H3K4 and H3K79

methylation (Briggs et al., 2002; Dover et al., 2002; Ng et al., 2002b; Sun and Allis, 2002), and *in vitro* H2Bub directly stimulates their MTases Set1 (Kim et al., 2009) and Dot1L (McGinty et al., 2008) respectively. Notably, Set1 and Dot1L are evolutionarily unrelated MTases, raising the question how does H2Bub stimulate both of the enzymes? This and related questions of crosstalk specificity will be addressed in subsequent chapters.

1.2.3.2 Functions of H2AK119ub

H2A was the first ubiquitylated protein identified, more than 30 years ago (Goldknopf and Busch, 1977; Hunt and Dayhoff, 1977). Despite this relatively long research record, and the abundance of this modification in chromatin (5-15% in mammalian cells), the function of H2Aub is still enigmatic.

H2Aub was initially linked to active transcription in *Drosophila* and mouse cell culture. Using biochemical chromatin fractionation and 2D-gel analysis, two groups determined that ubiquitylated mononucleosomes co-migrated with mononucleosomes from transcriptionally active (Barsoum and Varshavsky, 1985; Huang et al., 1986) and poised (Levinger and Varshavsky, 1982) loci. However, using a similar experimental system, co-migration was retained upon isopeptidase treatment, arguing that nucleosomes from these transcribed genes were not in fact ubiquitylated (Huang et al., 1986). The link between H2Aub and active transcription is also not supported globally, as H2Aub is not enriched in transcriptionally active or inactive chromatin pools (Dawson et al., 1991).

Subsequent *in vitro* nucleosome reconstitution experiments hinted at a function for H2Aub in chromatin compaction. Nucleosome arrays containing H2Aub exhibit a

somewhat higher propensity than unmodified arrays to oligomerize at high concentrations of divalent cations. However, H2Aub seemed to have no affect on intra-array compaction at lower divalent cation concentrations (Jason et al., 2001). The relative significance of these results is debatable because it is unclear which of these *in vitro* experimental models best mimics chromatin compaction *in vivo*.

The identification of Ring1B (a RING domain E3) as the major E3 ligase for H2AK119 in mammalian cells represented a major step forward (Wang et al., 2004). Ring1B knockout cells had been shown previously to have an embryonic lethal phenotype, emphasizing the potential importance of H2Aub in embryonic development (Voncken et al., 2003). Further, Ring1B is a member of PRC1 type PcG complexes and was shown to be necessary for repression of key developmental regulator genes, such as Hox genes (Cao et al., 2005; de Napoles et al., 2004; Wang et al., 2004; Wei et al., 2006). In support of H2Aub involvement in transcriptional repression, the ubiquitin hydrolase Ubp-M was shown to regulate transcriptional activation of Hox genes through deubiquitylation of H2Aub (Joo et al., 2007) and depletion of Ubp-M from *Xenopus* embryos resulted in homeotic phenotypes reminiscent of PcG mutants (Joo et al., 2007). Taken together these results established a firm link between H2Aub and developmentally regulated transcriptional repression.

Particularly relevant to this thesis, H2Aub was recently shown to participate in direct enzymatic crosstalk with an MTase involved in transcriptional activation. Nakagawa and colleagues tested whether H2Aub might inhibit transcription by directly inhibiting methylation of H3K4 by the MTase complex, MLL3 (Nakagawa et al., 2008). Indeed, nucleosomes reconstituted with endogenous H2Aub, but not endogenous H2A,

inhibited the MLL3 MTase activity while deubiquitylation allowed for efficient di- and trimethylation of H3K4, a marker of active transcription *in vivo*. Further, deubiquitylation stimulated *in vitro* transcription at the transcriptional initiation step (Nakagawa et al., 2008), which is generally in agreement with *in vivo* studies implicating H2Aub-mediated transcriptional repression specifically at the elongation step through RNA Pol II stalling (Stock et al., 2007) and inhibition of FACT-mediated chromatin remodeling of transcribed regions (Zhou et al., 2008).

However, genome-wide analysis of PcG-dependent H2Aub found minimal correlation between the level of H2Aub and transcription (Kallin et al., 2009), in contrast to genome wide studies of H2Bub (Minsky et al., 2008). Unlike PcG-dependent H3K27me3, the PcG-dependent H2Aub level at a promoters and transcription start sites is not a good predictor of transcription level.

A recent paper published by Müller and colleagues may offer some explanation and insights. Through a genetic screen for morphological PcG mutants in *Drosophila*, they identified a novel ubiquitin hydrolase for H2Aub, Calypso. Intriguingly, this H2Aub hydrolase biochemically purified with known PRC1 proteins and its hydrolase activity is required for transcriptional repression of PcG target genes *in vivo* (Scheuermann et al., 2010). This data argues against a simple model of H2Aub directly inhibiting transcription. Instead it suggests that for optimal gene repression, H2A may need to undergo cycles of ubiquitylation and deubiquitylation similar to those demonstrated for H2B in active transcription (Daniel et al., 2004; Henry et al., 2003; Wyce et al., 2007).

Also in 2010, Di Croce and colleagues identified an H2Aub binding protein, ZRF1, which displaces PRC1 from PcG-repressed genes in a developmentally regulated

fashion and de-represses their transcription (Richly et al., 2010). Rather than promote H2Aub involvement in transcriptional activation, the authors argue that H2Aub marks transcriptionally poised promoters (Richly et al., 2010)

Ubiquityation of H2A is also strongly implicated in the DNA damage response (DDR) in mammalian cells. Unlike transcription, where H2Aub and H2Bub are understood to broadly function antagonistically, in DDR, H2Aub and H2Bub function synergistically to promote DNA repair (Bekker-Jensen and Mailand, 2011).

1.2.4 "Designer" nucleosomes to study enzymatic crosstalk

The previous sections of this introductory chapter reviewed what is known about the biological function of four important histone PTMs: methylation of H3K27 and H3K79, and monoubiquitylation of H2BK120 and H2AK119. However, the astounding complexity in chromatin *in vivo* dictates that histone PTMs probably never function truly in isolation. Recent genome-wide profiling studies of histone PTMs are starting to reveal combinations of PTMs strongly associated *in vivo* with genome architecture and different chromatin states, including transcriptional status (Kharchenko et al., 2011; Roudier et al., 2011; Wang et al., 2008).

My major interest in this thesis work was to understand how combinations of histone PTMs are established. One important mechanism is crosstalk between pre-existing modifications on nucleosomes and the activity of other enzymatic activity on the same nucleosome. Carefully designed *in vitro* studies are important for furthering our understanding of crosstalk relationships. However, the inherent heterogeneity of histones and nucleosomes purified from endogenous sources has often obstructed efforts to

establish direct enzymatic crosstalk between PTMs. Histones expressed recombinantly in *E. coli*, devoid of PTMs, can be reconstituted into nucleosomes (Luger et al., 1999), but ideal substrates for enzymatic crosstalk studies require robust and specific installation of site-specific modifications on histones, and this has proved challenging. Fortunately, several groups have recently made large strides in developing chemical strategies for this purpose (Allis and Muir, 2011; Chatterjee et al., 2010; McGinty et al., 2008; McGinty et al., 2009b; Shogren-Knaak and Peterson, 2004; Simon et al., 2007; van Kasteren et al., 2007). For the purposes of this thesis I utilized several of these approaches to generate sufficient quantities of chemically defined H2AK119ub and H2BK120ub (Chatterjee et al., 2010; McGinty et al., 2008; McGinty et al., 2009b) (Chapter 2). These designer histones were incorporated into designer mononucleosomes for crosstalk studies with histone methyltransferases (Chapters 3-5).

CHAPTER 2: PREPARATION OF "DESIGNER" AND ENDOGENOUS NUCLEOSOMES

It is clear that post-translational modification of histone proteins plays a powerful role in regulating DNA templated processes such as transcriptional activation and repression, DNA replication, recombination, DNA damage repair, etc. However, in endogenous chromatin, dozens of PTMs exist on histone proteins, with multiple modifications on the same nucleosome, and found in myriad combinations. This complexity makes it challenging to isolate the function of a particular modification. Chemically defined histones and DNA sequences, when assembled into nucleosomes, can be a powerful tool to study the function of histone modifications without complications arising from the inherent heterogeneity of chromatin purified from endogenous sources. For this thesis, a set of nucleosomes was generated to study direct enzymatic crosstalk between histone ubiquitylation and histone methyltransferases, as described in subsequent chapters.

Two complimentary methods were used to quantitatively install monoubiquitin at position 119 in H2A and position 120 in H2B: semi-synthetic expressed protein ligation (nearly native) and disulfide-mediated (ssUb) (Figure 2.1). Installation by these methods is more specific for a particular lysine than *in vitro* enzymatic ubiquitylation, and they generate histone-ubiquitin linkages that differ minimally from the native isopeptide linkage (Chatterjee et al., 2010; McGinty et al., 2009b). The generation of these designer ubiquitylated histones and their incorporation into mononucleosomes is described below.

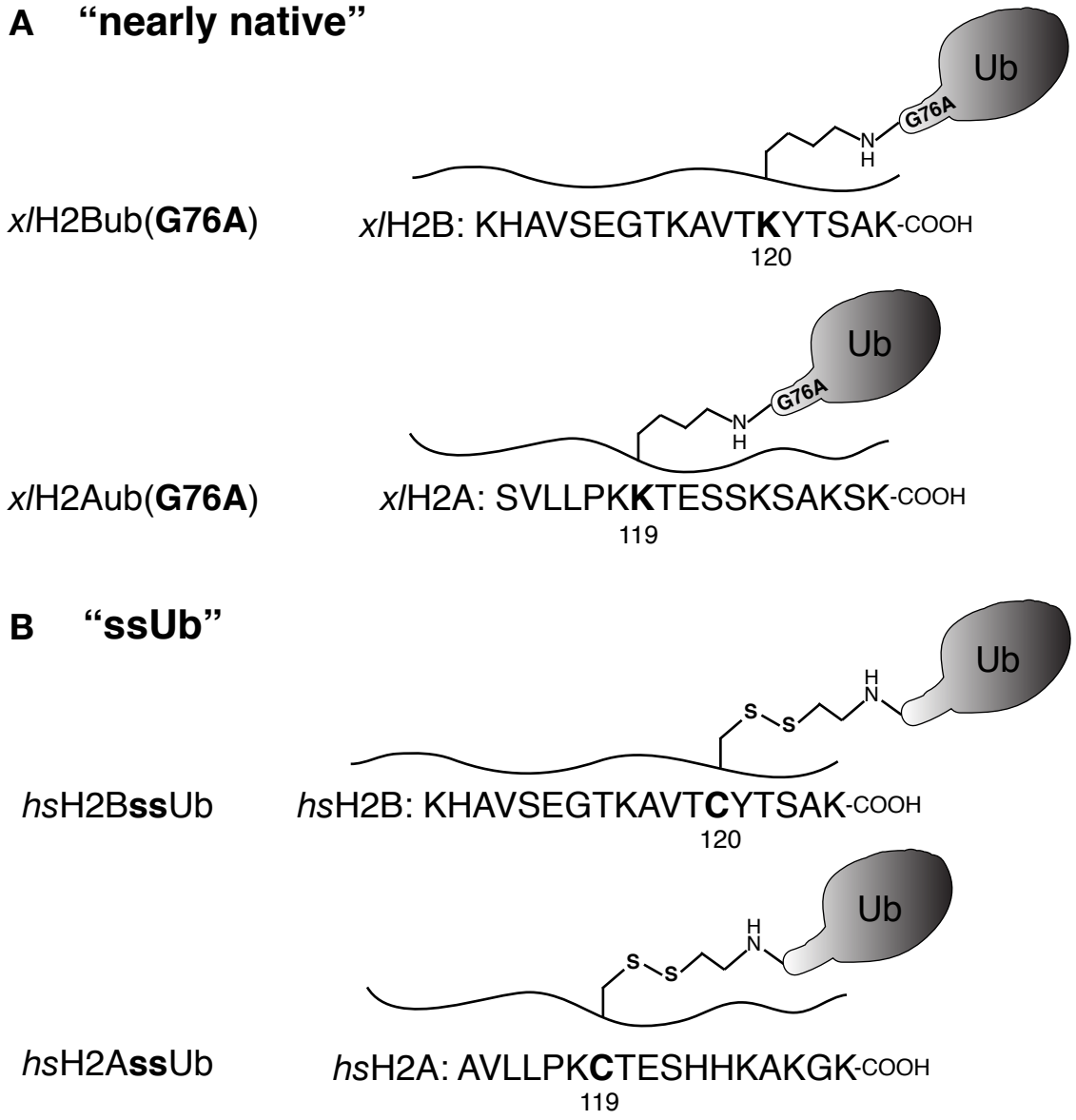

Figure 2.1 Site-specific monoubiquitylation to generate "nearly native" and "ssUb" H2Bub, H2Aub. The four site-specifically ubiquitylated histones described in this chapter are represented in cartoon form. Amino acid sequences of H2B and H2A C-termini are shown below a wavy line representing the peptide backbone. A) "nearly native" refers ubiquitylated histones generated by semi-synthetic expressed protein ligation. This strategy results in an isopeptide linkage identical to native *Xenopus laevis* H2BK120ub and H2AK119ub except for substitution of alanine for glycine as the final amino acid of ubiquitin (G76A). B)"ssUb" refers to ubiquitylated *Homo sapiens* histones generated through disulfide-mediated ubiquitylation at position 119 in H2A and position 120 in H2B.

In addition, native nucleosomes from endogenous sources were isolated and purified. Unlike designer nucleosomes, nucleosomes from endogenous sources carry a complex mixture of posttranslational modifications, DNA sequence, and nucleosome array lengths. Their ease of isolation allowed for preliminary studies of enzymatic activity before moving on to the more precious designer nucleosome substrates.

2.1 Expressed protein ligation to generate "nearly native" H2Bub(G76A)

Expressed protein ligation (EPL) is a semi-synthetic technique that allows the generation of a peptide bond between two polypeptides, one of recombinant origin and one of synthetic origin (Muir et al., 1998). The use of a polypeptide of synthetic origin allows the site-specific incorporation of a variety of biophysical probes, unnatural amino acids, and post-translational modifications (Flavell and Muir, 2009). More specifically, EPL is a ligation between a polypeptide with a C-terminal thioester and one with N-terminal cysteine. Ligations proceed through a reversible *trans*-thioesterification of the C-terminal thioester by the N-terminal cysteine thiol, followed by an irreversible S- to N-acyl shift, resulting in peptide bond between the two polypeptides (Figure 2.2A). Synthetic peptides with a N-terminal cysteine thiol can be prepared by solid phase peptide synthesis (SPPS), and recombinant proteins with a C-terminal thioester can be generated by thiolysis of an intein fusion protein. With the addition of thiols, a modified intein spontaneously cleaves itself out of a fusion protein, leaving a C-terminal thioester on the recombinant protein of interest (Figure 2.2B).

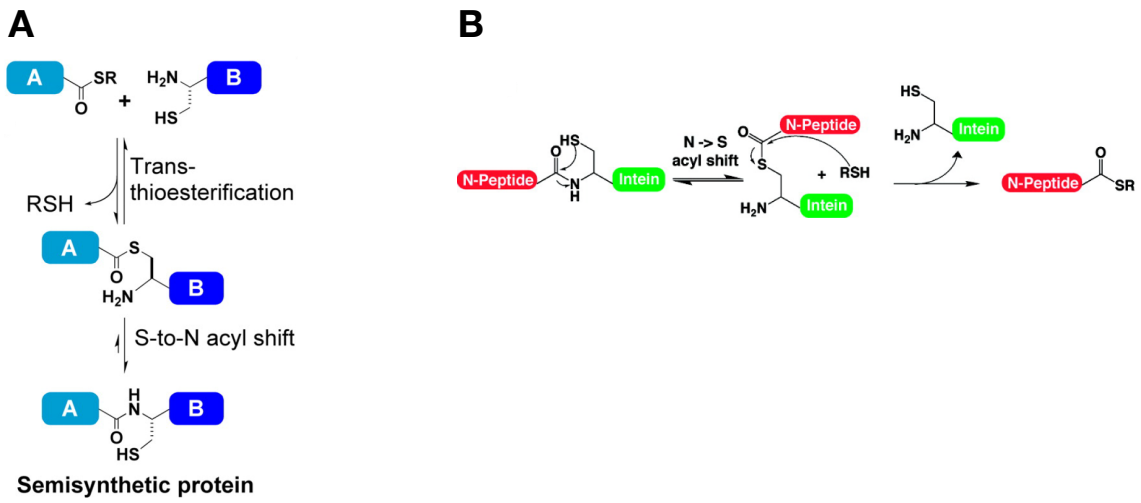

Figure 2.2 Expressed protein ligation. A) basics of expressed protein ligation between a polypeptide with a C-terminal thioester and a polypeptide with an N-terminal cysteine, resulting in a peptide bond between them. Adapted from (Chatterjee and Muir, 2010). B) generation of a polypeptide with a C-terminal thioester by intein-mediated thiolysis for use in expressed protein ligation. Adapted from (Flavell and Muir, 2009).

Dr. Robert McGinty, while a MD-PhD student in the lab of Dr. Tom W. Muir at The Rockefeller University, harnessed EPL to produce H2B homogenously monoubiquitylated at K120, the major H2B ubiquitylation site in chromatin. In this synthesis he ligated two recombinantly expressed proteins to the same synthetic peptide to generate the desired branched protein with the native isopeptide bond between them (Figure 2.3).

Xenopus laevis H2B(1-116) and Ubiquitin(1-75) were expressed as fusion proteins with the *Mycobacterium xenopi* GyrA intein and a C-terminal CBD (chitin binding domain). Soluble fusion protein was purified from *E. coli* lysate with chitin resin. Intein-mediated cleavage with the thiol 2-mercaptoethanesulfonic acid (MESNa) resulted in H2B(1-116)-α-MES and Ub(1-75)-α-MES thioesters. The H2B(117-125) C-terminal

peptide required two cysteines, one for each ligation reaction. For this purpose, a cysteine was installed via an isopeptide bond to the ε-NH_2 of H2BK120, which in addition to providing the nucleophilic thiol for an EPL reaction also provided a linker to replace glycine76 of ubiquitin in the final protein. Additionally, the first amino acid in the synthetic peptide, representing alanine117, was changed to cysteine and reversibly protected as a thiazolidine for the first ligation reaction, to limit ubiquitin ligation to the desired internal site. Before the second ligation with H2B(1-116) thioester, thiazolidine was converted to cysteine by treatment with methoxylamine at pH 5.

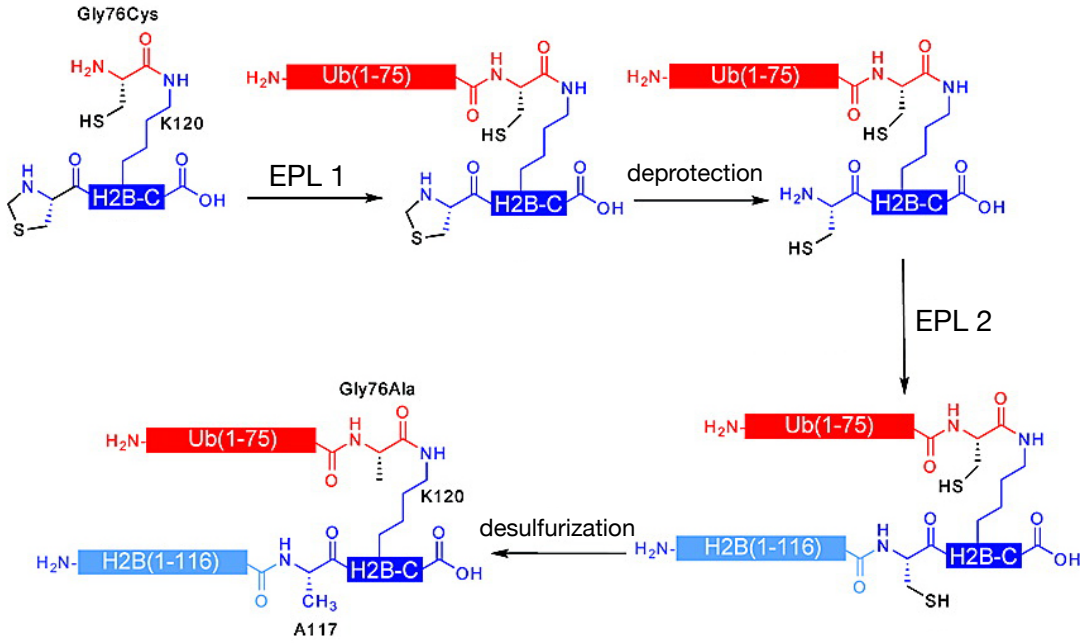

Figure 2.3 Scheme for synthesis of xlH2Bub(G76A). As published by McGinty and colleagues (McGinty et al., 2009), xlH2Bub(G76A) was generated by two sequential expressed protein ligation reactions between H2BC synthetic peptide and the thioesters Ub(1-75)-α-MES (EPL1) and H2B(1-116)-α-MES (EPL2). The product of the first ligation was treated with methoxylamine at pH 5 to deprotect the N-terminal thiol on H2BC. After the second ligation reaction, the cysteines at both ligation junctions were desulfurized to alanines, finally resulting in the native xlH2B sequence and the point mutation in ubiquitin (G76A). Figure adapted from (McGinty et al., 2009).

EPL ligation reactions result in cysteines at each ligation junction. As these cysteines are not in the endogenous sequence of H2Bub, desulfurization was performed to convert the cysteines to alanines (He et al., 2003). Raney nickel (Yan and Dawson, 2001) or radical-initiated (Wan and Danishefsky, 2007) desulfurization was used to convert H2B(A117C) to the native H2B(A117), resulting in a traceless ligation, and Ub(G76C) was converted to Ub(G76A) (Figure 2.3).

It had been previously observed that H2Bub was required for detectable methylation of H3K79 *in vivo* (Briggs et al., 2002; Ng et al., 2002b; Sun and Allis, 2002), but the molecular basis of this crosstalk was unknown. Dr. McGinty incorporated his EPL prepared H2Bub into nucleosomes and performed methyltransferase assays to show that H2Bub can directly stimulate Dot1L MTase activity on H3K79, ruling out, at least *in vitro*, the need for bridge/mediator proteins to generate the striking crosstalk between these modifications (McGinty et al., 2008; McGinty et al., 2009b). Additionally, as these experiments were performed with mononucleosomal substrates rather than with nucleosomal arrays, they argued against H2Bub functioning merely as a wedge between nucleosomes to expose nucleosomal axial surfaces for Dot1L binding and methylation of H3K79. Whether ubiquitylation of H2BK120 allosterically regulates Dot1L or modifies nucleosomal structure/dynamics remains an important open question.

2.2 Application of expressed protein ligation to generate "nearly native" H2Aub(G76A)[1]

Dr. McGinty's elegant work with H2Bub and its stimulation of Dot1L illustrated the power of using chemical-biology techniques to generate defined nucleosomal substrates for *in vitro* enzymatic assays. Consequently, I was interested in using EPL to site-specifically install ubiquitin on H2AK119, in order to study the function of this abundant but enigmatic modification.

2.2.1 Traceless EPL at alanine to generate *hs*H2Aub(G76A)

Analogous to H2Bub(G76A), nearly native H2Aub requires ligation of Ub(1-75) and H2A_ΔC-term thioesters to a synthetic peptide containing the H2A C-terminus ($H2A_C$). Standard EPL utilizes the amino acid cysteine at ligation junctions, which can be subsequently desulfurized to alanine. In order to generate a traceless ligation between ubiquitylated $H2A_C$ and H2A_ΔC, the ligation site should be placed immediately before an alanine. There are two alanines in the C-terminus of *Homo sapiens* H2A, at positions 103 and 113 (Figure 2.4A), and ligation at either of these sites would be compatible with $H2A_C$ synthetic peptide synthesis. However, the identity of the final amino acid in the thioester must also be considered when choosing a ligation site. Proline, valine or isoleucine in that position are particularly detrimental to ligation efficiency and/or thiolysis yield (Blaschke et al., 2000). Isoleucine is present at position 102 in human H2A, ruling this out as a suitable ligation site for EPL (Figure 2.4A). Therefore, position Q112/A113 was chosen as the H2A ligation site. Using this ligation site, the three

[1] Performed in close collaboration with Dr. Robert McGinty and Dr. Beat Fierz, then members of the Laboratory of Synthetic Protein Chemistry at the Rockefeller University

components to produce nearly native *hs*H2Aub(G76A) by EPL are H2A(1-112)-α-COSR and Ub(1-75)-α-COSR thioesters from intein mediated thiolysis and H2A(113-129) synthetic peptide (Figure 2.4B,C).

The necessary synthetic peptide was synthesized by Dr. McGinty, and contributed as part of our collaboration (Figure 2.4B). Two modifications were made to the H2A C-terminal sequence, one at each ligation site. For ligation to H2A(1-112)-α-COSR, the first amino acid in the peptide, representing A113, was changed to cysteine and reversibly protected as a thiazolidine. For ligation to Ub(1-75)-α-COSR, cysteine was installed via an isopeptide bond to the ε-NH_2 of the lysine representing K119. This isopeptide linked cysteine serves as a nucleophilic thiol for the EPL reaction and also provides the linker to replace glycine76 of ubiquitin in the final protein (Figure 2.4C).

The Ub(1-75)-α-MES thioester was generated by thiolysis with MESNa of an Ubiquitin-GyrA-CBD fusion protein, as described above. The Ub-thioester ligated efficiently to the $H2A_C$ peptide, generating Ub-$H2A_c$ ligation product. Deprotection of the N-terminal cysteine of Ub-H2Ac for next ligation with H2A(1-112)-α-COSR was also accomplished efficiently.

However, recombinant expression of the *hs*H2A(1-112)-GyrA fusion protein presented unanticipated challenges. Full-length histones are typically expressed at high levels in *E. coli* and can be purified from inclusion bodies in denaturing conditions. However, *hs*H2A(1-112)-GyrA fusion protein was expressed at extremely low levels in both soluble and insoluble fractions. Inclusion of an N-terminal FLAG-tag increased expression somewhat, but expression yields were still quite low. A variety of *E. coli* expression strains, growth temperatures, and Isopropyl β-D-1-thiogalactopyranoside

(IPTG) concentrations were tried in an effort to increase expression of the fusion protein. The small about of protein that was expressed was affinity purified using either chitin-agarose or Ni-NTA-agarose resin, for CBD and 6xHis tagged fusion proteins respectively.

Poor expression was compounded by inefficient H2A(1-112) thioester generation. Intein mediated thiolysis requires the intein domain to be properly folded, necessitating cleavage of solubly expressed protein or refolded protein purified denatured from inclusion bodies (Flavell et al., 2008). Whether using solubly expressed fusion protein or refolded protein purified denatured from inclusion bodies, thiolysis was quite inefficient. Thiolysis efficiency was not significantly aided by cleavage in solution as opposed to on-column.

After massive scale up of protein expression and thioester generation processes, a small amount of purified H2A(1-112)-α-MES thioester was available for the final EPL reaction with Ub-H2Ac. However, this ligation was significantly less efficient than the first EPL between Ubiquitin and H2Ac peptide and we were never able to achieve reliable mass spectrometry confirmation of HPLC purified products. Further, we were not able to confirm the ubiquitylation site by western blot with an antibody specific for H2AK119ub (Figure 2.4D), perhaps because the antibody is sensitive to having a cysteine rather than glycine as the final amino acid in ubiquitin, right at the isopeptide junction between the two proteins. Due to lack of other suitable ligation sites in the H2A C-terminal tail, I abandoned an EPL approach to generate *hs*H2Aub(G76A) and instead invested in a "disulfide-mediated" approach (Ch 2.3) to generate chemically-defined H2Aub for enzymatic crosstalk studies with histone metyltransferases.

Figure 2.4 Scheme for synthesis of *hs*H2Aub(G76A). A) *Homo sapiens* H2Aub showing ubiquitylation at the native site, K119, and the sequence surrounding this C-terminal tail modification. B) H2A(1-112)-GyrA-CBD/6xHis construct designed for expression in *E. coli*, affinity purification, and intein-mediated thiolysis to generate H2A(1-112)-α-MES. The $H2A_c$ peptide synthesized by Dr. Robert McGinty is shown below. C) Modeled after the synthesis of *xl*H2Bub(G76A), the synthetic scheme to generate *hs*H2Aub(G76A) called for two sequential expressed protein ligation steps between $H2A_C$ synthetic peptide and the thioesters Ub(1-75)-α-MES and H2A(1-112)-α-MES. The product of the first ligation was treated with methoxylamine at pH 5 to deprotect the N-terminal thiol on $H2A_C$. After the second ligation, cysteines at both ligation junctions were desulfurized to alanines, finally resulting in the native *hs*H2A sequence and the point mutation in ubiquitin (G76A). D) as discussed in the text, final yields of *hs*H2Bub(G76A) was extremely low and mass spectrometry was not able to confirm the identity of the final product. Western blot analysis shown here confirms that the *hs*H2Bub(G76A) generated is recognized by anti-H2A antibody, but the ubiquitylation site, K119, could not be confirmed using a site-specific antibody, anti-H2AK119ub. This result may be a false negative as it cannot be ruled out that the antibody is sensitive to the identity of the final amino acid in ubiquitin at the branch point between the polypeptides H2A and Ub.

Figure 2.4

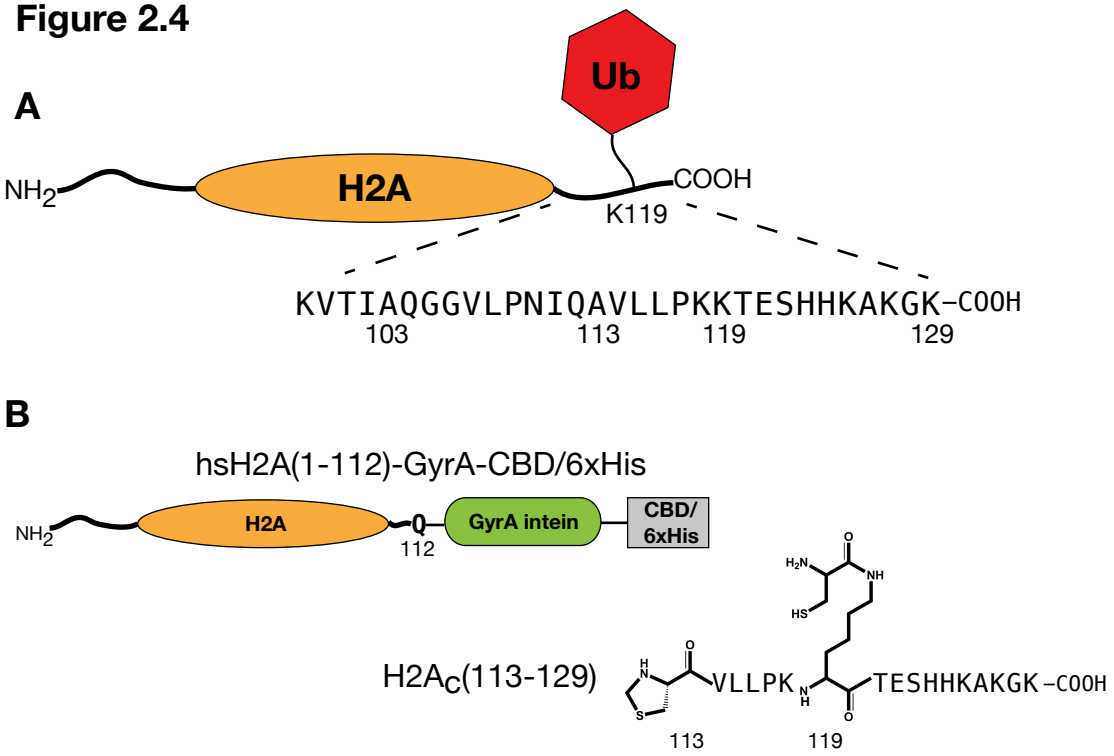
A
Ub
H2A
NH2
COOH
K119
KVTIAQGGVLPNIQAVLLPKKTESHHKAKGK-COOH
103
113
119
129
B
hsH2A(1-112)-GyrA-CBD/6xHis
NH2
H2A
Q
112
GyrA intein
CBD/
6xHis
H2Ac(113-129)
VLLPK
TESHHKAKGK-COOH
113
119
C
Gly76Cys
K119
H2A-C
113
Ub(1-75)
EPL 1
deprotection
EPL 2
Gly76Ala
Gly76Cys
desulfurization
H2A(1-112)
Ala113
Ala113Cys
D
kDa
HeLa nuclei
H2Aub(G76A)
50
36
22
16
6
H2Aub(G76A)?
H2AK119ub (endogenous)
H2A
direct blue
anti-H2A
anti-H2AK119ub

2.2.2 Traceless EPL at valine to generate *xl*H2Aub(G76A)

Dr. Beat Fierz, then a post-doctoral fellow in the lab of Dr. Tom Muir at the Rockefeller University, continued to explore other methods to generate "nearly-native" H2Aub. His efforts targeted ubiquitylation of the *Xenopus laevis* H2A sequence rather than the human sequence due to improved expression characteristics of the *xl*H2A_ΔC-terminal polypeptide. Perhaps more critically, he pursued modified chemistries that made other ligation sites available in the H2A C-terminal sequence. Standard EPL utilizes a N-terminal cysteine for ligation with a C-terminal thioester (Figure 2.2). As recently described (Haase et al., 2008), substitution of β,β-dimethylcysteine for cysteine allows for effective ligation and can be desulfurized to the amino acid valine. A valine exists at position 114 in H2A, and this ligation site proved to be dramatically more amenable to traceless EPL generation of nearly native H2Aub. Dr. Beat Fierz graciously provided me with sufficient sample for the crosstalk studies presented in Chapter 4.

2.3 Disulfide-directed ubiquitylation of H2B and H2A[2]

Concurrent with my attempts to generate nearly native *hs*H2Aub(G76A), Dr. Champak Chatterjee, then a post-doctoral fellow in the lab of Dr. Tom Muir at The Rockefeller University, was developing a disulfide-directed strategy to specifically install monoubiquitin on histone proteins. The highly nucleophilic sulfhydryl side chain of cysteine presents a convenient site to add functional groups to mimic natural post-translational modifications of proteins, and such an approach had previously been used by several groups to site-selectively install sulfur-containing analogs of lysine

[2] Performed in close collaboration with Dr. Champak Chatterjee, then a member of the Laboratory of Synthetic Protein Chemistry at the Rockefeller University

methylation (Simon et al., 2007) and glycosylation (van Kasteren et al., 2007). Dr. Chatterjee recognized that histones and ubiquitin are perfectly suited for disulfide-directed strategies because these proteins lack cysteines in their native sequence (except for C110 of histone H3, which can be mutated to alanine without appreciably affecting nucleosome structure (Simon et al., 2007)). This characteristic allows for great specificity in installation with minimal additional effort to reversibly protect other sulfhydryls.

Dr. Chatterjee developed an efficient and rapid method to generate *Xenopus laevis* H2BssUb as an analog to nearly native H2Bub(G76A) for structure/function studies of Dot1L stimulation by monoubiquitylated histones (Chatterjee et al., 2010). The resulting disulfide linkage between ubiquitin and H2B is one atom longer (~ 2.4 Å) than the native isopeptide bond (Figure 2.5E), but importantly, H2BssUb mimicked nearly native H2Bub in Dot1 stimulation assays (Chatterjee et al., 2010). Unable to generate sufficient quantities of sufficient quality of nearly native H2Aub(G76A) by EPL (Chapter 2.2), this disulfide-directed strategy provided me with an alternative method to generate chemically-defined ubiquitylated H2A.

Figure 2.5 Scheme for synthesis of H2AssUb and H2BssUb by disulfide-mediated ubiquitylation. As published by Chatterjee and colleagues (Chatterjee et al., 2010), site-specificity of disulfide-mediated monoubiquitylation is achieved by genetic substitution of the thiol containing cysteine at the desired ubiquitylation site. A) Full-length *Homo sapiens* H2AK119C and H2BK120C were expressed in *E. coli* and purified, cysteine sulfhydryl circled in blue. B) Intein-mediated thiolysis of full-length ubiquitin and concomitant addition of aminoethanethiol to the C-terminus. C) The C-terminal thiol of ubiquitin-aminoethanethiol was protected by treatment with 2,2'-dithiobis(5-nitropyridine) (DTNP) in acetic acid. D) Formation of the desired asymmetric disulfide bond between H2AK119C or H2BK120C and Ub-aminoethanethiol. E) The disulfide bridge between histone-cysteine and ubiquitin-aminoethanethiol results in a linkage ~ 2.4 Å longer than the native isopeptide bond. Figure adapted from (Chatterjee et al., 2010).

Figure 2.5

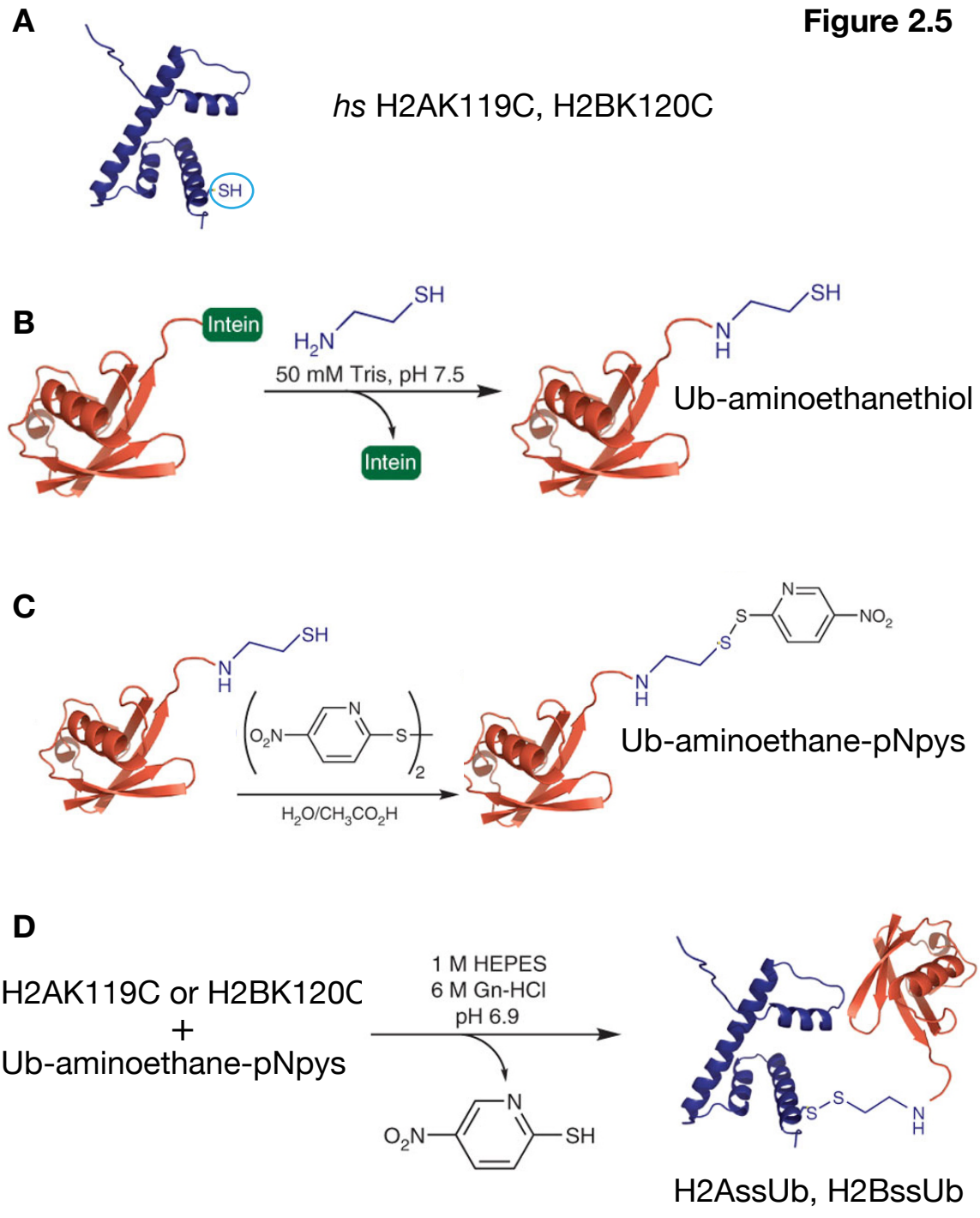
A
SH
hs H2AK119C, H2BK120C
B
Intein
SH
H_2N
50 mM Tris, pH 7.5
Intein
SH
N
H
Ub-aminoethanethiol
C
SH
N
H
O_2N
N
S
2
H_2O/CH_3CO_2H
N
S
S
NO_2
N
H
Ub-aminoethane-pNpys
D
H2AK119C or H2BK120C
+
Ub-aminoethane-pNpys
1 M HEPES
6 M Gn-HCl
pH 6.9
O_2N
N
SH
S
S
N
H
H2AssUb, H2BssUb
E
O
HN
N
H
O
H
N
isopeptide bond
O
HN
S
S
H
N
O
N
H
disulfide mediated

In order to generate H2AssUb and H2BssUb (Figure 2.1B), the lysines at position 119 and 120, in human H2A and H2B sequences respectively, were genetically modified to cysteine (Figure 2.5A). Full-length histones carrying the K to C mutation were expressed in *E. coli* and purified from inclusion bodies. During histone purification and affinity tag cleavage, β-ME was used as a reducing agent because of its compatibility with Ni-NTA resin. However, this results in the formation of β-ME-H2AK119C and β-ME-H2BK120C disulfide adducts, leaving the histone sulfhydryls unavailable for disulfide formation with ubiquitin. The undesired β-ME adducts were reduced with 20mM Tris(2-carboxyethyl)phosphine) (TCEP) and reducing agents removed by HPLC purification before H2AK119C and H2BK120C could be used in ligation reactions with ubiquitin.

Full-length ubiquitin was expressed as a fusion protein with GyrA intein and CBD and then purified on chitin resin. The desired sulfhydryl group and two-carbon linker were introduced onto the C-terminus of ubiquitin by intein-mediated thiolysis with cystamine-dihydrochloride followed by an intra-molecular S- to N-acyl shift (Figure 2.5B). The C-terminal thiol group was then activated/protected by reacting it with 2,2'-dithiobis(5-nitropyridine) (DTNP) and HPLC purified (Figure 2.5C). Before proceeding to disulfide formation with either H2AK119C or H2BK120C, Ub-aminoethane-pNpys (Ub-pNpys) was HPLC purified away from any remaining unreacted cystamine in order to prevent it from competing with Ub-pNpys in disulfide formation with H2AK119C and H2BK120C (Figure 2.5D). Failure to remove unreacted cystamine before ligation resulted in large reductions in the final yield of H2AssUb and H2BssUb.

2.4 Designer octamer generation

With *xl*H2Bub(G76A) (Chapter 2.1), *xl*H2Aub(G76A) (Chapter 2.2.2), *hs*HBAssUb and *hs*H2AssUb (Chapter 2.3) in hand, unmodified histones were prepared for designer octamer generation. Briefly, N-terminal 6xHis tagged histones were expressed in *E. coli*, extracted from inclusion bodies and purified with Ni-NTA affinity resin. TEV or Precision proteases were employed to remove the 6xHis tag from H3.2C110A, H4, H2A, and H2B. Note that because the integrity of the eventual disulfide bond between H2AK119C, H2BK120C and Ub-aminoethanethiol is extremely sensitive to reducing agents, any residual reducing agents from all histone preps (not only H2AK119C and H2BK120C, as described above) were removed by extensive dialysis and/or HPLC purification.

Unmodified and ubiquitylated histones were assembled into designer octamers of 7 types: *Xenopus* unmodified, H2Bub(G76A) H2Aub(G76A); human unmodified, H2AssUb, H2BssUb, and H2AssUb/H2BssUb. Briefly, denatured histones were combined in dialysis buttons such that H3 and H4 were slightly limiting and dialyzed into high salt buffer. Octamers were purified from unincorporated dimers, individual histones and aggregates by Superdex 200 size exclusion FPLC (Figure 2.6). Pooled fractions corresponding to octamers (biased towards the front of the peak because H3/H4 tetramers do not separate well from octamers by Superdex 200 size exclusion chromatography) were verified by SDS-PAGE (Figure 2.7, 2.8A).

Figure 2.6 Assembly and purification of designer octamers. Unmodified and ubiquitylated histones were appropriately combined in denaturing buffer and dialyzed into high salt buffer to assemble 7 designer octamers: *Xenopus* unmodified, H2Bub(G76A) and H2Aub(G76A); human unmodified, H2AssUb, H2BssUb, and H2AssUb/H2BssUb. Octamers were purified by size exclusion chromatography using Superdex 200 columns from GE Healthcare, a PC 3.2/30 column for assemblies < 1 mg, or a 10/300 GL column for larger-scale assemblies. Representative chromatograms are shown, A280 absorbance graphed as a function of time. Octamer peak fractions were pooled as indicated (red box).

Figure 2.6

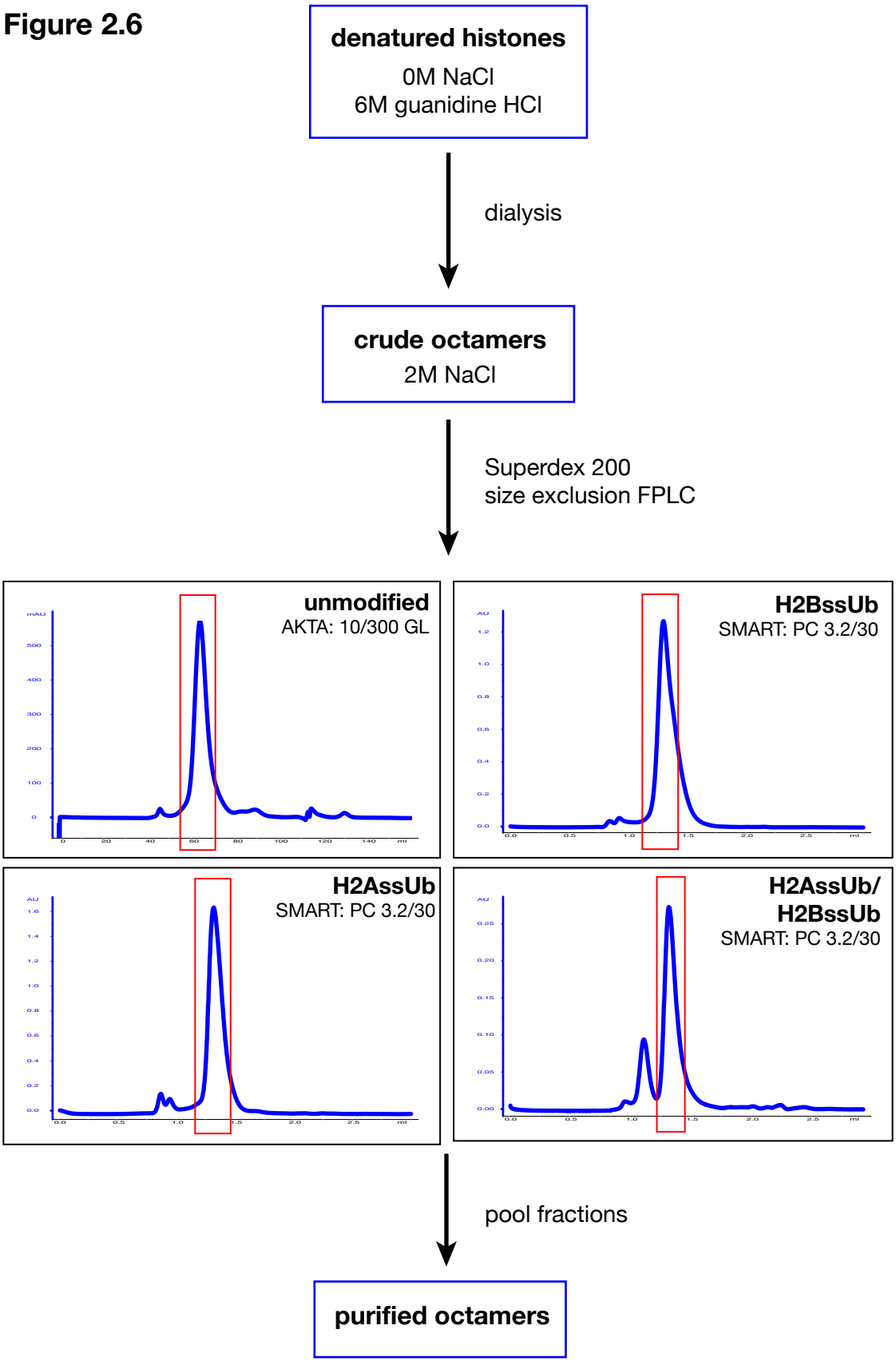
denatured histones
0M NaCl
6M guanidine HCl
dialysis
crude octamers
2M NaCl
Superdex 200
size exclusion FPLC
unmodified
AKTA: 10/300 GL
H2BssUb
SMART: PC 3.2/30
H2AssUb
SMART: PC 3.2/30
H2AssUb/
H2BssUb
SMART: PC 3.2/30
pool fractions
purified octamers

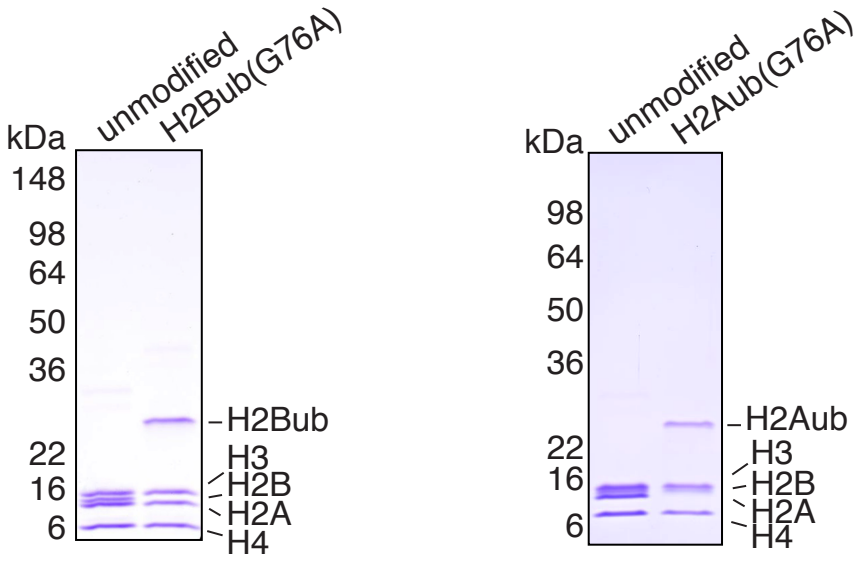

Figure 2.7 Characterization of "nearly native" ubiquitylated *Xenopus* octamers. The purity and expected 1:1:1:1 ratio of histones H3, H4, H2A/H2Aub, and H2B/H2Bub of *Xenopus* octamers was assessed by Coomassie staining of SDS-PAGE gels.

For ssUb octamers, the specificity of ubiquitin attachment and its reversibility with reducing agents were confirmed by western blot analysis with antibodies specific for H2AK119ub and for H2BK120ub (Figure 2.8C). For reasons that are not clear, the disulfide bridge between ubiquitin and H2AK119C or H2BK120C is nearly completely reduced if run on a standard SDS-PAGE Tris-Glycine precast gel made by Invitrogen but not on a seemingly equivalent precast gel made by Bio-Rad, or on standard "hand poured" SDS-PAGE Tris-Glycine gels (Figure 2.8B).

Figure 2.8 Characterization of "ssUb" human octamers. Octamers assembled from human unmodified and ssUb histones were electrophoresed on SDS-PAGE gels. A - B) octamer quality was assessed by Coomassie staining. C) SDS-PAGE separated octamer samples -/+ beta-mercaptoethanol (β-ME) were transferred to PVDF membrane, stained with Direct Blue, and subjected to western blotting with the indicated antibodies. Nuclei from mouse embryonic stem cells (ESC) were used to mark the migration position of endogenous H2AK119ub and H2BK120ub.

Figure 2.8

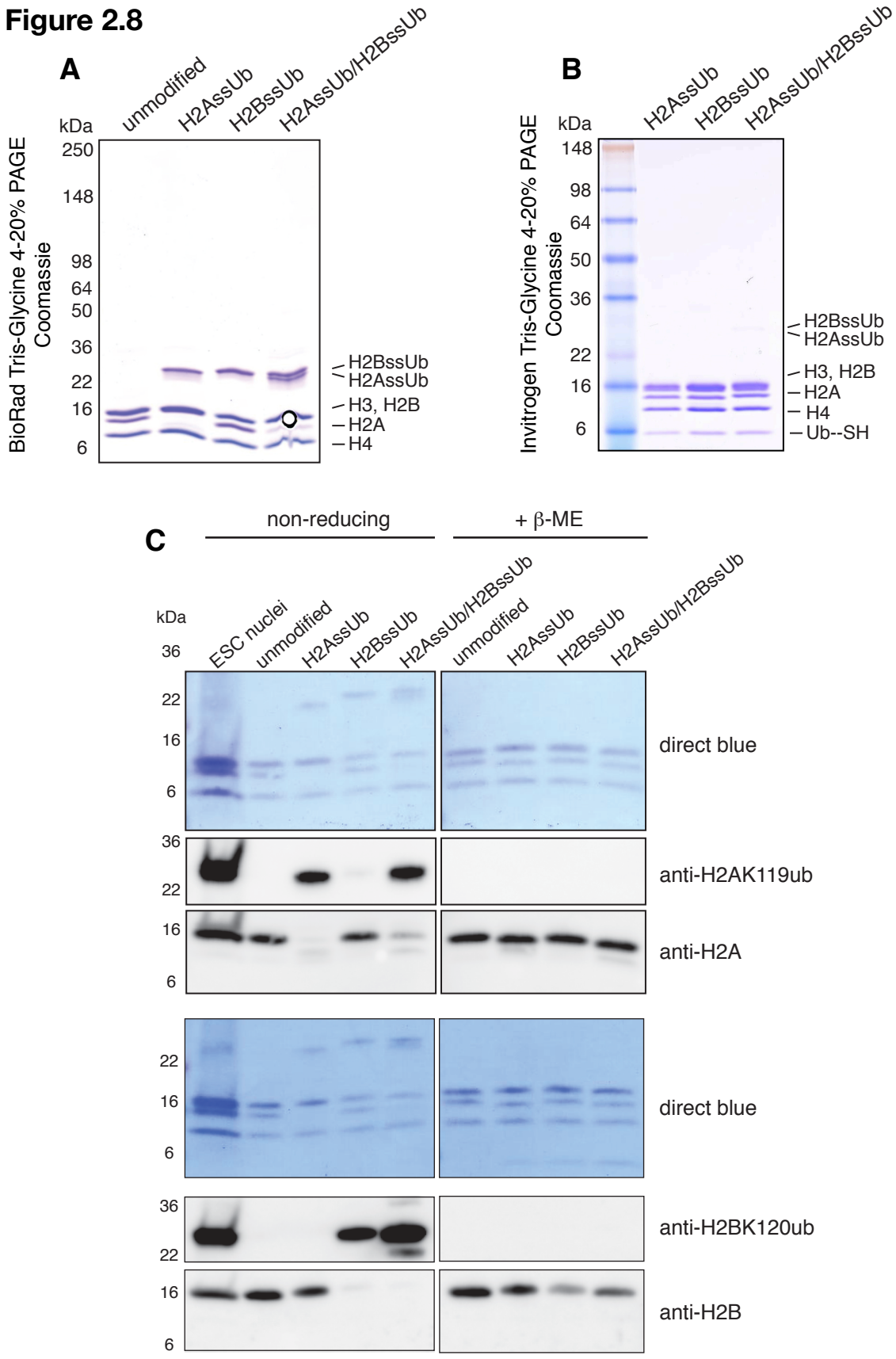
A
unmodified
H2AssUb
H2BssUb
H2AssUb/H2BssUb
kDa
250
148
98
64
50
36
22
16
6
BioRad Tris-Glycine 4-20% PAGE
Coomassie
H2BssUb
H2AssUb
H3, H2B
H2A
H4
B
H2AssUb
H2BssUb
H2AssUb/H2BssUb
kDa
148
98
64
50
36
22
16
6
Invitrogen Tris-Glycine 4-20% PAGE
Coomassie
H2BssUb
H2AssUb
H3, H2B
H2A
H4
Ub--SH
C
non-reducing
+ β-ME
kDa
ESC nuclei
unmodified
H2AssUb
H2BssUb
H2AssUb/H2BssUb
unmodified
H2AssUb
H2BssUb
H2AssUb/H2BssUb
36
22
16
6
direct blue
anti-H2AK119ub
anti-H2A
direct blue
anti-H2BK120ub
anti-H2B

2.5 Designer mononucleosome generation

Relative to other histone PTMs, monoubiquitylation is an extremely bulky modification (itself being ~ 60% of the molecular weight of histones H2A and H2B). For enzymatic crosstalk studies I wanted to eliminate the possibility that ubiquitylation dependent changes in array conformation could alter the accessibility of a target lysine for subsequent methylation. Therefore, I assembled octamers into mononucleosomes using a 153bp sequence containing the 601 strong positioning sequence (Lowary and Widom, 1998). DNA fragments for mononucleosome assemblies were prepared by EcoRV digest of 32x153bp tandem repeats cloned into pUC19 (a kind gift from Dr. Kyle Chiang, Tom Muir Laboratory) (Figure 2.9A). After extensive digest, plasmid backbone fragments were PEG precipitated, and soluble 153bp fragments were purified with several phenol/chloroform extractions and ethanol precipitated (Figure 2.9B).

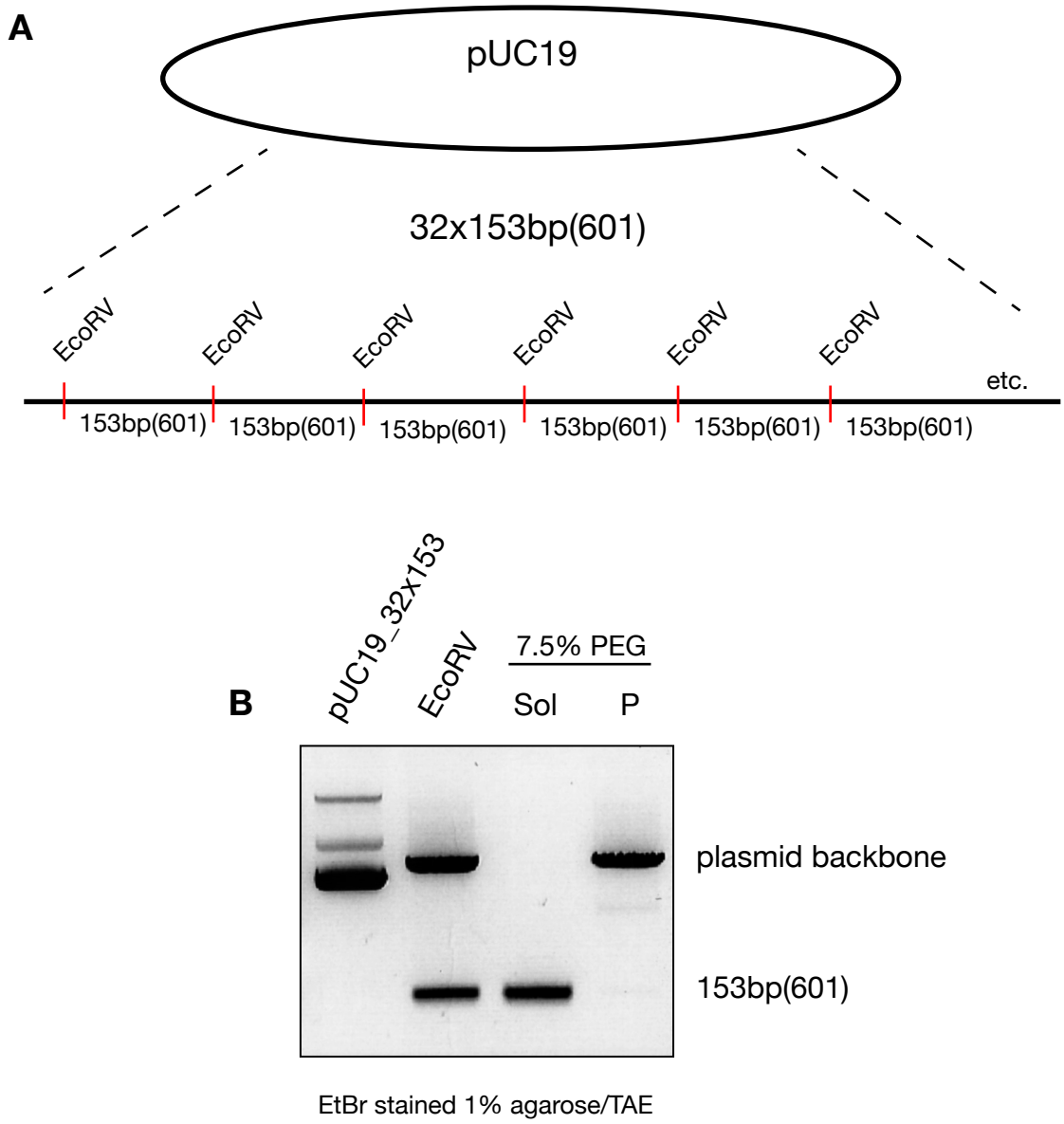

Figure 2.9 Preparation of 601 positioning sequence DNA for mononucleosome assemblies. A) 153bp DNA fragments containing the 147 bp 601 positioning sequence were prepared by EcoRV restriction digest of 32x153bp tandem repeats of the 601 sequence cloned into pUC19. B) EtBr stained 1% agarose gel of the 153bp DNA purification procedure. Plasmid DNA was digested with EcoRV. 153bp DNA fragments were purified by plasmid backbone precipitation in 500 mM NaCl and 7.5% polyethylene glycol (PEG-6000).

Mononucleosomes were assembled by gradient dialysis from high salt to low salt over approximately 24 hours, as previously described (Ruthenburg et al., 2011). The precise molar ratio of octamer to nucleosome positioning sequence is critical for successful nucleosome assemblies. However, histone proteins are low in aromatic amino acids (tryptophan, tyrosine, and phenylalanine), and so absorb 280nm light poorly, making accurate assessments octamer concentrations difficult. Therefore, with each batch of octamers, small scale assemblies were carried out, carefully titrating the octamer:DNA ratio. Too little DNA results in poor nucleosome assembly yield, while too much DNA results in soluble unincorporated DNA (Figure 2.10A). Most enzymes that act upon chromatin substrates have DNA binding activity. Recognizing that unincorporated DNA could influence the results of enzymatic activity assays, all assemblies were checked for free DNA by native 5% polyacrylamide gel electrophoresis and ethidium bromide staining (EtBr) (Figure 2.10).

Native gel electrophoresis was also used to assess the structural homogeneity of mononucleosome assemblies. Typically mononucleosome assemblies resulted in one shifted EtBr stained band. However, my initial assemblies with *xl*H2Bub(G76A) and *xl*H2Aub(G76A) octamers resulted in two shifted bands (Figure 2.10B). This was a puzzling result as 153bp DNA should not be long enough to allow for nucleosome positional isomers, and attempts to heat reposition nucleosomes at 55 degrees had no impact. If hexamers contaminated the octamer pool, they could result in multiple shifted EtBr stained bands on a native gel. However, the position of the lower band appeared to be too high to be the result of DNA associated with a hexamer (H3/H4 tetramer plus one H2A/H2Bub dimer), and Coomassie staining of the octamer pools did not suggest that

H3/H4 were present at greater than equimolar amounts (Figure 2.7). Interestingly, assemblies using extremely high ratios of nearly native ubiquitylated octamers to DNA (1.9 H2Bub oct:1 DNA; 2.3 H2Aub oct:1 DNA) resulted in only one shifted band (Figure 2.10B,C), solving the assembly problem with these designer octamers. Interestingly, H2AssUb, H2BssUb, and not even H2AssUb/H2BssUb nucleosomes assemblies ever gave this doublet pattern, suggesting that ubiquitylated octamers are not inherently refractory to efficient mononucleosome assembly. However, I was not able to determine why nearly native ubiquitylated octamers behaved differently from ssUb octamers in these assemblies.

Anticipating the disulfide linkage in the ssUb nucleosomes could present challenges for biochemical studies given the frequent necessity of reducing conditions for enzymatic activity, I performed a titration with dithiothreitol (DTT) to ascertain whether there are low concentrations of reducing agent that would leave the histone-ubiquitin disulfide bond appreciably intact (Figure 2.11). However, even at 5 μM DTT, the mobility of H2AssUb and H2BssUb nucleosomes on native PAGE gels indicated partial disulfide reduction. Additionally, H2AssUb mononucleosomes were found to be approximately 3 times more sensitive to DTT than their H2BssUb counterparts. This is reminiscent of the differential accessibility of H2AK1119ub and H2BK120ub to trypsin: H2AK119ub in endogenous chromatin is trypsin sensitive while H2BK120ub is resistant (Bohm et al., 1982; Bohm et al., 1980).

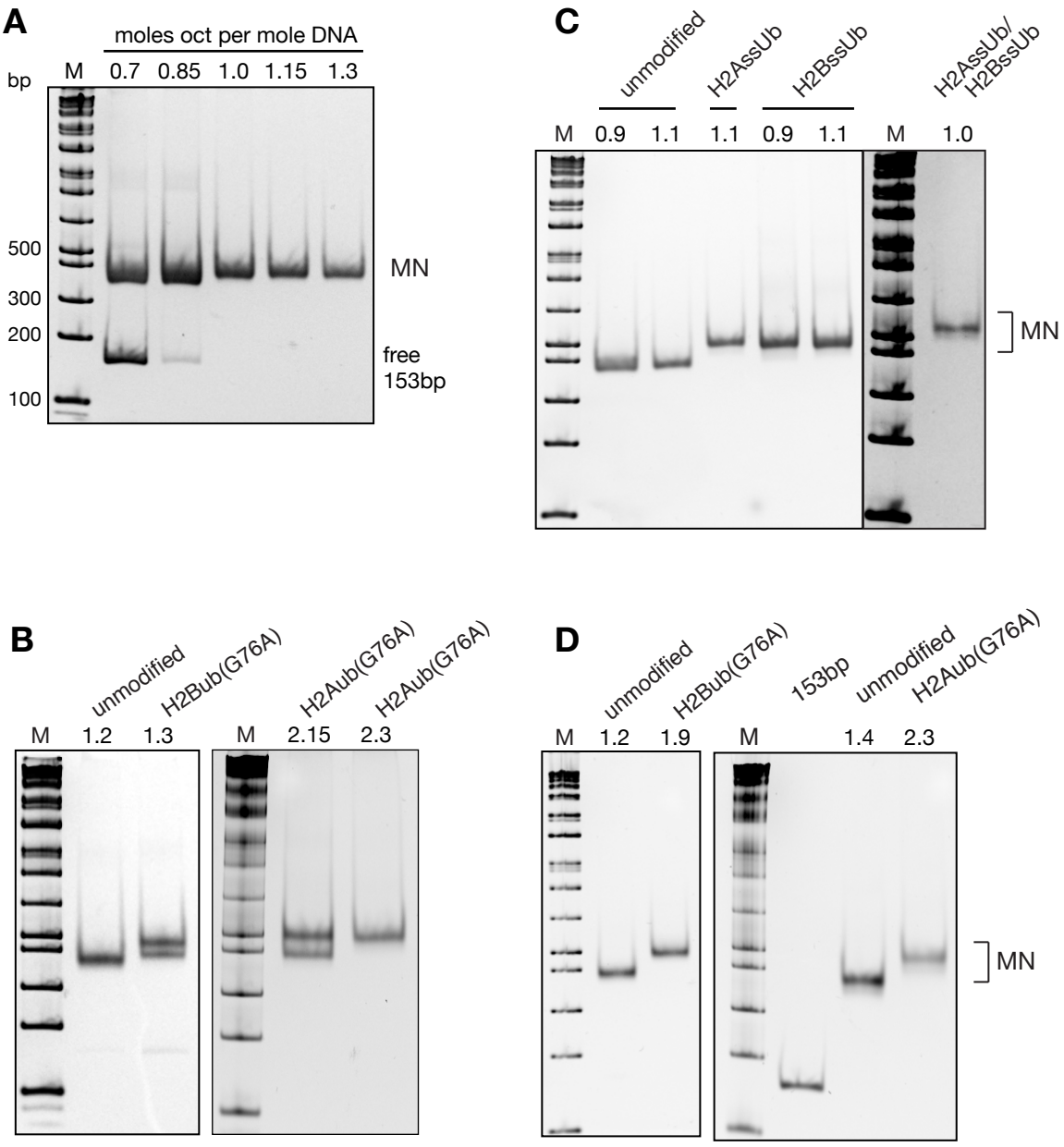

Figure 2.10 Designer mononucleosomes. "Designer" octamers were assembled into mononucleosomes with 153 bp (601) positioning sequence DNA. Mononucleosome (MN) assembly quality was assessed by native 5% PAGE and EtBr staining. 1 kb plus ladder (M) from NEB. Numbers above lanes are molar ratios of octamers : DNA used in nucleosome assembly. A) titration of octamers (oct) to DNA. B) relatively high ratios of nearly native ubiquitylated octamers are required for high quality mononucleosome assemblies, see text. C-D) Representative nucleosome assemblies of high quality are shown.

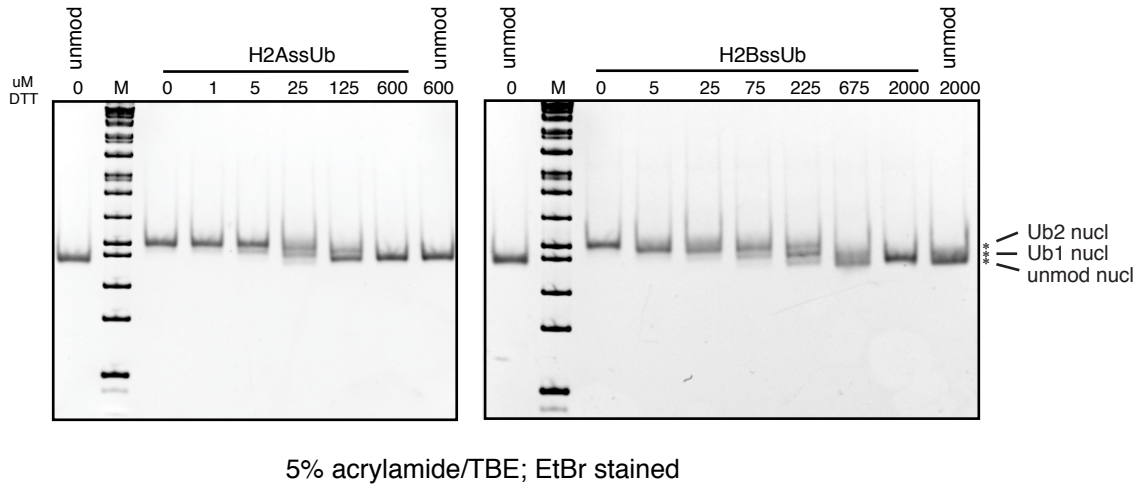

Figure 2.11 Characterization of sensitivity of ssUb nucleosomes to reducing agents. H2AssUb and H2BssUb mononucleosome assemblies were adjusted to the indicated dithiothreitol (DTT) concentrations and incubated at 37° C for 3 hours before separation on native 5% polyacrylamide gels. The gels were stained with EtBr to assess the stability of the disulfide bond between histone and ubiquitin. Unmodified human nucleosomes were used as a marker for where de-ubiquitylated ssUb nucleosomes should migrate.

2.6 Endogenous HeLa nucleosomes

To complement the designer ubiquitylated mononucleosomes described above, endogenous nucleosomes were purified from HeLa cells. With only minor alterations to a published protocol (Fang et al., 2004), pools of native nucleosomes of differing array lengths were isolated (Figure 2.12). It seems likely that these different pools of nucleosomes, with different MNase digestion properties, may represent biochemically and perhaps physiologically different chromatin domains. Western blotting revealed that acetylation and methylation PTMs were well preserved through the isolation and purification procedure, however, the bulk of ubiquitylation on H2A and H2B was lost, presumably due to residual ubiquitin isopeptidase activity in the chromatin extracts.

Briefly, HeLa nuclei were prepared by detergent cell lysis and mild douncing. Nuclei were subjected to relatively mild MNase digestion, and most non-histone proteins were stripped off MNase solubilized chromatin with 750 mM NaCl. Solubilized chromatin fragments of variable length were fractionated on a linear 5-30% sucrose gradient with ultracentrifugation. Fractions near the top of the gradient contain mononucleosomes and fractions near the bottom of the gradient contain long oligonucleosome arrays, with intermediary length arrays concentrated in the middle fractions (Figure 2.12A). In addition to fractionating based on chromatin fragment length, these gradients also separated nucleosome-associated proteins from nucleosomal histones. Fractions in lower part of the gradient contain virtually no detectable protein besides core histones, but fractions near the top of the gradient contain significant quantities of contaminating proteins (Figure 2.12B). "Relatively clean" oligonucleosome fractions were pooled and split in half. One half was subjected to additional mild MNase digestion (to generate mono, di and tri nucleosomes), and then both halves were purified and fractionated again on 5-30% sucrose gradients. Finally, gradient fractions were pooled according to array length (Figure 2.12C). Coomassie staining of these pools revealed them to be nearly devoid of non-histone proteins (Figure 2.12D).

These endogenous nucleosome pools, with relatively native and complex PTM profiles, provide substrates for enzymatic crosstalk experiments that are complimentary to the chemically defined designer mononucleosomes described above. Further, their ease of preparation allowed for many pilot experiments before using the more precious designer mononucleosomes.

Figure 2.12 Preparation of endogenous nucleosomes from HeLa cells. MNase solubilized and salt extracted HeLa chromatin can be fractionated over linear sucrose gradients to yield nucleosome fractions that can be pooled based on nucleosome array length. A-B) after one round of MNase digest and sucrose gradient purification, fractions containing oligonucleosomes and relatively free of non-histone proteins were pooled. C-D) a portion of these pooled oligonucleosomes was digested further with MNase, before a second round of purification and fractionation on sucrose gradients. Final nucleosome fractions were pooled based on nucleosome array length (into a – f) and the absence of detectable non-histone proteins was confirmed by SDS-PAGE electrophoresis and Coomassie staining.

Figure 2.12

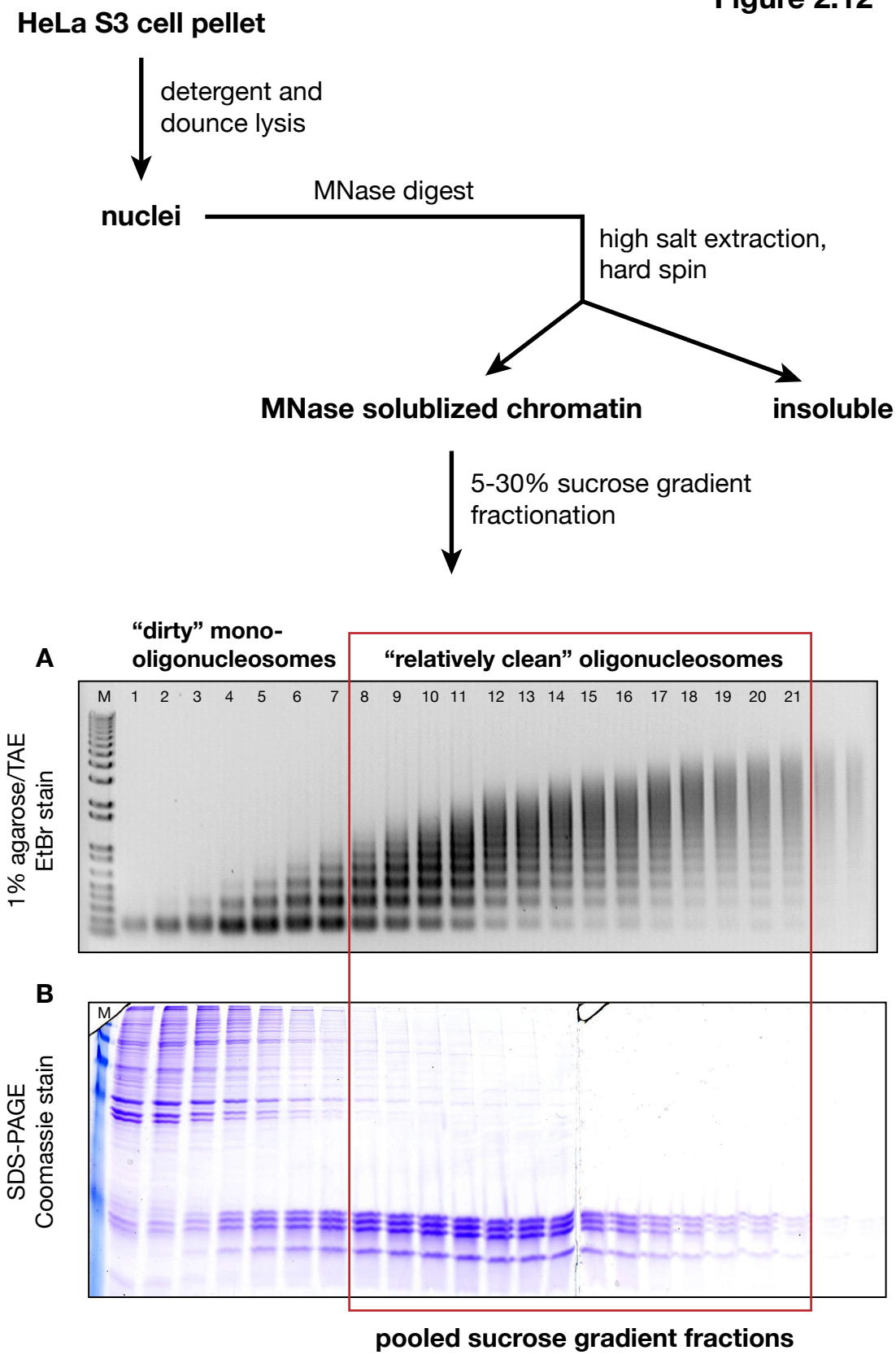
HeLa S3 cell pellet
detergent and
dounce lysis
nuclei
MNase digest
high salt extraction,
hard spin
MNase solublized chromatin
insoluble
5-30% sucrose gradient
fractionation
A
"dirty" mono-
oligonucleosomes
"relatively clean" oligonucleosomes
M 1 2 3 4 5 6 7 8 9 10 11 12 13 14 15 16 17 18 19 20 21
1% agarose/TAE
EtBr stain
B
M
SDS-PAGE
Coomassie stain
pooled sucrose gradient fractions

Figure 2.12

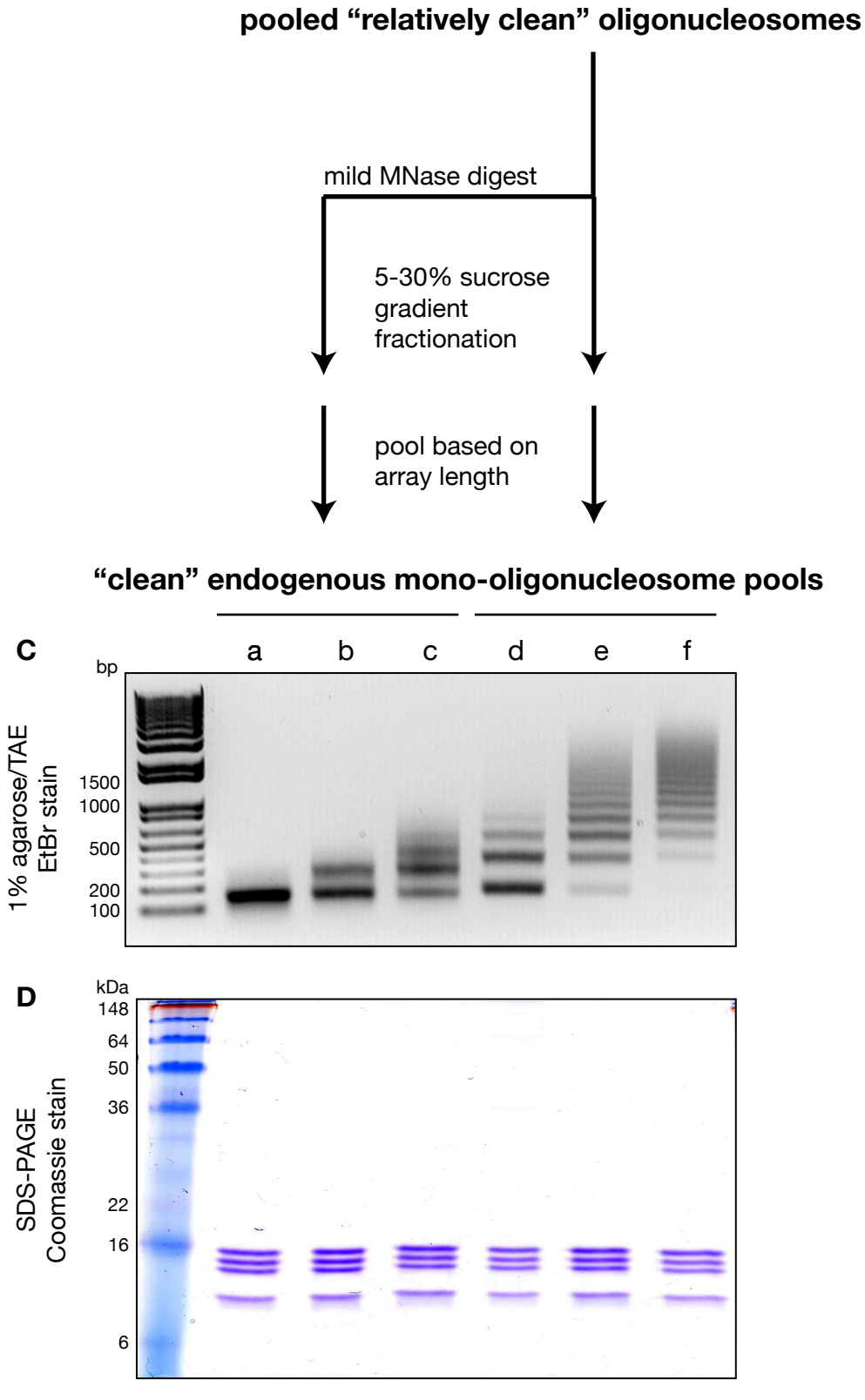
pooled “relatively clean” oligonucleosomes
mild MNase digest
5-30% sucrose gradient fractionation
pool based on array length
“clean” endogenous mono-oligonucleosome pools
C
a
b
c
d
e
f
bp
1% agarose/TAE
EtBr stain
1500
1000
500
200
100
D
kDa
148
64
50
36
22
16
6
SDS-PAGE
Coomassie stain

CHAPTER 3: SPECIFICITY OF ENZYMATIC CROSSTALK BETWEEN HISTONE UBIQUITYLATION AND H3K79 METHYLATION

One of the key outstanding questions in chromatin biology is how histone PTMs are coordinately regulated to generate meaningful combinations of "marks" at physiologically appropriate genomic locations. One important mechanism is "crosstalk" between pre-existing histone PTMs and enzymes that add or remove subsequent modifications on chromatin. Dot1 methyltransferase for H3K79 is one such enzyme whose activity is sensitive to the presence of pre-existing PTMs on its nucleosomal substrate (Figure 3.1). The set of designer ubiquitylated and endogenous nucleosomes prepared in Chapter 2 allowed me to do a series of *in vitro* enzymatic assays to investigate the specificity and plasticity of crosstalk between H2BK120ub, H2AK119ub, and H3K79me.

3.1 Dot1, evolutionarily conserved methyltransferase for H3K79

Dot1 is an evolutionarily conserved methyltransferase specific for K79 in histone H3 (Feng et al., 2002; Lacoste et al., 2002; Ng et al., 2002a; van Leeuwen et al., 2002). Dot1 family MTases are is critical for telomeric maintenance, DNA damage response, and many developmental processes including embryogenesis (Jones et al., 2008), hematopoeisis and leukemia (Feng et al., 2010), and cardiac development (Nguyen et al., 2011). Therefore, understanding how Dot1 activity is regulated is an important question to be addressed.

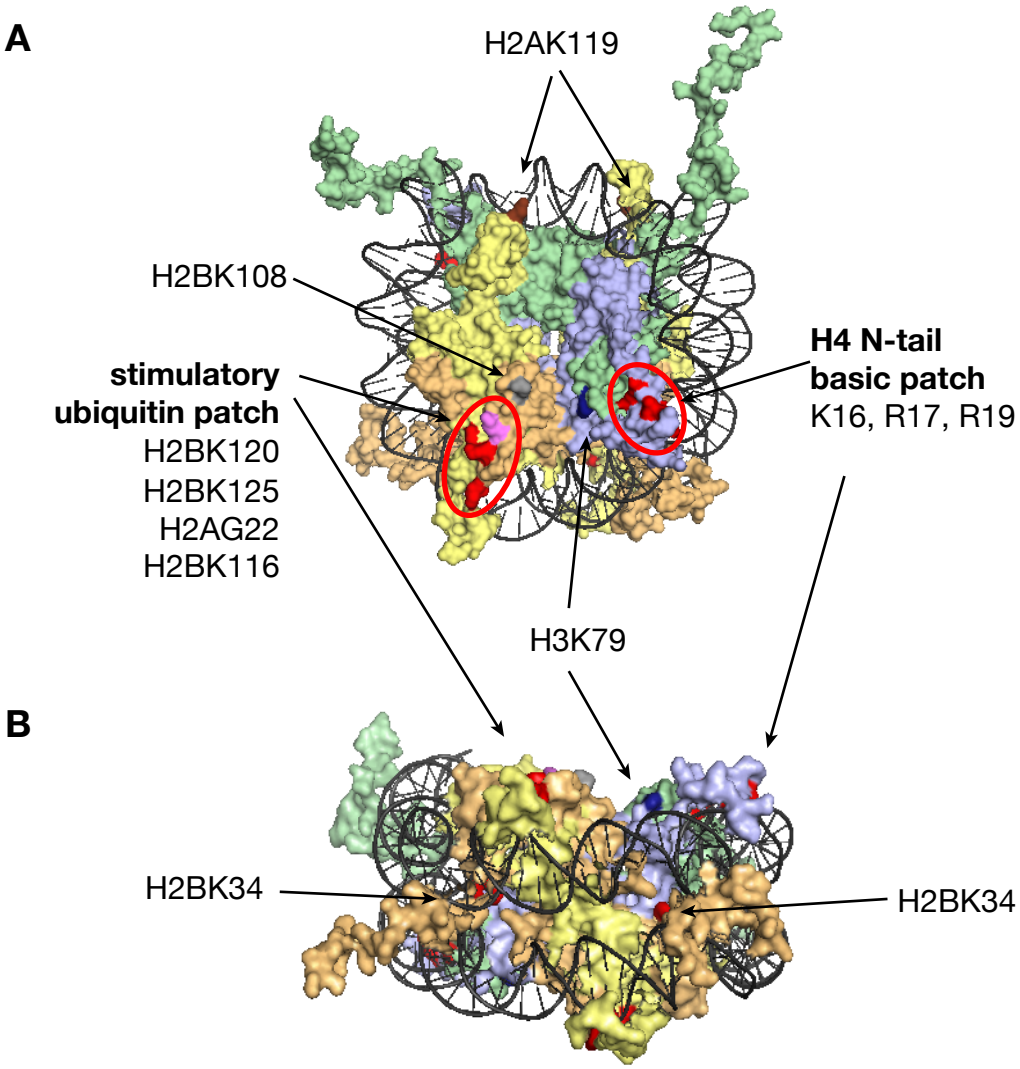

Figure 3.1 Histone features that affect Dot1 methyltransferase activity in their nucleosomal context. Surface rendition of mononucleosome structure, Protein Data Bank code 1KX5. A) axial view, B) radial view. DNA is colored in black and the histones H3, H4, H2A, and H2B are colored green, lavender, yellow, and orange respectively. The Dot1 methylation site, H3K79, is colored in dark blue. Two patches of amino acid residues are circled in red, the "H4 N-tail basic patch" and the stimulatory ubiquitin patch. H4 K16, R17 and R19 are colored in red because they are critical for Dot1 activity towards H3K79. Similarly, within the "stimulatory ubiquitin patch", positions that when ubiquitylated strongly stimulate Dot1 activity are colored in red. Ubiquitylation at H2BK116 only moderately stimulates Dot1 and is colored in pink. Outside of the stimulatory patch, H2BK108 is colored in grey because ubiquitylation at this position does not stimulate Dot1 activity. H2AK119, located at the opposite side of the nucleosome axial face is colored in brown. H2BK34, located between DNA gyres, is colored in red as ubiquitylation at this site greatly stimulates Dot1 methyltransferase activity.

The yeast yDot1p and human hDot1L have been most extensively studied, and they share a strongly conserved catalytic core, but outside of this relatively small region of homology, their protein sequences differ significantly, as highlighted in Figure 3.2. Most obviously, hDot1L is approximately 3 times larger in size than yDot1p. Secondly, the position of the only other annotated region, the lysine rich region, relative to the methyltransferase domain differs between yDot1p and hDot1L. These structural differences in the polypeptides may contribute to differences in regulation of yDot1p and hDot1L's shared catalytic activity.

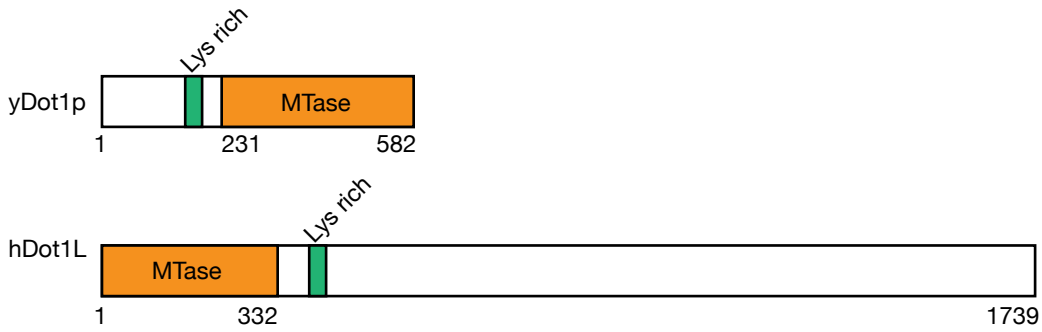

Figure 3.2 Domain structure of yeast and human Dot1 methyltransferase. The domain structure of yDot1p (Q04089) and hDot1L (Q8TEK3) are represented. Methyltransferase domains, highly conserved between the yeast and the human proteins, are shown in orange (MTase). Lysine rich regions, ~ 65 amino acids in length, are indicated in green. Amino acid positions are indicated below.

The *in vivo* steady state levels of K79 unmodified, monomethyl (me1), dimethyl (me2), and trimethyl (me3) differ greatly between yeast and human cells. Approximately 90% of yeast H3 is methylated at K79, the majority of which is in the trimethylated state (Garcia et al., 2007; van Leeuwen et al., 2002). Whereas, in mouse and human cells only

about 50% of H3K79 is methylated, with monomethyl being the predominant state and trimethylation being undetectable by mass spectrometry (Garcia et al., 2007). Whether or not these differences in steady state levels are due to intrinsic differences in Dot1 enzymatic activity, differential regulation *in vivo*, or to differential activity of yet to be discovered demethylation machinery *in vivo* is not known at this time.

3.2 DNA binding is critical for Dot1 methyltransferase activity

As mentioned above, both yeast and human Dot1 proteins contain an unstructured, highly basic patch, rich in lysines and arginines, either N-terminal to (in the case of yDot1p) or C-terminal to (in the case of hDot1L) the methyltransferase domain. There is little sequence conservation between these regions, but their importance for DNA binding and catalytic activity is conserved. Specifically, this region is essential for enzymatic activity (Feng et al., 2002; Min et al., 2003; Sawada et al., 2004). Even a 17 amino acid deletion (removing 9 of the 15 positive charges in this basic region) is sufficient to very strongly repress catalytic activity (Min et al., 2003). Gel shift experiments with Dot1 protein mutants and mononucleosomes, suggested that this same basic region of Dot1 is necessary for DNA binding, thereby conferring intrinsic nucleosome binding activity to the yeast Dot1p (Sawada et al., 2004). Further, Dot1 does not methylate H3 unless in the context of chromatin or nucleosomes (Feng et al., 2002; van Leeuwen et al., 2002). This data suggests that the lysine-rich region is necessary for catalytic activity because of its role in substrate binding. However, the defect in catalytic activity of yDot1p missing this lysine rich region can be nearly rescued by pre-incubation

with short pieces of DNA (30-150 bp) (Sawada et al., 2004), suggesting that the role of this lysine rich region and DNA binding is more complicated than simple recruitment.

3.3 Indirect *in vivo* crosstalk between H4K16Ac and H3K79methylation

In addition to intrinsic DNA binding activity, Dot1 methylation activity also requires binding to a basic patch in the H4 N-terminal tail (y16-20) (Altaf et al., 2007), located very close to H3K79 on the axial surface of the nucleosome (Luger et al., 1997) (Figure 3.1). It is tempting to speculate that the function of this interaction is to correctly position Dot1 for methylation of H3K79. Binding to this region of the H4 tail is exquisitely sensitive to the charge state at position R17 and R19, but is unaffected by acetylation (removal of positive charge) on K16. In contrast to the *in vitro* results, H4K16 acetylation *in vivo* facilitates H3K79me by disrupting the binding of heterochromatic protein Sir3, which competes with Dot1 for binding to the nucleosome (Altaf et al., 2007). Therefore, *in vivo* H4K16Ac participates in indirect crosstalk with H3K79methylation.

3.4 Direct Enzymatic crosstalk between H2Bub and H3K79methylation

In landmark papers for trans-histone tail crosstalk, monoubiquitylation of H2BK120 was shown to be an *in vivo* requisite for methylation of H3K79 (Briggs et al., 2002; Ng et al., 2002b; Sun and Allis, 2002). Although crucial first steps, these yeast genetic studies were not able to rule out indirect effects as the cause of the observed striking ubiquitin-methylation crosstalk. However, subsequent work by McGinty and colleagues using semi-synthetic H2Bub incorporated into designer nucleosomes and

purified enzyme, showed that H2Bub directly stimulates Dot1L methylation of H3K79 (McGinty et al., 2008). Dot1L binding to nucleosomes was not shown to be sensitive to the presence of H2Bub (McGinty et al., 2008; McGinty et al., 2009b), arguing against a simple recruitment function for H2Bub in the stimulatory crosstalk.

3.5 Preparation of recombinant hDot1L methyltransferase

Interested in exploring mechanism of ubiquitin-mediated modulation of Dot1 activity, I took an *in vitro* approach using recombinant Dot1 and the designer mononucleosomes described in Chapter 2. Aware of the potential differences in regulation of yDot1p and hDot1L, I chose not to mix organisms and used recombinant human Dot1L as well as nucleosomes of human origin, either assembled from recombinant/designer human histones or purified from the human cell line, HeLa.

Full-length human Dot1L protein was over-expressed in insect cells and purified (Figure 3.3). Briefly, soluble FLAG-hDot1L was affinity purified with M2 resin and eluted with multiple rounds of incubation with excess 3xFLAG peptide. Elutions were pooled. Although degradation products were detectable by Coomassie staining and M2 western blotting, the quality of the prep (in terms of integrity of full length Dot1L) was comparable to those regularly obtained by members of the Muir laboratory. Purified methyltransferase was sufficiently active to use at 1 mole enzyme : 30 moles nucleosomal substrate in the following experiments.

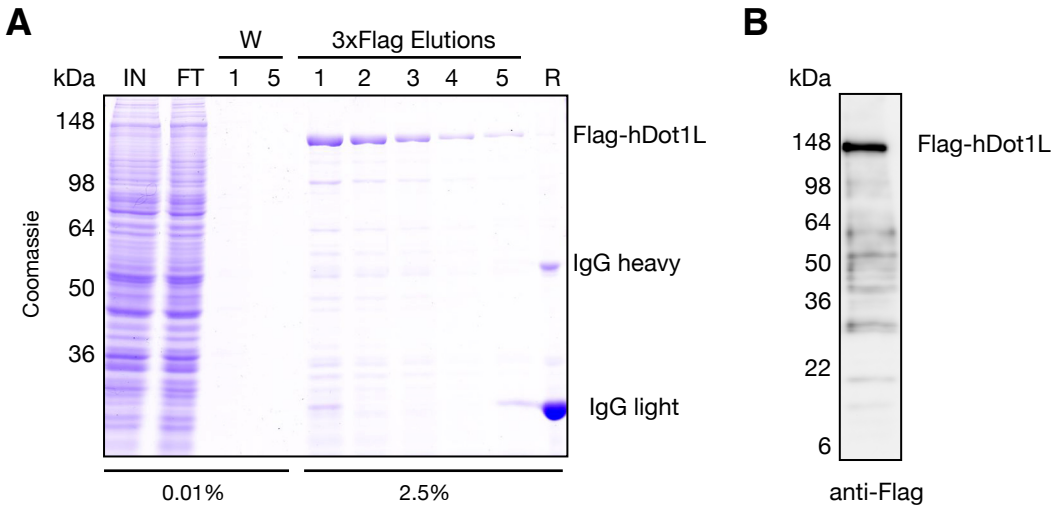

Figure 3.3 Purification of recombinant Flag-hDot1L. Flag-hDot1L was expressed and purified from baculovirus infected Sf9 cells. A) Coomassie stained SDS-PAGE gel of samples from the purification procedure. Flag-hDot1L was purified from soluble cell lysate with M2 anti-FLAG affinity resin and serially eluted with 3xFLAG peptide. B) Elutions 1-5 were pooled and western blotted with M2 antibody to confirm the major band as Flag-hDot1L. Lanes are labeled: soluble cell lysate (IN), M2 resin flow through (FT), washes 1, 5 (W), M2 resin after elutions (R).

3.6 Ubiquitin stimulates Dot1L activity *in cis*

I asked whether free ubiquitin could affect HMTase activity in trans. Dot1L binding of free ubiquitin could stimulate activity on unmodified nucleosomes (if ubiquitin functions allosterically) or could inhibit activity by competing with nucleosomes for binding of Dot1L. However, I found that neither 2 nor 20 molar equivalents (to nucleosomal substrates) of free ubiquitin had any significant impact on Dot1L HMTase activity on mononucleosomes purified from HeLa cells (Figure 3.4), similar to the findings of others (McGinty et al., 2008). In further support of this result, Chatterjee and colleagues used a modified ubiquitin moiety containing a variable length

glycine linker to show that the native distance between the globular fold of ubiquitin and the nucleosomal surface was optimal for Dot1L stimulation (Chatterjee et al., 2010).

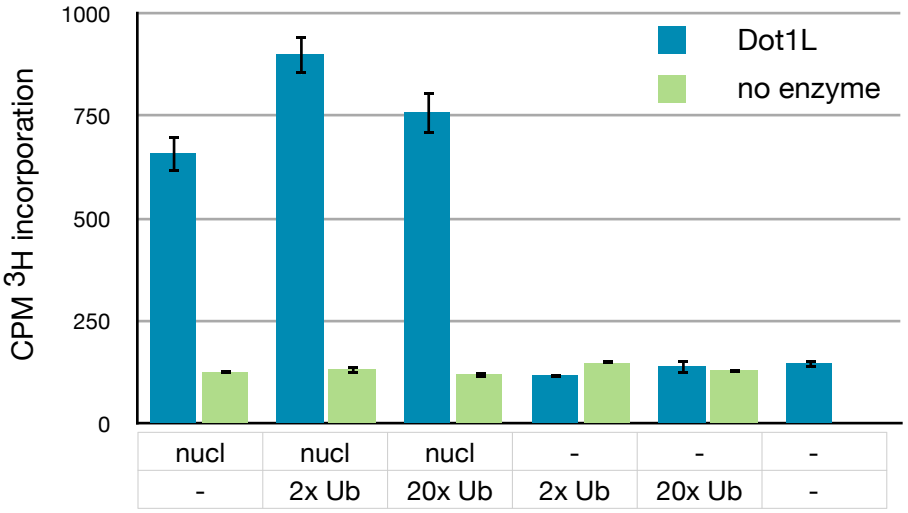

Figure 3.4 Ubiquitin does not stimulate Dot1L activity in *trans*. MTase reactions were assembled with Flag-hDot1L, HeLa nucleosomes and soluble ubiquitin, as indicated. Soluble ubiquitin was either absent from the reaction or added in 2x or 20x nucleosome molar equivalents. Methyltransferase activity was quantitated by filter binding and scintillation counting of incorporated 3H-CH3. Error bars represent the standard deviation of replicate scintillation counts.

3.7 Histone ubiquitylation positional plasticity in Dot1L MTase stimulation

Interested in investigating the specificity/plasticity of monoubiquitylation stimulated Dot1L activity, and guided by atomic level structural knowledge of the nucleosome (Luger et al., 1997), Chatterjee et al. used lysine to cysteine mutagenesis of histone sequences and disulfide-directed monoubiquitylation to move the ubiquitylation site around on the axial surface of the nucleosome (Chatterjee et al., 2010). This panel of monoubiquitylated nucleosome was used as substrates for Dot1L MTase assays to query the spatial and sequence specificity of ubiquitin stimulation of Dot1L. Specifically,

ubiquitin was attached at position G22 of H2A, and K116, 125, and 108 of H2B (in order of increasing distance from the native H2BK120 site. Of these positional isomers, only attachment at position 108 of H2B failed to stimulate HMTase activity. This analysis revealed that Dot1L stimulation does not strictly depend on the sequence surrounding the ubiquitylation site or the precise position of the attachment on the nucleosomal surface. However, not all ubiquitylation sites were equally stimulatory. In fact, despite being extremely close to the native attachment site, ubiquitylation at H2BK116 was only moderately stimulatory. Notably, nucleosomes assembled with the weakest stimulators (ubiquitylation at K108 and K116 of H2B) also migrated faster than the others in the panel on native gel electrophoresis. This suggests that the precise ubiquitin attachment site may influence the surface-charge or nucleosome structure, characteristics which may also affect the ubiquitylated nucleosome's ability to stimulate Dot1L HMTase activity.

Additionally, disulfide-directed and expressed protein ligation approaches were used to incorporate structural relatives of ubiquitin, Smt3, Nedd8, and Hub1, at H2BK120 and compared the ability of these modifications to mimic the stimulatory effect of H2BK120ub on Dot1L activity. Neddylation at H2B position 120 could fully substitute for ubiquitylation at the same position. However, Smt3 and Hub1were not able to stimulate Dot1L activity (Chatterjee et al., 2010; McGinty et al., 2009b). These results raised the possibility, that it is not merely the general size and fold of monoubiquitin that stimulates Dot1, but that the crosstalk is sensitive to specific structural or sequence elements on the surface of ubiquitin (and Nedd8) that are not mimicked in Hub1 or Smt3.

As valuable as these studies are to our understanding of Dot1L function, they utilize nucleosome substrates that have not been observed *in vivo*. However, very

recently, a novel H2B ubiquitylation site was discovered that also dramatically stimulates Dot1L activity *in vitro* and *in vivo* (Wu et al., 2011). This site, H2BK34, has additional interest because of its relatively great distance from H2BK120 and because rather than being solvent exposed on the axial surface of the nucleosome, it is located between the DNA gyres on the radial edge (Wu et al., 2011)(Figure 3.1). Taken together, these data reveal significant positional plasticity in the histone ubiquitylation site for enzymatic stimulation of Dot1.

The location of H2AK119ub, on the opposite end of the nucleosome axial face, and its approximately 10 times greater abundance *in vivo* relative to H2BK120ub, make H2Aub an interesting test case for the extent of Dot1L stimulation plasticity. Additionally, H2Bub and H2Aub are known to have opposite effects on methylation of H3K4 *in vitro* (Kim et al., 2009; Nakagawa et al., 2008), which begs the question whether a similar antagonism exists in regulating H3K79methylation.

3.8 Dot1L activity is stimulated by Mg^{2+} and insensitive to DTT

Putative H2Aub inhibition of Dot1L activity would be difficult to detect *in vitro* using published enzymatic assay conditions that have shown Dot1 activity on unmodified nucleosomes to nearly undetectable (Chatterjee et al., 2010; McGinty et al., 2008). In the course of this thesis work, various MTase reaction buffers were tried, and it was found that Dot1L *in vitro* activity is extremely sensitive to the concentration of the divalent cation, Mg^{2+} (Figure 3.5A). Even 1 mM Mg^{2+} is sufficient to increase Dot1 activity on unmodified nucleosomes by approximately 10 fold over activity at 0 mM. In the presence of Mg^{2+}, Dot1L activity is high enough to allow detection of H2Aub inhibition, if present.

Importantly, increased Mg^{2+} concentrations did not significantly change the strong substrate preference of Dot1 for H2Bub nucleosomes as compared to unmodified nucleosomes.

Before conducting crosstalk experiments between H2Aub and K79me, I first confirmed that Dot1L methyltransferase activity is undiminished in non-reducing conditions (Figure 3.5B). This characteristic of hDot1L activity allowed the use of ssUb nucleosomes described in Chapter 2 to rigorously test for potential crosstalk between H2Aub and H3K79methylation.

3.9 Use of ssUb nucleosomes to investigate potential crosstalk between H2Aub and Dot1L

Dot1L methyltransferase activity on unmodified mononucleosomes was compared to activity on 3 types of ubiquitylated nucleosomes: H2AssUb, H2BssUb, and H2AssUb/H2BssUb (nucleosomes containing both H2AssUb and H2BssUb). As previously reported (Chatterjee et al., 2010), H2BssUb greatly stimulates Dot1L activity on nucleosomal H3. However, H2AssUb has little appreciable impact on Dot1L activity relative to unmodified nucleosomes, and activity on H2AssUb/H2BssUb nucleosomes was comparable to that on H2BssUb nucleosomes (Figure 3.6). The precise extent of Dot1L stimulation by H2AssUb/H2BssUb nucleosomes varied between experiments more than other substrate types, in some cases being slightly more stimulating to Dot1L than H2BssUb alone, and in some cases being slightly less stimulating, as shown. Based on these experiments I conclude that H2Aub does not influence Dot1L HMTase activity *in vitro*.

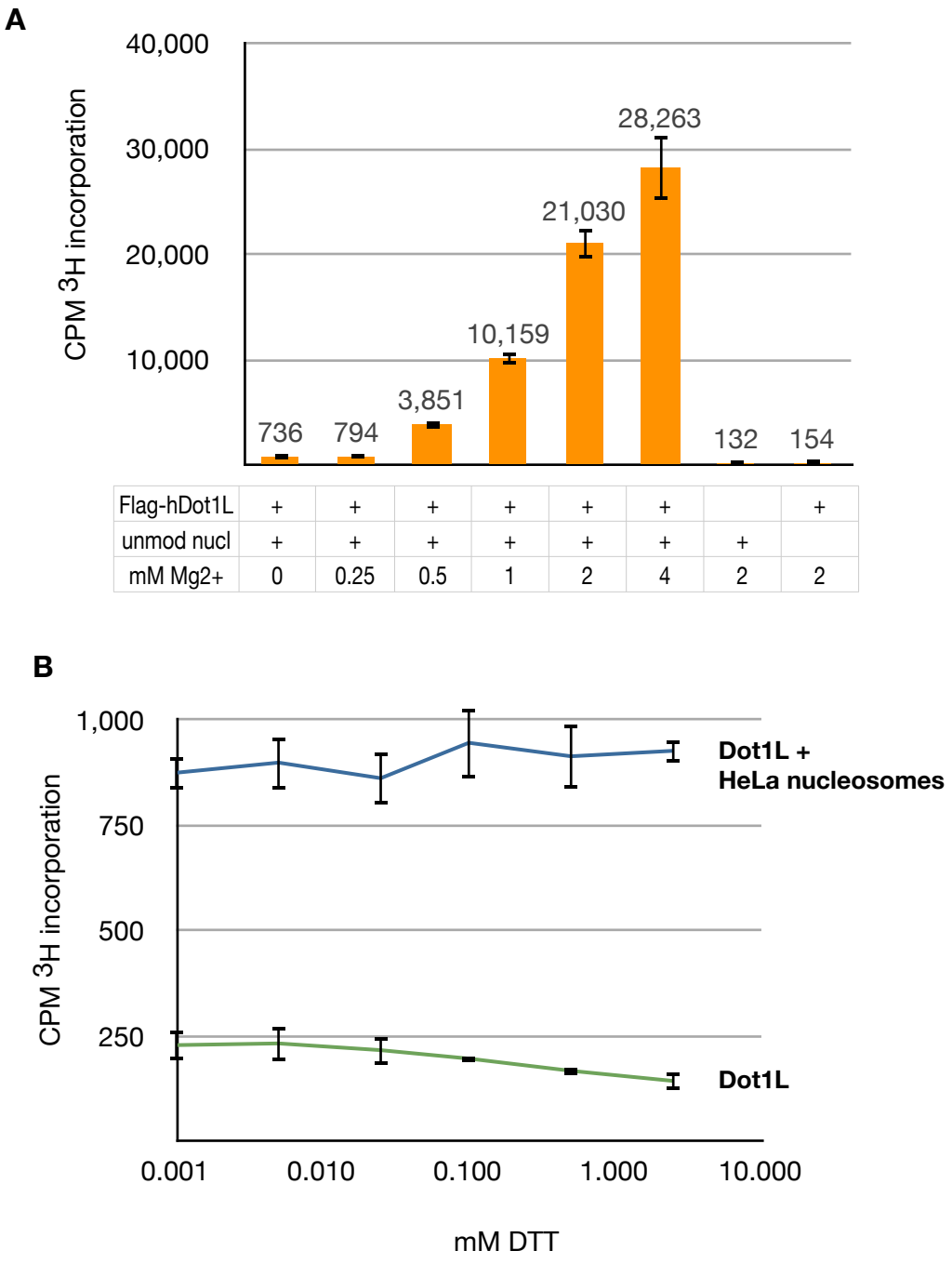

Figure 3.5 Dot1L activity is stimulated by Mg2+ and insensitive to reducing agent concentration. A) Mg2+ titration of Dot1L methyltransferase activity on unmodified mononucleosomes. B) DTT titration of Dot1L methyltransferase activity on HeLa nucleosomes (blue) or without nucleosome substrates (green). Methyltransferase activity was quantitated by filter binding and scintillation counting of incorporated 3H-CH3. Error bars represent the standard deviation of replicate scintillation counts.

Figure 3.6 Presence of H2Aub in mononucleosomes does not affect Dot1L MTase activity. Dot1L activity was tested on human unmodified and "ssUb" mononucleosomes as indicated. ¾ of each reaction was separated by SDS-PAGE and Coomassie stained (A) and activity was assessed by fluorography (B). Activity was also assessed by filter binding and scintillation counting of ¼ of each reaction (C). Error bars indicate the standard deviation of replicate scintillation counts of the same filter paper. The asterisk above the rightmost bar indicates an atypically high (~ 5x greater than normal) scintillation count due to a technical artifact and is not from Dot1L self-methylation activity. Note that the same sample produced no detectable fluorography signal (B).

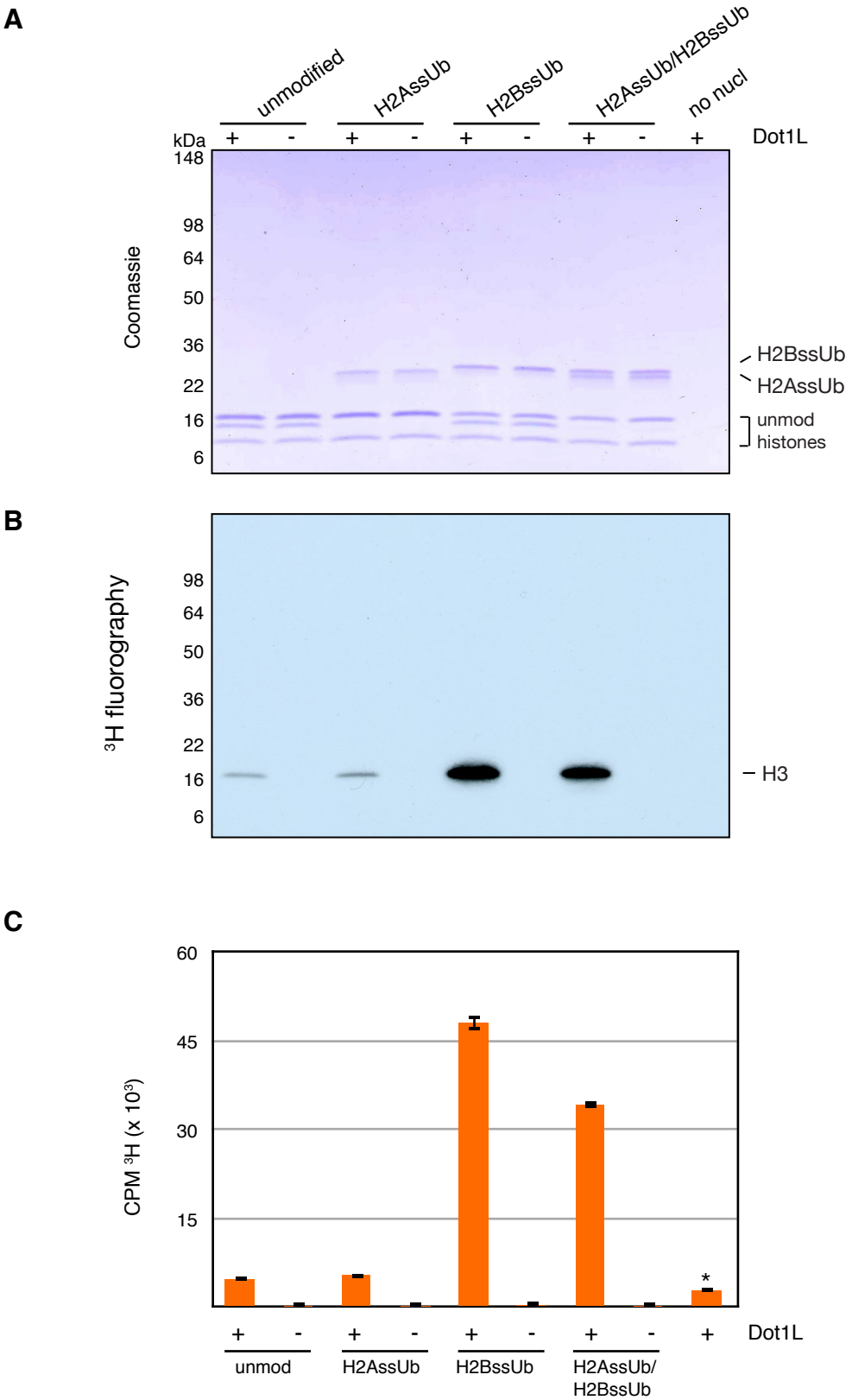
A
unmodified
H2AssUb
H2BssUb
H2AssUb/H2BssUb
no nucl
kDa
+ - + - + - + - +
Dot1L
148
98
64
50
36
22
16
6
Coomassie
H2BssUb
H2AssUb
unmod
histones
B
98
64
50
36
22
16
6
3H fluorography
H3
C
60
45
30
15
CPM 3H (x 10^3)
*
+ - + - + - + - +
Dot1L
unmod
H2AssUb
H2BssUb
H2AssUb/
H2BssUb

Although others have shown that Dot1L can be stimulated by ubiquitylation at a variety of nucleosomal locations (Figure 3.1), under these assay conditions, plasticity of stimulation does not extend to H2Aub. However, two lines of evidence may have suggested that H2Aub would actually inhibit Dot1 activity: H2Aub and H2Bub have roughly antagonistic roles in transcriptional regulation (Chapter 1), and they have been shown to have opposite affects on the *in vitro* activity of methyltransferases for H3K4 (Kim et al., 2009; Nakagawa et al., 2008). Although H2Aub was found to neither activate nor repress Dot1L activity *in vitro*, the results presented here provide further evidence of differential function of H2Aub and H2Bub (Chapter 1).

CHAPTER 4: TESTING FOR CROSSTALK BETWEEN HISTONE UBIQUITYLATION AND H3K27 METHYLATION

In Chapter 3, experiments to investigate modulation of Dot1L H3K79 MTase activity by histone monoubiquitylation were presented. Previous studies had shown that Dot1 activity is stimulated by histone monoubiquitylation at a variety of positions on the nucleosome axial surface and even on the radial edge (Chatterjee et al., 2010; Wu et al., 2011). However, this plasticity of ubiquitylation position does not extend to H2AK119, as shown in Figure 3.6.

Here in Chapter 4, studies of potential crosstalk between histone ubiquitylation and histone methyltransferases were extended to the methyltransferase Polycomb Repressive Complex 2 (PRC2). Initially discovered as factors necessary for maintained transcriptional repression of developmentally regulated genes (Kennison, 1995), PRC2 is now known to be the multimeric protein complex responsible for H3K27 dimethylation and trimethylation *in vivo* (Cao et al., 2002). Numerous studies have shown PRC2-mediated transcriptional repression and H3K27 methylation to be involved in cellular differentiation, stem cell identity, X inactivation, cell-cycle regulation, and cancer (Margueron and Reinberg, 2011). Genes targeted by PRC2 have been mapped in a variety of cellular contexts, and in many cases these genes can be either methylated on H3K27, H3K4, or both, depending on the particular cellular/developmental context. In fact, it has been proposed that the balance between H3K4me2/3 and H3K27me2/3 may be an important mechanism of regulating transcription of many genes, particularly those involved in cellular differentiation programs (Schuettengruber et al., 2007).

Intriguingly, both H2Bub and H2Aub participate in direct enzymatic crosstalk with methyltransferases for H3K4, however in antagonistic directions: H2Bub is required for Set1-mediated methylation of H3K4 (Kim et al., 2009), while deubiquitylation of H2Aub is required for MLL3-mediated methylation of H3K4 (Nakagawa et al., 2008). Presented here in Chapter 4 are experiments to address whether the antagonistic crosstalk between H2Aub and H2Bub on methylation of H3K4 is mirrored in antagonistic crosstalk on PRC2-mediated methylation of H3K27 (Figure 4.1).

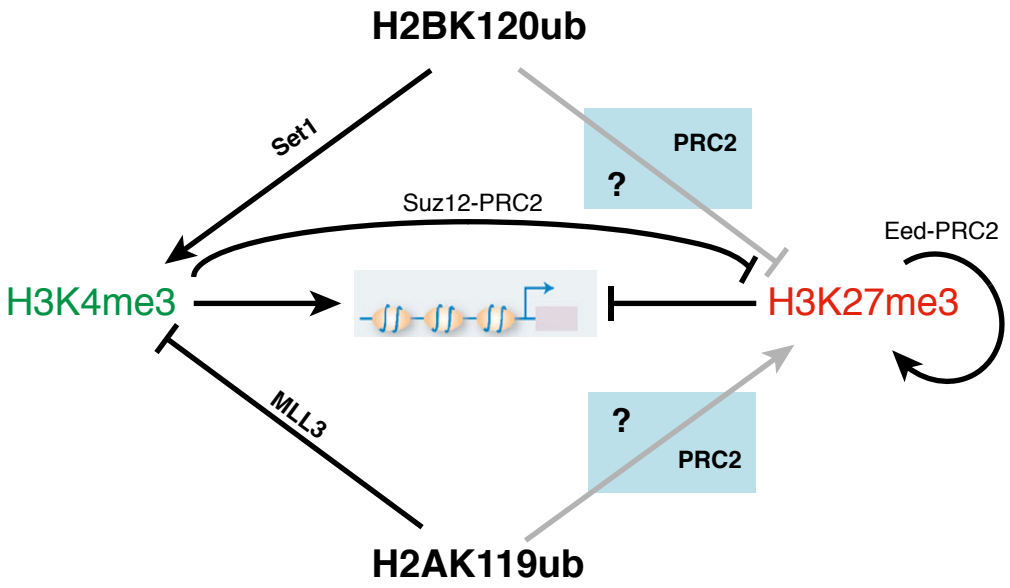

Figure 4.1 Putative antagonistic crosstalk of H2Aub and H2Bub on H3K27 methylation. Outlined are established and hypothesized crosstalk relationships between H2Bub, H2Aub, H3K4me3, and H3K27me3. Validated direct enzymatic crosstalk between H2Bub/H3K4me3, H2Aub/H3K4me3, H3K4me3/H3K27me3, and H3K27me3/H3K27me3 are shown with solid arrows and with the relevant methyltransferase indicated above. Note that H2Bub and H2Aub have opposing effects on H3K4 methylation *in vitro*. The regulation of transcription of a generic gene is located in the center, showing the opposing action of H3K4me3 and H3K27me3 in transcriptional regulation. Hypothesized crosstalk between H2Bub and H2Aub on PRC2-mediated H3K27 methylation is indicated with grey arrows and question marks.

4.1 Evolutionary conservation of Polycomb Repressive Complex 2

Genetic, biochemical, and bioinformatic approaches have identified and characterized PRC2 components in organisms as divergent as plants, *Drosophila*, and humans. Complexes purified from these diverse sources share H3K27-directed MTase and transcriptional repression activity (Hennig and Derkacheva, 2009). Although fungi might be expected to have PRC2 components given their common ancestor with plants and animals, PcG proteins have yet to be identified in unicellular fungi, such as yeast. However, *Neurospora crassa*, a filamentous fungus, has homologs of PRC2 components (Schuettengruber et al., 2007). Given that PcG proteins are critical for cellular differentiation, my colleagues and I speculated that genes for PRC2 components have been retained in *Neurospora* because they contribute to the multicellular developmental stages of this organism (Whitcomb et al., 2007).

4.2 Mammalian PRC2 core complex composition

PRC2 complexes have been isolated from a variety of cell culture systems revealing some diversity in composition. However, regardless of the details of complex purification, the core components present in mammalian PRC2 are Ezh2, Suz12, Eed, and RbAp46/48 (Cao et al., 2002; Kuzmichev et al., 2002) (Figure 4.2A).

Ezh2 is the catalytic component of mammalian PRC2 and its MTase activity is dependent upon the highly conserved SET domain (Chapter 1.2.2.1) (Cao et al., 2002; Muller et al., 2002) (Figure 4.2B). Over the approximately 800 million years since the divergence of our common ancestor, the human Ezh2 SET domain retained 86% amino acid sequence identity and 93% similarity with the SET domain of its *Drosophila*

homolog, E(z) (Whitcomb et al., 2007). Just N-terminal to the SET domain is another highly conserved region, called the Pre-SET domain. This cysteine-rich region is required for SET domain mediated methylation. Additionally, Ezh2 contains two SANT domains that are predicted to bind histone tails (Boyer et al., 2004).

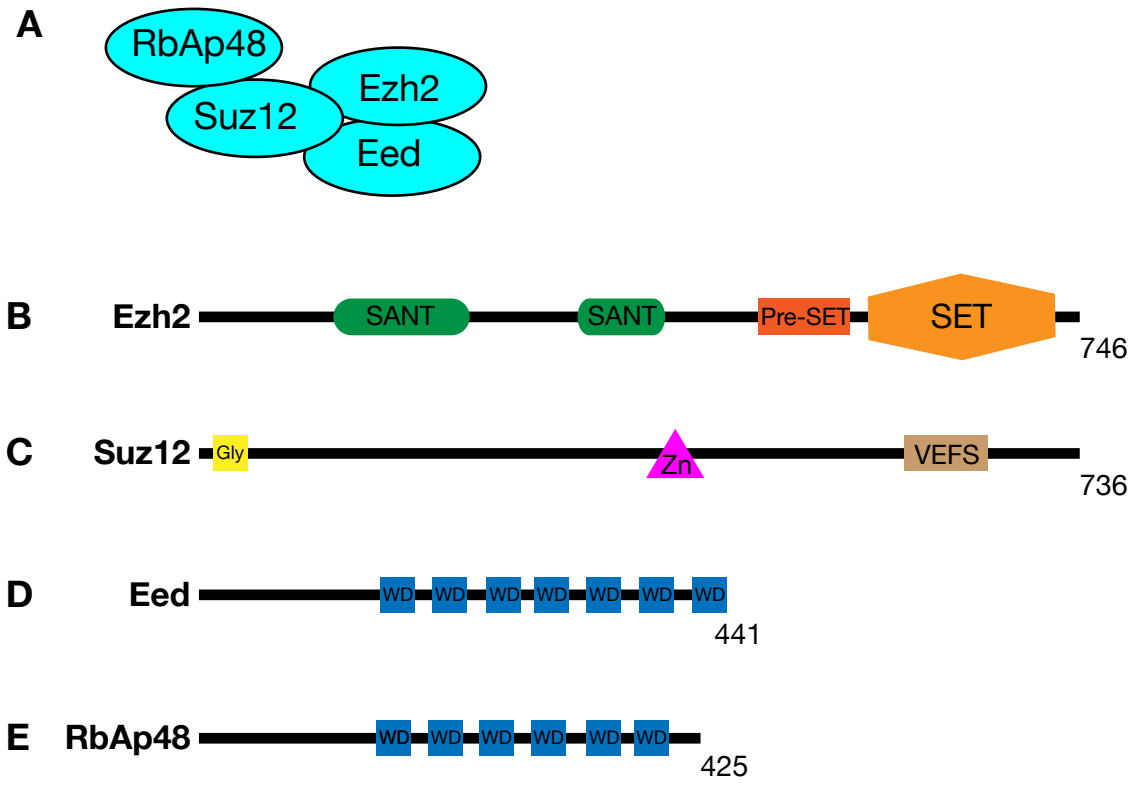

Figure 4.2 Mammalian PRC2 core complex composition. A) subunits of core mammalian PRC2 complex. Contacts shown do not necessarily represent those required for PRC2 complex assembly. B-E) domain structures of the four core members of mammalian PRC2. Numbers below each polypeptide indicate amino acid length. Methylation of H3K27 is mediated by the catalytic SET domain in Ezh2 (orange). Other domains and motifs described in the text are indicated: SANT (green), Pre-SET (dark orange), glycine-rich (yellow), C2H2 Zinc finger (pink), VEFS-box (khaki), and WD-40 repeats (blue).

Suz12 contains a classical C_2H_2 zinc finger domain similar to those found in sequence specific DNA binding proteins which likely contributes to PRC2 binding to nucleosomes (Birve et al., 2001; Nekrasov et al., 2005) (Figure 4.2C). At its N-terminus is a short glycine-rich region and at its C-terminus Suz12 has a so-called VEFS-box, named because this sequence is highly conserved between Suz12 and plant homologs VRN2, EMF2, and FIS2 (Birve et al., 2001). The VEFS-box is required for Suz12 interaction with Ezh2 (Ketel et al., 2005; Yamamoto et al., 2004).

Eed is a WD-40 repeat protein that folds into a 7-bladed β-propeller (Han et al., 2007) (Figure 4.2D). As is typical of WD-40 repeat proteins, the Eed β-propeller serves as a large protein-protein interaction surface, important for complex assembly. It is on one face of this propeller that Ezh2 binds. In the center of the Eed β-propeller donut-like structure, but on the opposite face from the Ezh2 interaction surface, is an aromatic cage capable of binding multiple histone peptides with methylated lysines. Although peptides for H1K26me3, H3K9me3, H3K27me3, and H4K20me3 all bind with similar affinities in the aromatic cage of Eed, methylated lysines associated with active transcription such as H3K4me3 (Bernstein et al., 2005; Santos-Rosa et al., 2002), H3K36me3, and H3K79me3 do not bind (Margueron et al., 2009). It seems that evolution of the Eed protein has selected for a β-propeller fold that selectively binds methylation states associated with repressed transcription and excludes methylated lysines associated with active transcription.

The final core member of mammalian PRC2 is RbAp46/48. Like Eed, it is a WD-40 repeat protein that folds into a 7-bladed β-propeller (Murzina et al., 2008) (Figure 4.2E). Recently it was shown that the β-propeller of the *Drosophila* RpAp46/48

homolog, Nurf55, binds unmodified H3 N-tail peptide but not the H3K4 trimethylated peptide (Schmitges et al., 2011). Although Nurf55 interaction with the H3 N-tail is not critical for PRC2 binding to nucleosomes (Schmitges et al., 2011), it appears to allosterically influence Ezh2 activity, as will be discussed below.

4.3 *In vitro* PRC2 HMTase activity

Ezh2 is inactive as a methyltransferase *in vitro* unless associated with other PRC2 complex members (Czermin et al., 2002; Muller et al., 2002). Eed and Suz12 are especially crucial for Ezh2 activity, both *in vitro* and *in vivo* (Cao and Zhang, 2004; Montgomery et al., 2005; Pasini et al., 2004), and the addition of RbAp48 to Ezh2-Eed-Suz12 further stimulates MTase activity (Cao and Zhang, 2004).

It was recently shown that when added in *trans*, H3K27me3 peptide, but not other methylated histone peptides, stimulates H3K27 methylation by PRC2 on nucleosomes (Margueron et al., 2009; Xu et al., 2010). This end-product (H3K27me3) stimulation of the enzyme (PRC2) was dependent upon amino acids in the Eed aromatic binding pocket for methylated lysines (see above). Given that H3K27me3 was provided as a peptide in *trans*, the stimulation is unlikely to be due to increased recruitment of PRC2 complex to nucleosomal substrates. The authors proposed an allosteric effect on Ezh2 MTase activity mediated by Eed-trimethylated lysine binding. If the role of H3K27me3 peptide in these experiments can be played by nucleosomal H3 tails carrying methylated K27, then perhaps these results point to a mechanism of H3K27methylation spreading *in vivo*.

Intriguingly, H3K4 methylation also can allosterically modulate PRC2 methyltransferase activity, although in the opposite direction of H3K27me3 (Schmitges

et al., 2011) (Figure 4.1). Pre-methylation of H3K4 inhibits subsequent methylation of K27 in the same H3 N-terminal tail (Schmitges et al., 2011). This presents an appealing model for how Eed-mediated H3K27methylation spreading is restricted from transcriptionally active genes.

4.4 Recombinant PRC2 complex preparation

Interested in exploring further how pre-existing histone PTMs, notably monoubiquitylation on H2A and H2B, might modulate PRC2 methyltransferase activity (Figure 4.1), I obtained recombinant PRC2 complex purified by Dr. Susan Wu, then a PhD student in the laboratory of Yi Zhang at the University of North Carolina. Briefly, Ezh2, FLAG-Eed, Suz12, and RbAp48 were co-expressed in Sf9 cells using a standard baculovirus expression system, purified using M2 anti-FLAG affinity resin, and eluted with 3xFLAG peptide. Eluates were pooled and PRC2 complex was purified away from incomplete complex and other contaminating proteins by size exclusion chromatography (Figure 4.3A).

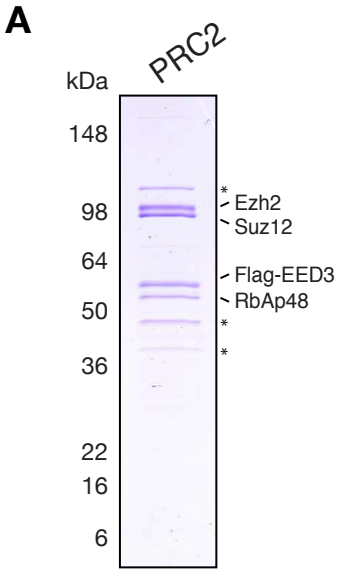

Figure 4.3 PRC2 activity is sensitive to the concentration of cations and reducing agents. A) Coomassie stained SDS-PAGE gel of reconstituted human PRC2 complex, courtesy of Dr. Wu. (*) denote contaminating proteins or proteolytic products. B-D) characterization of PRC2 methyltransferase sensitivity to the concentration of Mg^{2+}, Li^{+}, and reducing agents, as quantitated by scintillation counting of incorporated $^{3}H\text{-}CH_3$. Error bars represent the standard deviation of replicate scintillation counts. D) DTT titration of PRC2 methyltransferase activity on unmodified mononucleosomes (blue) or in the absence of nucleosomal substrates (green).

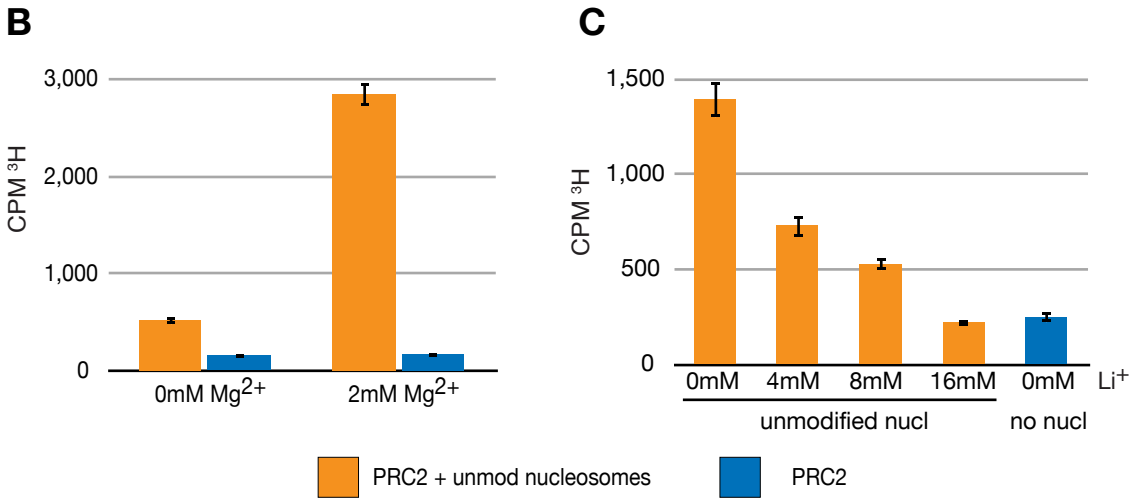

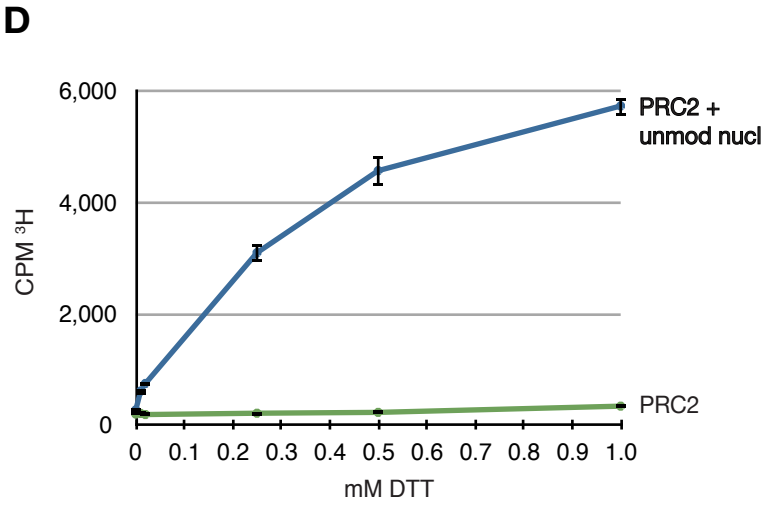

4.5 PRC2 activity is sensitive to the concentration of Mg^{2+}, Li^{+}, and reducing agents

Before beginning crosstalk studies I performed several experiments to characterize PRC2 activity on unmodified nucleosomes. Having observed that Dot1L MTase activity is strongly stimulated by Mg^{2+} (Figure 3.5A), I tested recombinant PRC2 complex for the same sensitivity. PRC2 activity was also found to be sensitive to the concentration of Mg^{2+}, although not as drastically as Dot1L (Figure 4.3B). PRC2 activity on unmodified mononucleosomes was approximately 6x higher at 2 mM Mg^{2+} than in the absence of Mg^{2+}. This increased activity was practically useful because it allowed the use of far less PRC2 complex per enzymatic activity assay. Contrary to the stimulatory effect Mg^{2+}, the monovalent cation Li^{+} has a strong inhibitory effect on PRC2 methyltransferase activity (Figure 4.3C). 16 mM Li^{+} is sufficient to depress PRC2 activity on unmodified mononucleosomes to background levels.

Thinking forward to potential crosstalk experiments using the designer ssUb nucleosome set described in Chapter 2, the sensitivity of PRC2 activity to the concentration of reducing agents needed to be critically assessed. Unlike Dot1L activity that showed essentially no sensitivity to reducing agent concentration (Figure 3.5B), PRC2 activity is strongly stimulated by DTT (Figure 4.3D). The drastically different behavior of Dot1L and PRC2 histone methyltransferases in the presence of reducing agents may be due to the presence of the cysteine-rich "pre-SET" domain (Figure 4.2) in Ezh2 but absence of a similar motif in Dot1L. In the absence of reducing agents, cysteines in this domain may form disulfide bonds that are unfavorable for SET domain catalytic activity or nucleosomal substrate binding. Unfortunately, at DTT concentrations

compatible with ssUb nucleosomes (0-10 μM), PRC2 activity is several orders of magnitude below maximal activity and very close to the background auto-methylation activity level. Thus, one unexpected challenge I confronted was the need to optimize PRC2 activity with reducing equivalents without altering the ubiquitin linkage of the H2Aub substrates being used in these crosstalk experiments (see below).

4.6 *In vitro* enzymatic ubiquitylation of H2A for PRC2 crosstalk studies[3]

Having found H2AssUb nucleosomes to be an unsuitable substrate for PRC2 assays (Figure 2.11, Figure 4.3D), and struggling to generate "nearly native" H2Aub (Chapter 2.2.1), I instead pursued *in vitro* enzymatic means to generate nucleosomes containing H2Aub. The Polycomb Repressive complex 1 (PRC1) protein Ring1B is the major E3 ligase for H2AK119ub *in vivo* and can efficiently ubiquitylate H2A *in vitro*. As for Ezh2, Ring1B catalytic activity is strongly enhanced by association with a Polycomb Repressive Complex member. A structural study suggested that fellow PRC1 member Bmi1 enhances Ring1B activity by stabilizing the interaction between the E2 ligase, Ring1B, and the substrate nucleosome (Li et al., 2006). Additionally, Bmi1 directs self-ubiquitylation of Ring1B in the form of atypical-mixed chains that are necessary for H2A monoubiquitylation activity (Ben-Saadon et al., 2006). For the following *in vitro* ubiquitylation reactions, full-length human Ring1B-6xHis and GST-Bmi1 proteins were co-expressed in *E. coli* and Ring1B/Bmi1 complex purified by tandem-affinity chromatography performed by Dr. Ronen Sadeh.

---

[3] The work in this section was performed with the collaboration of Dr. Ronen Sadeh in the Laboratory of Chromatin Biology and Epigenetics at The Rockefeller University.

In vitro ubiquitylation of nucleosomal H2A was performed with Ring1B/Bmi1 (E3), UbcH5c (E2), E1, monoubiquitin, and ATP. ATP can be purchased as a salt with several different cations, but for these studies only ATP-Mg was used to accommodate subsequent PRC2 activity assays (Figure 4.4A). Mg^{2+} has a stimulatory effect on PRC2 activity, while Li^{+} has an inhibitory effect (Figure 4.3B,C)

Briefly, designer nucleosomes of two types, either WT or with H2AK118,119 mutated to arginines (H2A_RR), were incubated with active (+ E1) or inactive (- E1) ubiquitylation machinery. Using active machinery, nearly all WT H2A is monoubiquitylated, while only trace amounts of H2A_RR was ubiquitylated (Figure 4.4B,C). Western blot analysis with an antibody specific for H2AK119ub confirmed that H2AK119 is the major ubiquitylation site using this *in vitro* enzymatic ubiquitylation set-up. To further confirm the site-specificity, mass spectrometry analysis was performed by Joe Fernandez at The Rockefeller University Proteomics Resource Center. This analysis confirmed that H2AK119 is the major ubiquitylation site, with some minor H2AK118 ubiquitylation, and trace amounts of H2AK36 and H2AK95 ubiquitylation.

Figure 4.4 H2A ubiquitin ligase machinery inhibits PRC2 MTase activity. In order to test for potential H2Aub crosstalk with PRC2, sequential ubiquitin ligase and methyltransferase reactions were performed on human WT or H2A_RR mononucleosomes. After completing both reaction steps, each sample was divided to assess H2A ubiquitylation and H3 methylation (A). B-D) ½ of each sample was used to assess Ring1B/Bmi1-mediated ubiquitin ligase activity by western blot. E) ¼ of each reaction was spotted onto P81 filter paper, washed and PRC2-mediated incorporated ^{3}H-CH_3 was quantitated by scintillation counting. F) PRC2-mediated methylation of H3 was also assessed by fluorography of ¼ of each sample separated on an SDS-PAGE gel.

Figure 4.4

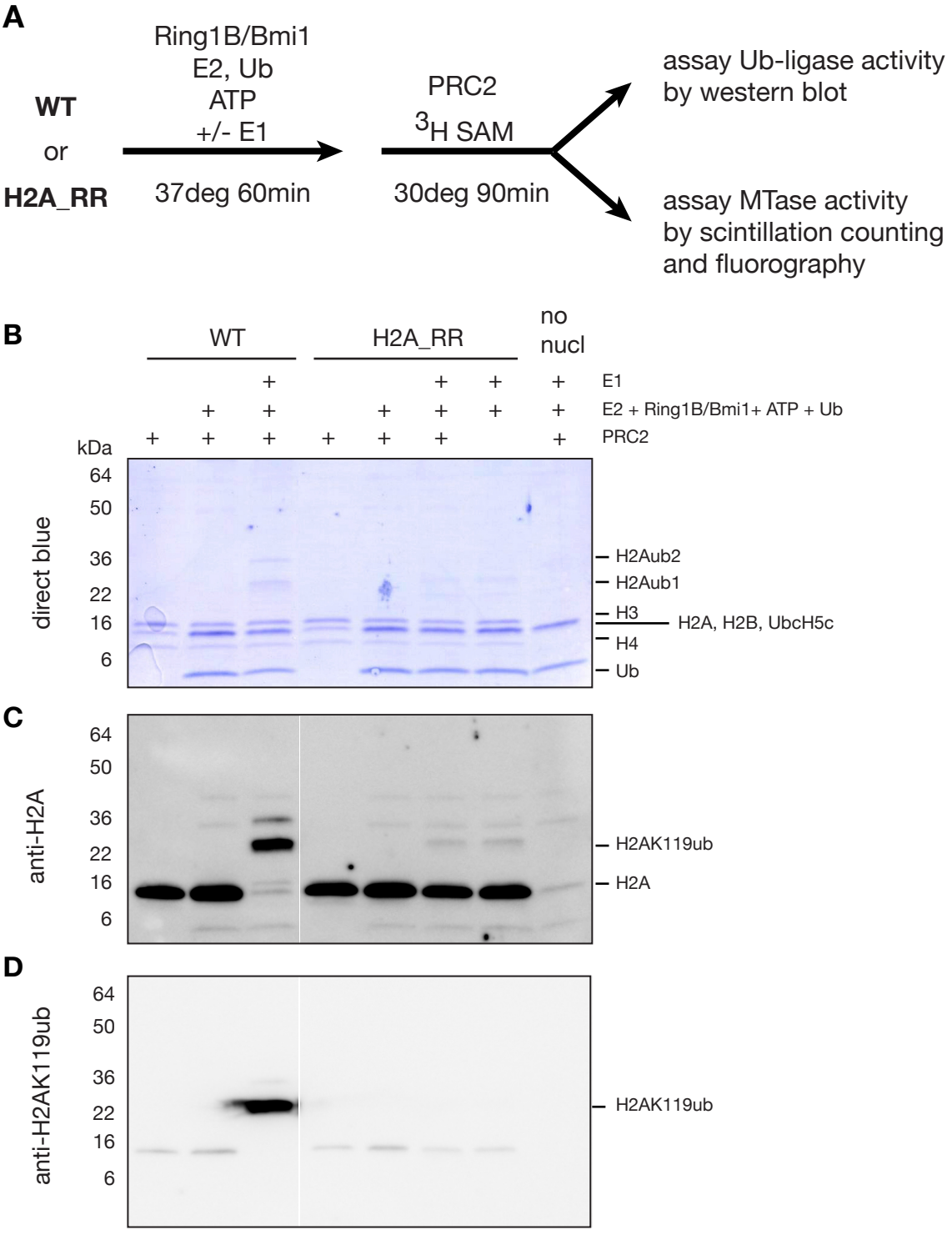
A
WT
or
H2A_RR
Ring1B/Bmi1
E2, Ub
ATP
+/- E1
37deg 60min
PRC2
3H SAM
30deg 90min
assay Ub-ligase activity
by western blot
assay MTase activity
by scintillation counting
and fluorography
B
WT
H2A_RR
no
nucl
E1
E2 + Ring1B/Bmi1+ ATP + Ub
PRC2
kDa
64
50
36
22
16
6
direct blue
H2Aub2
H2Aub1
H3
H2A, H2B, UbcH5c
H4
Ub
C
anti-H2A
H2AK119ub
H2A
D
anti-H2AK119ub
H2AK119ub

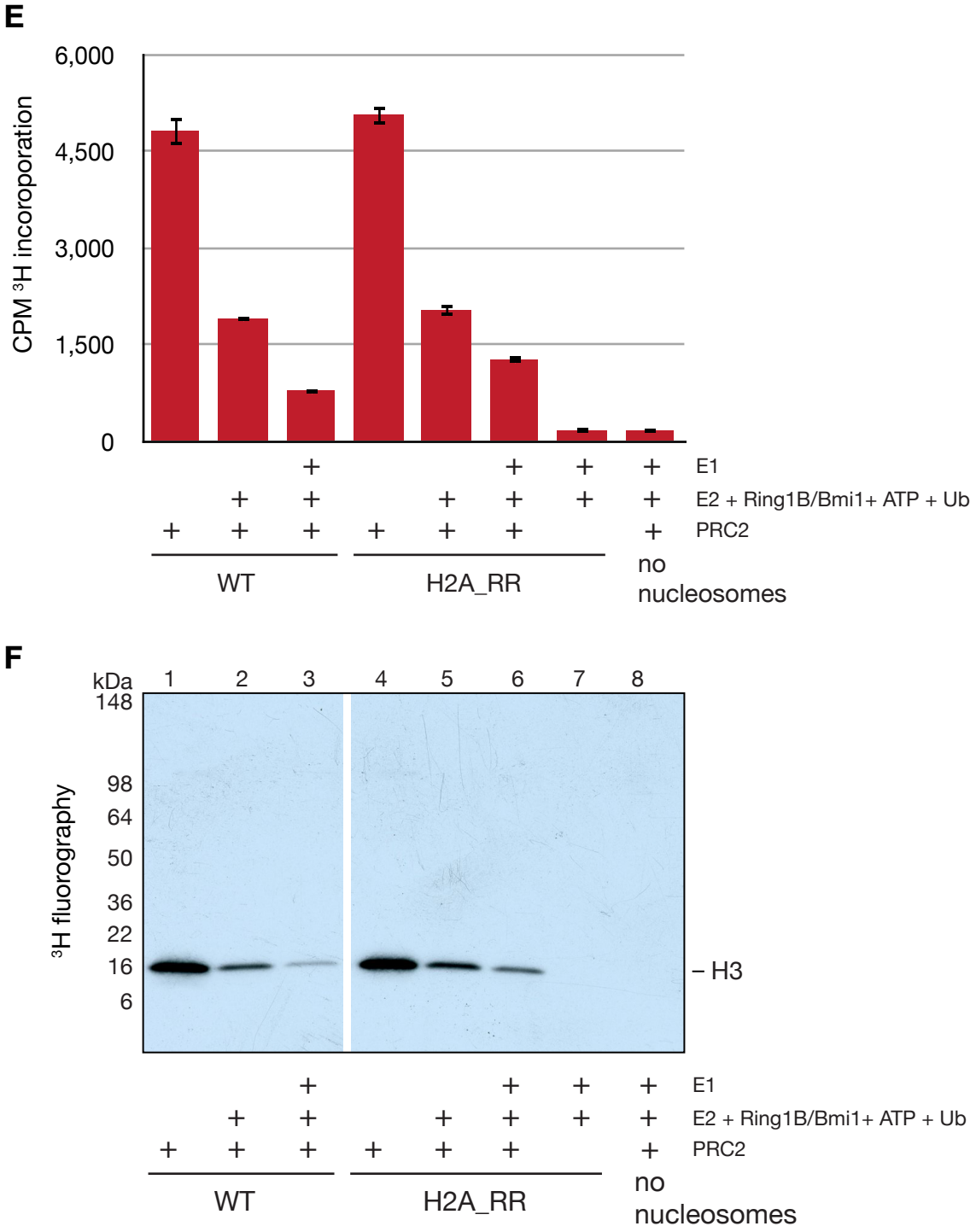
E
6,000
4,500
3,000
1,500
0
CPM ³H incoroporation
E1
E2 + Ring1B/Bmi1+ ATP + Ub
PRC2
WT
H2A_RR
no nucleosomes
F
kDa
1 2 3 4 5 6 7 8
148
98
64
50
36
22
16
6
³H fluorography
– H3
E1
E2 + Ring1B/Bmi1+ ATP + Ub
PRC2
WT
H2A_RR
no nucleosomes

4.7 H2A ubiquitylation machinery inhibits PRC2 methylation of H3K27

As described above, H2Aub mononucleosomes can be generated by *in vitro* enzymatic ubiquitylation. Using sequential ubiquitylation and methylation reactions, I sought to test whether the presence of H2Aub affects PRC2 activity *in vitro* (Figure 4.4). H2A_RR nucleosomes were used as a control for nucleosomes ubiquitylated on sites other than H2AK118,119, and (-) E1 reactions were used as a control for effects not attributable to an active ubiquitylation machinery. After sequential ubiquitylation and methylation reactions, the samples were split to assay for levels of H2Aub and for H3K27methylation (Figure 4.4A).

As shown by anti-H2A western blot signal, H2A in WT nucleosomes was nearly quantitatively ubiquitylated (Figure 4.4C). Ubiquitylation was E1-dependent, and no appreciable ubiquitylation of H2A_RR was detected.

As expected, in the absence of ubiquitylation machinery WT and H2A_RR nucleosomes were found to be equally good substrates for PRC2 MTase (Figure 4.4E-F, compare lanes 1 and 4). Surprisingly, addition of "inactive" ubiquitin ligase machinery (Ring1B/Bmi1, E2, Ub, ATP, but missing E1) strongly inhibited PRC2 activity. Free ubiquitin and ATP have no effect on PRC2 activity (not shown), but several groups have reported stable nucleosome binding activity of Ring1B/Bmi1. Perhaps pre-incubation of nucleosomes with Ring1B/Bmi1 blocks access of PRC2 to the nucleosome or to H3K27 specifically, thereby explaining the inhibition of PRC2 activity following nucleosome incubation with inactive ubiquitylation machinery.

Interestingly and curiously, "active" ubiquitylation machinery (+ E1) inhibited PRC2 activity even further. However, this inhibition was not dependent on ubiquitylation

of H2AK119 because the same effect was observed on WT and H2A_RR nucleosomes (Figure 4.4E,F). Western blots to determine whether components of PRC2 are ubiquitylated in this assay were inconclusive (not shown), and therefore it cannot be ruled out that ubiquitylation of a PRC2 component by Ring1B may directly inhibit PRC2 MTase activity on H3. However, even with these uncertainties, there is no *in vivo* evidence that PRC1 activity inhibits PRC2 mediated H3K27methylation.

4.8 H2Aub modestly inhibits PRC2 activity

Very near the completion of this thesis, "nearly native" *Xenopus* H2Aub(G76A) became available thanks to the work of Dr. Beat Fierz (Chapter 2.2.2). This reagent, paired with *xl*H2Bub(G76A) (Chapter 2.1), allowed me to test whether the antagonistic crosstalk between H2Aub and H2Bub on methylation of H3K4 is mirrored in antagonistic crosstalk on PRC2-mediated methylation of H3K27 (Figure 4.1). To my knowledge these experiments are the first to investigate potential PRC2 crosstalk with histone ubiquitylation.

However, H2Aub modestly, but reproducibly, inhibits PRC2 MTase activity (Figure 4.5). This was an unexpected result since both H3K27me and H2Aub are transduced by Polycomb Repressive Complexes (PRC2 and PRC1, respectively) with well-established roles in gene repression. However, several recent publications provide evidence that the functional link between H2Aub and transcriptional repression is not as clear as was once thought (Eskeland et al., 2010; Richly et al., 2010; Scheuermann et al., 2010), and these will be discussed further in Chapter 6.

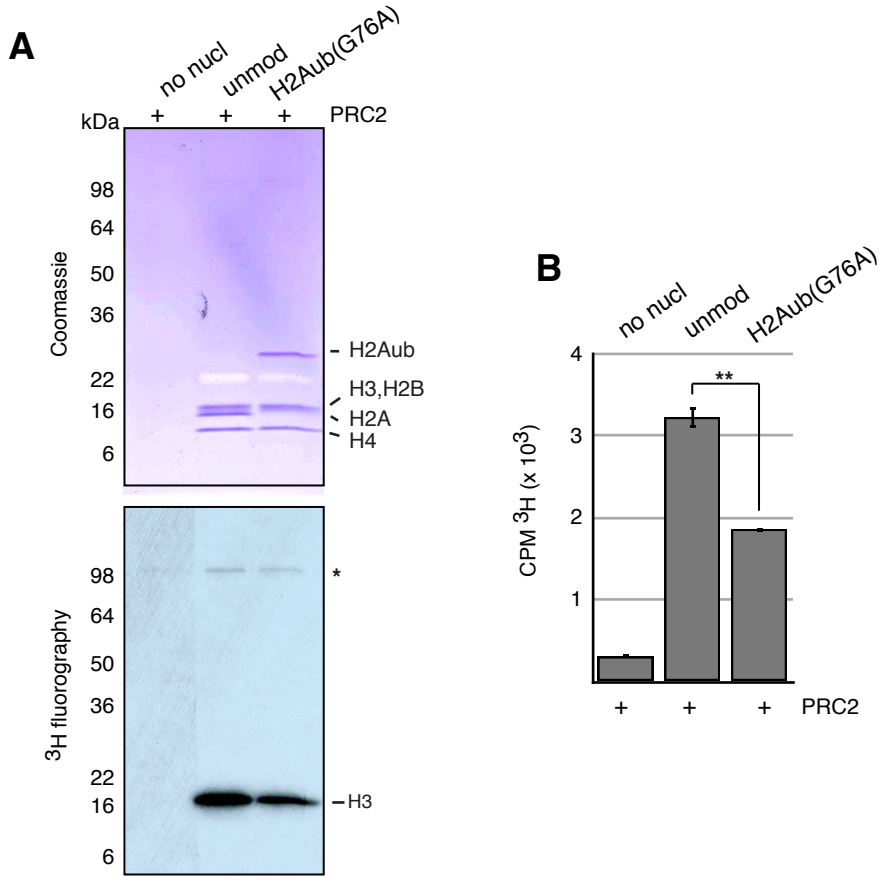

Figure 4.5 H2Aub inhibits PRC2 methyltransferase activity on mononucleosomes. PRC2 methyltransferase activity was tested in reducing conditions on Xenopus unmodified and H2Aub(G76A) mononucleosomes. A representative experiments is shown. Reactions were separated by SDS-PAGE, Coomassie stained, and activity assessed by fluorography (A). Automethylation activity is indicated (*). Activity was also assessed by scintillation counting of incorporated ^{3}H into ¼ of each reaction (B). Error bars indicate the standard deviation of multiple scintillation counts of the same reaction. Paired student's test is indicated, $p<0.0001$ (**).

4.9 Presence of H2Bub in nucleosome doesn't appreciably influence PRC2 activity

As described in Chapter 3, nucleosomes containing H2BK120ub directly stimulate Set1 and Dot1 histone methyltransferase activity directed towards H3K4 and H3K79 respectively. However, it is still far from clear how monoubiquitylation on

H2BK120 stimulates both of these enzymes. Set1 and Dot1 are both histone lysine methyltransferases, but they are evolutionarily unrelated. Set1 activity requires the participation of its complex members while Dot1 is an active MTase on its own and is not known to belong to a stable protein complex. Perhaps H2Bub is a general stimulator of HMTases. Or perhaps its stimulatory action is restricted to MTases involved in transcriptional activation (*e.g.* Set1 and Dot1). Further, given the role of H2Bub in active transcription, perhaps it antagonizes methylation states involved in transcriptional repression.

To investigate these possibilities, I performed *in vitro* methyltransferase experiments to test for crosstalk between H2Bub and PRC2-mediated H3K27methylation. My results show that PRC2 activity is unaffected by the presence of H2Bub in nucleosomal substrates (Figure 4.6). Based on time course analysis, the kinetics of methylation also did not appreciably differ between the substrates (Figure 4.6D-E). By this measure also, H2Bub nucleosomes were equally good substrates for PRC2 as unmodified nucleosomes, ruling out the possibility that nucleosomal H2Bub represses PRC2-mediated methylation in these assay conditions.

As was outlined above, H2Bub and H2Aub have opposing effects on methyltransferase activity directed towards H3K4 (Figure 4.1), and I hypothesized that this may be a more general mechanism of regulating histone methyltransferases. In particular, PRC2-mediated H3K27methylation was an attractive candidate because of its antagonistic role to H3K4 methylation in regulating transcription. However, the *in vitro* MTase assays presented here suggest that, contrary to expectation, H2Aub inhibits PRC2 while H2Bub had no appreciable effect on MTase activity.

Figure 4.6 H2Bub crosstalk with HMTases does not extend to PRC2. PRC2 methyltransferase activity was tested on *Xenopus* (*xl*) unmodified and H2Bub(G76A) mononucleosomes under reducing conditions. A-C) ½ of each reaction was separated by SDS-PAGE and Coomassie stained (A) and activity was assessed by fluorography (B) the lower panel is a short exposure of the upper panel. Activity was also assessed by scintillation counting of $^{3}H\text{-}CH_3$ incorporation in ½ of each reaction (C). Error bars indicate the standard deviation of replicate scintillation counts of the same filter paper. D-E) reactions were incubated for the indicated times and the entire reaction assessed by fluorography.

Figure 4.6

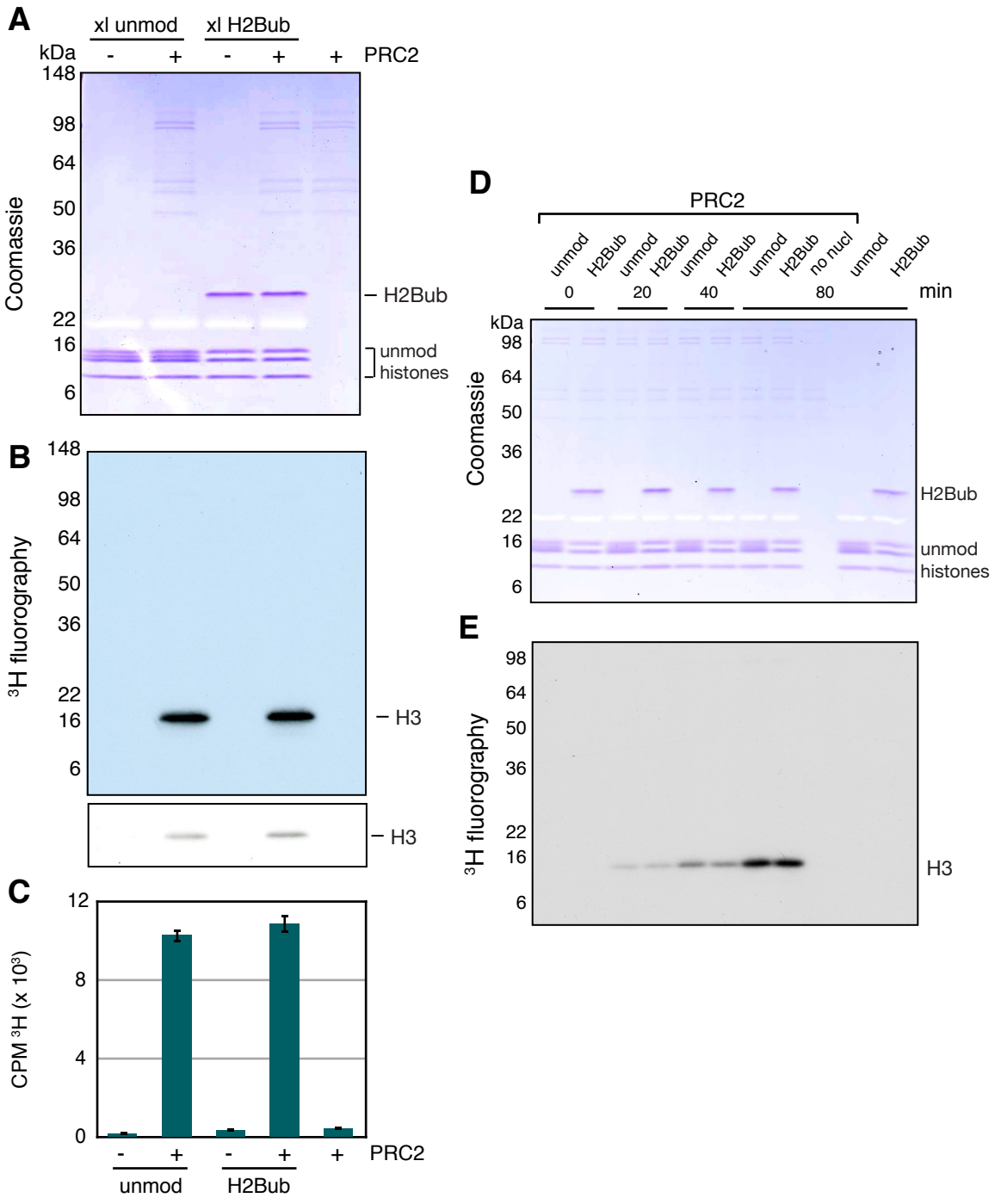
A
xl unmod
xl H2Bub
kDa
-
+
-
+
+
PRC2
148
98
64
50
36
22
16
6
Coomassie
H2Bub
unmod
histones
B
148
98
64
50
36
22
16
6
3H fluorography
H3
H3
C
12
8
4
0
CPM 3H (x 10³)
-
+
-
+
+
PRC2
unmod
H2Bub
D
PRC2
unmod
H2Bub
unmod
H2Bub
unmod
H2Bub
unmod
H2Bub
no nucl
unmod
H2Bub
0
20
40
80
min
kDa
98
64
50
36
22
16
6
Coomassie
H2Bub
unmod
histones
E
98
64
50
36
22
16
6
3H fluorography
H3

CHAPTER 5: TESTING FOR CROSSTALK BETWEEN H3 VARIANTS, H3.3 PHOSPHORYLATION AND H3K27ME3[4]

As discussed in Chapter 1, multiple mechanisms exist to selectively introduce complexity into the chromatin fiber. This thesis has thus far emphasized the importance of histone post-translational modifications and has investigated mechanisms for how meaningful combinations of modifications are generated and maintained. Site and process-specific incorporation of variant histone proteins is another major mechanism to introduce complexity and increase the epigenetic coding potential of chromatin. In this chapter, H3 variant-specific and phosphomimetic nucleosomes are used in crosstalk experiments with PRC2 MTase for H3K27.

5.1 Mammalian histone H3 variants

Mammalian cells express three H3 variants, H3.1, H3.2, and H3.3, in addition to the more divergent centromere-specific variant, CENP-A. The amino acid sequence of H3.3 differs from the canonical H3.2 and H3.1 proteins at only 4-5 positions (Figure 5.1A) but has distinct chromatin deposition properties. H3.1 and H3.2 expression is restricted to S-phase and their chromatin deposition is coupled to DNA replication, whereas H3.3 is expressed constitutively throughout the cell cycle and its deposition is independent of DNA replication (Ahmad and Henikoff, 2002; Ray-Gallet et al., 2011). In non-replicating cells, H3.3 replaces canonical H3 in chromatin over time (Pina and Suau, 1987).

[4] The work in this chapter was performed as part of a collaboration with Dr. Laura Banaszynski in the Laboratory of Chromatin Biology and Epigenetics at The Rockefeller University.

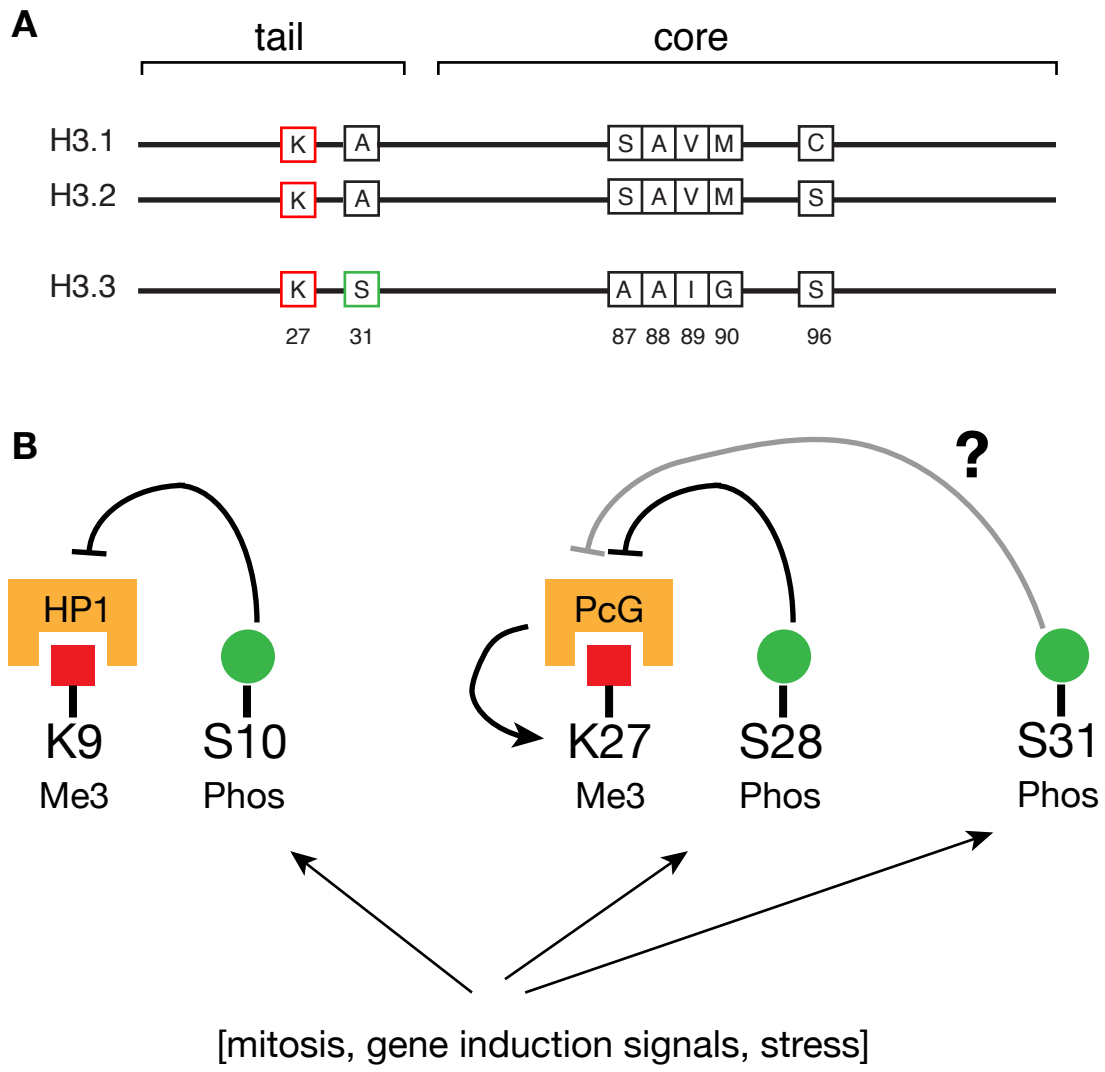

Figure 5.1 Mammalian H3 variants and methyl/phos "switches" on H3. Differential sequence features of mammalian H3 variants H3.1, H3.2, and H3.3 are shown (A). H3.1 and H3.2 only differ at one position, 96, whereas H3.3 differs from H3.1 and H3.2 at 4-5 positions, both in the H3 folded core and in the N-terminal tail. Serine 31, a potential phospho-acceptor residue, is colored in green to emphasize its restriction to the H3.3 variant and its proximity to the conserved lysine 27, a methyl acceptor, colored in red. B) outlined are established and hypothesized methyl/phos switches on the N-terminal tail of H3. Validated interference of H3S10phos and H3S28phos on HP1 and PcG binding to adjacent methylated lysines, are shown with black blunt-headed arrows. A hypothesized H3.3S31phos/H3K27me3 "switch" is indicated with a grey blunt-headed arrow and question mark.

Initial studies of H3.3 function linked this histone variant with active transcription. In the ciliate *Tetrahymena thermophila*, an H3.3-like protein is specifically targeted to the transcriptionally active macronucleus but excluded from the highly compacted and transcriptionally inactive micronucleus (Allis et al., 1980). Subsequent studies have shown that H3.3 enrichment at actively transcribed regions of the genome is conserved in multicellular eukaryotes as well (Ahmad and Henikoff, 2002; Goldberg et al., 2010; Mito et al., 2005). H3.3 is also enriched in constitutive heterochromatin at telomeres (Goldberg et al., 2010; Wong et al., 2009) and at cis-regulatory elements (Jin and Felsenfeld, 2006), including PcG binding sites (Mito et al., 2007). It has been proposed that H3.3 enrichment in particular regions is due in large part to locally high turnover of nucleosomes (Mito et al., 2007). The mechanism of deposition and functional significance of H3.3 incorporation at these various classes of genomic regions is an active area of investigation.

5.2 Histone H3 Methyl/Phos switches

An understudied aspect of H3.3 biology is the significance of having a serine at position 31, where canonical H3 (H3.1/2) has an alanine (Figure 5.1A). Unlike alanine, serine is a potential phospho-acceptor residue, and in fact, phosphorylated S31 in H3.3 was identified in mitotically arrested cells (Hake et al., 2005). Although the function of H3.3S31phos is almost completely unknown, histone phosphorylation on other sites is clearly linked to critical processes such as mitosis (H3S10phos, H3S28phos, H3T3phos), apoptosis (H2BS14phos), DNA repair (H2A.XS139phos), and inducible gene activation (H3S10phos, H3S28phos)(Baek, 2011; Berger, 2010). In the case of H3S10 and H3S28,

phosphorylation critically disrupts binding of effector proteins to the trimethylated lysine adjacent to the phosphorylated serine (Figure 5.1B), so called "methyl-phos switches" (Fischle et al., 2005; Fischle et al., 2003; Gehani et al., 2010; Lau and Cheung, 2011).

HP1-association is a hallmark of constitutive heterochromatin, and binding to H3K9me3 is critical for proper chromatin localization of HP1. During mitosis, the bulk of HP1 dissociates from chromatin despite no significant change in H3K9me3 levels on condensed chromosomes. Adjacent to K9 is S10, which is phosphorylated in M-phase by Aurora B kinase. HP1 binding to H3K9me3 is incompatible with H3S10phos, and phosphorylation of H3S10 is sufficient to eject HP1 from chromatin during M-phase (Fischle et al., 2005; Hirota et al., 2005). Recently, the H3K27/S28 pair was also discovered to participate in a methyl/phos switch triggered mitogens, stress and differentiation signals (Figure 5.1B). Phosphorylation of H3S28 by MSK1 at promoters of PcG-repressed genes disrupts PRC1 and PRC2 binding and results in a reduction of H3K27me3 and transcriptional de-repression (Gehani et al., 2010; Lau and Cheung, 2011).

Almost nothing is known about the function of the H3.3 variant-specific S31phos, but its proximity to H3K27 hints that it may impact PRC2-mediated methylation of H3K27. We wondered whether K27/S31 might function as a methyl/phos switch similar to K9/S10 and K27/S28.

5.3 Testing for differential PRC2 MTase activity on canonical H3.2 and H3.3 nucleosomes

Dr. Laura Banaszynski, a post-doctoral fellow in the Allis lab, has been studying the function of H3.3 in lineage specification during ESC differentiation. In agreement with studies linking H3.3 with active transcription, she found H3.3 mononucleosomes in ESC to be enriched in H3K4me3 and depleted in H3K27me3 relative to H3.1 mononucleosomes. However, in the absence of H3.3, transcription of a subset of developmental genes is upregulated, accompanied by reduced PcG occupancy and reduced H3K27me3 at the promoters of these genes. Taken together, these data suggest that at least for some genes, H3.3 is important for PcG-mediated transcriptional repression.

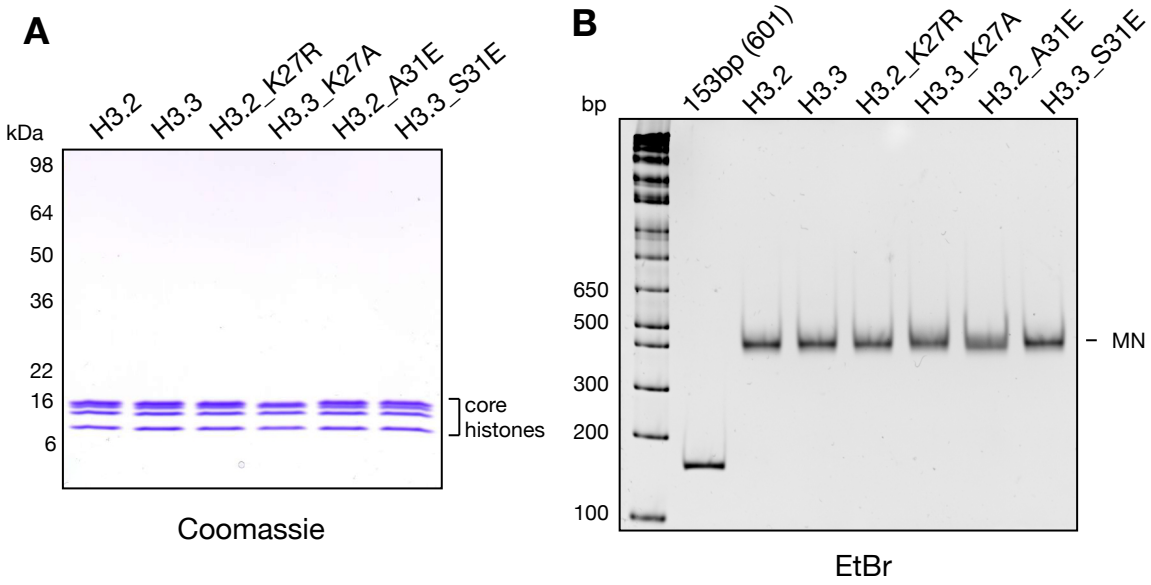

Figure 5.2 H3.2 and H3.3 designer octamer and mononucleosomes. Octamers containing core histones H3.2, H3.3, H3.2_K27R, H3.3_K27A, H3.2_A31E, or H3.3_S31E were assembled and incorporated into mononucleosomes as described in Chapter 2.4,5. Coomassie stained SDS-PAGE gel of octamers (A) and EtBr stained native PAGE gel of mononucleosomes, MN (B).

We wanted to test whether H3.3 nucleosomes are intrinsically better substrates for PRC2-mediated H3K27methylation than canonical H3 nucleosomes. To do so, I assembled a set of designer human octamers with either H3.2, H3.3, or with point mutants at the PRC2 methylation site, H3.2_K27R, H3.3_K27A (Figure 5.2A). Note that the H3.2 octamers used in this chapter are identical to the unmodified octamers described in Chapter 2 and used in crosstalk studies in Chapters 3 and 4. Mononucleosomes were assembled with these octamers and 153bp (601) DNA (Figure 5.2B), as described in Chapter 2.5.

In methyltransferase assays with ^{3}H-SAM, H3.3 nucleosomes were found to be slightly better substrates for PRC2 MTase than canonical H3.2 nucleosomes (Figure 5.3). This difference is indeed subtle, but was reproducible across different mononucleosome assemblies, time course of MTase reaction, and over a 4-fold change in PRC2:nucleosome molar ratio (Figure 5.3A-C).

Figure 5.3 Putative H3 variant-specific crosstalk with PRC2-mediated H3K27methylation. Mononucleosomes containing H3.2, H3.3, H3.2_K27R, H3.3_K27A, H3.2_A31E, or H3.3_S31E were used in methyltransferase assays with ^{3}H-SAM (or cold SAM (D)) and PRC2. Activity was assessed by fluorography (A, B, F) or scintillation counting of incorporated ^{3}H-CH_3 (C, G). As expected, no ^{3}H-CH_3 incorporation was observed on nucleosomes containing H3.2_K27R or H3.3_K27A (A, F, G). PRC2 MTase activity was shown to be slightly, but reproducibly, higher on H3.3 containing nucleosomes using different reaction times (B), enzyme concentration (C), and nucleosome assembly batches (A-C, F, G). D), mass spectrometry analysis was performed on methyltransferase samples to assess whether the relative proportion of H3K27Kme0,1,2,3 differed between H3.2 and H3.3. Numbers represent the percent of H3K27 in the given methylation state after incubation with PRC2 and SAM. Red boxes around the percent unmodified and the percent dimethylated highlight differences in PRC2 activity and processivity on H3.2 and H3.3 nucleosomes. Chemical structures of phosphoserine and the phosphoserine-mimetic, glutamic acid, are shown in (E). Incorporation of glutamic acid at position 31 reduced PRC2 activity to about 60% of its activity on WT H3.2 and H3.3 nucleosomes (F, G).

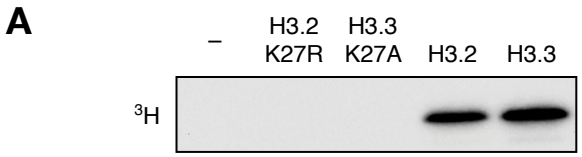

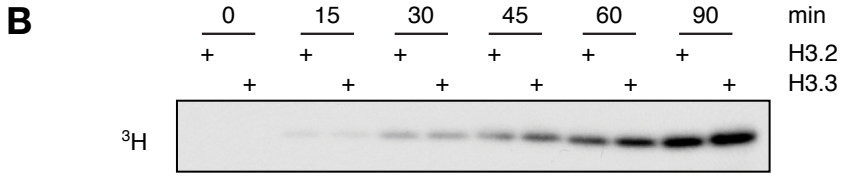

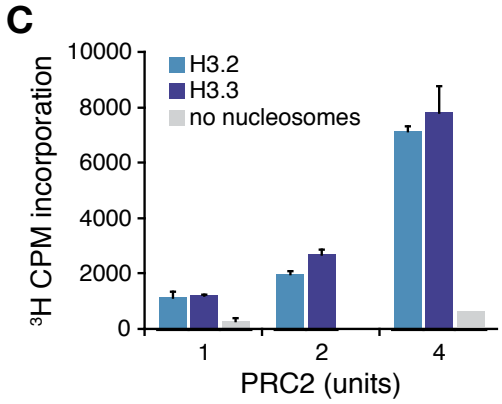

D

	H3.2	H3.3
no modification %	71.7	64.5
H3K27me1 %	27.8	28.7
H3K27me2 %	0.5	6.7
H3K27me3 %	0.01	0.1

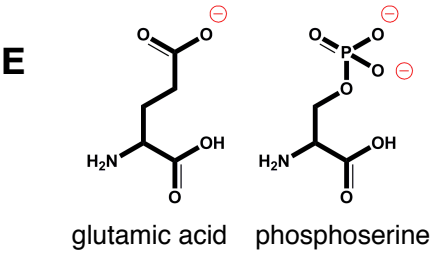

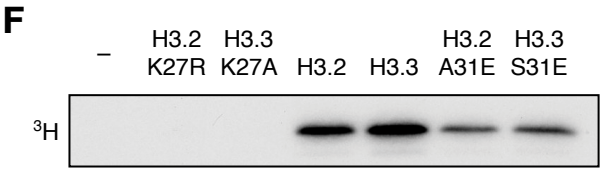

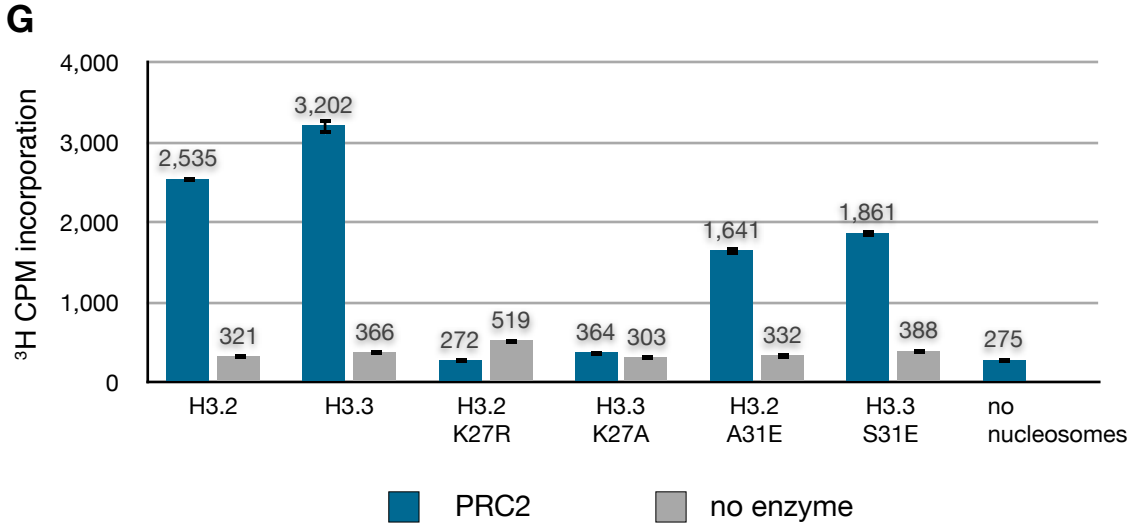

In vitro core-PRC2 enzymatic activity assays (Nekrasov et al., 2007; Sarma et al., 2008) show that H3K27me1 is the predominant methylation state produced *in vitro*. We wondered whether increased $^{3}H_{3}C$ incorporation on H3.3 nucleosomes was the result of increased processivity of PRC2 in converting monomethyl to di- and trimethyl, or whether it was the result of increased monomethylation only. To measure the distribution of K27me1, me2, and me3 on H3.2 and H3.3, the products of PRC2-mediated methylation reactions were subjected to mass spectrometry. As expected, H3K27me1 is the predominant methylation state observed for both H3.2 and H3.3 containing nucleosomes. Interestingly, preliminary analysis revealed that enhanced activity on H3.3 nucleosomes was likely due to the incorporation of higher order methylation, as H3K27me2 was only significantly observed on this substrate (Figure 5.3D). As described above, H3.2 and H3.3 amino acid sequences differ at only 4 positions: position 31 in the N-terminal tail, and 3 positions within the histone fold domain (Figure 5.1A). The proximity of position 31 to K27 makes it a good candidate for potential regulation of enzymatic activity on K27. Future experiments using H3.2_A31S nucleosomes will test whether a serine at position 31 is sufficient for increased higher order K27methylation *in vitro*. Alternatively, it is possible that amino acid differences in the histone fold domain of H3.2 and H3.3 might affect nucleosomal stability in a way that affects PRC2 MTase processivity.

If H3.3 facilitates higher order methylation of H3K27 *in vivo*, then it may have an impact on gene regulation. Based on peptide and nucleosome binding studies, one would expect PcG binding to H3K27me1 chromatin to be significantly less than to H3K27me2/3 chromatin (Bernstein et al., 2006; Margueron et al., 2009), and H3K27me1

is unable to allosterically stimulate PRC2 methyltransferase activity (Margueron et al., 2009). Taken together, these data may point to a role of H3.3 in tuning PcG-mediated transcriptional repression.

5.4 Putative methyl/phos switch between K27me and H3.3S31phos

Having shown that H3.3 nucleosomes are intrinsically slightly better substrates for PRC2 methylation than canonical H3 nucleosomes, we wondered whether phosphorylation at S31 in H3.3 might also influence PRC2 activity. Might H3.3S31phos participate in a methyl/phos switch with PRC2 and H3K27me3 (Figure 5.1B)?

In order to begin to address this question, H3.2 and H3.3 recombinant proteins carrying the serine-phosphomimetic glutamic acid (Figure 5.3E) were incorporated into designer octamers and assembled into designer nucleosomes (Figure 5.2). Strikingly, the presence of glutamic acid at position 31 inhibited PRC2 methylation activity significantly on both H3.2 and H3.3 mononucleosomes (Figure 5.3F,G). The slightly increased signal still observed on the mutant H3.3 nucleosomes with respect to their H3.2 counterparts suggests that amino acid differences in the core, and not only at position 31, contribute to enhanced PRC2 methyltransferase activity.

In summary, studies on the function of H3.3 in mouse lineage determination led to the identification of a putative H3 variant-specific methyl/phos regulatory link, although mechanistic details remain unclear. We look forward to knowing whether the observed *in vitro* inhibition of PRC2 by a phosphomimetic at position 31 will extend to phosphorylated H3.3 and whether the *in vitro* crosstalk identified in this chapter will be validated *in vivo*.

CHAPTER 6: DISCUSSION

Chromatin is the biological substrate for all DNA-templated processes, including transcription, mitosis, meiosis, DNA replication, and DNA repair. The diversity of processes regulated by chromatin is mirrored by the immense structural and compositional complexity of chromatin itself (Chapter 1.1). Even mononucleosomes, the minimal repeating units of chromatin, are endowed with extensive variation in the form of variant histone incorporation and a multitude of histone PTMs. It is of central importance to understand how variation in the chromatin fiber, signal transduction pathways, and all types of DNA metabolism are coordinately regulated to produce functional outcomes, and conversely, how misregulation results in disease.

6.1 Designer ubiquitylated nucleosomes to study crosstalk with methyltransferases

An important mechanism of regulatory coordination is histone PTM crosstalk: enzymatic installation or removal of a histone PTM that is influenced by pre-existing PTMs. In theory, a pre-existing PTM can influence enzymatic activity in *cis* and in *trans* (Figure 1.2). For example, a histone PTM may interact in *trans* with a modification-specific binding domain in the enzyme or its associated complex. Interactions of this type may lend specificity and/or affinity to the enzyme's interaction with chromatin and may be particularly important for processive enzymes, like many MTases (Walsh, 2006). Conversely, a PTM may block enzyme association with its nucleosome substrate or inhibit the precise positional binding required for productive enzymatic activity. Alternatively, a PTM may function in *cis* by altering the biophysical properties of the

nucleosome or the chromatin fiber, making nucleosomes more dynamic for example, or the fiber less compact. These differences may expose surfaces or target residues in a way that influences enzymatic activity.

The inherent heterogeneity of histones and nucleosomes purified from endogenous sources has historically obstructed efforts to confirm that observed *in vivo* crosstalk is mediated directly by a particular PTM. Recently several groups have developed chemical strategies for robust and site-specific installation of histone PTMs (Chatterjee and Muir, 2010). Chemically-defined histones bearing desired modifications can be reconstituted into designer nucleosomes, which can serve as potentially powerful substrates in enzymatic crosstalk studies (Allis and Muir, 2011).

One leader in designer chromatin methodologies is the lab of Dr. Tom Muir, at Princeton University, with whom I've been fortunate to collaborate throughout my thesis research. Among other advances, they were the first to adapt chemical ligation techniques to generate H2B homogenously monoubiquitylated at K120, requiring demanding semi-synthetic peptide chemistry and two chemical ligation steps (McGinty et al., 2008).

Using designer mononucleosomes, Dr. McGinty and colleagues were able to conclusively show that H2Bub can *directly* stimulate Dot1L-mediated H3K79 methylation (McGinty et al., 2008), an *in vivo* crosstalk relationship first revealed in striking fashion by yeast genetics (Briggs et al., 2002; Ng et al., 2002b). It had been suggested that *in vivo* Dot1 is stimulated *indirectly* by H2Bub, perhaps by serving as a "wedge" between adjacent nucleosomes and thereby exposing the nucleosome axial surface, where H3K79 resides (Figure 1.3), for methylation. But since the *in vivo* crosstalk relationship was recapitulated *in vitro* using mononucleosome substrates,

H2Bub-mediated chromatin fiber decompaction is unlikely to be the main mechanism of stimulation. Designer nucleosomes were also utilized to show that H2Bub can *directly* stimulate Set1-mediated H3K4 methylation (Kim et al., 2009), another *in vivo* crosstalk relationship first revealed by yeast genetics (Briggs et al., 2002; Dover et al., 2002; Sun and Allis, 2002).

Interestingly, Dot1 and Set1 are evolutionarily unrelated, and the local structural environments of their target lysines are very different (H3K79 being located on the axial surface of the nucleosome and H3K4 being located near the end of the relatively unstructured H3 N-terminal "tail")(Figure 1.3). These observations elicit the question, how are the activities of both Set1 and Dot1 drastically stimulated by the presence of H2Bub in the nucleosome substrate?

Recently, using nucleosomes reconstituted with endogenous H2Aub or H2A, Nakagawa and colleagues showed that deubiquitylation of H2Aub allowed for efficient methylation of H3K4 by the HMTase MLL3 complex (Nakagawa et al., 2008), suggesting that H2Aub, in addition to H2Bub, also participates in enzymatic crosstalk with histone MTases, albeit of an inhibitory nature and antagonistic to transcription. This study in combination with the H2Bub/H3K79me and H2Bub/H3K4me crosstalk studies suggested that it may be a general feature of histone ubiquitylation to participate in enzymatic crosstalk with histone methyltransferases.

6.2 Summary and discussion of experimental results

For this thesis I was interested in exploring the specificity and range of crosstalk relationships between histone monoubiquitylation and histone methyltransferases. For

this purpose I utilized expressed protein ligation and disulfide-mediated ubiquitylation strategies to generate sufficient quantities of chemically-defined H2AK119ub and H2BK120ub (Chatterjee et al., 2010; McGinty et al., 2008; McGinty et al., 2009b) (Chapter 2). In order to isolate putative direct enzymatic crosstalk functions of these modified histones, rather than indirect effects on chromatin higher-order structure that manifest in enzymatic activity differences, I chose mononucleosomes as substrates for these studies. As noted above, H2Bub and H2Aub have opposing influences on methylation of H3K4 *in vitro*. I wanted to test whether H2Aub also functions antagonistically to H2Bub in crosstalk with other HMTases, specifically Dot1L (Chapter 3) and PRC2 (Chapter 4). The main results of these experiments are summarized below and in Figure 6.1A.

Dot1L MTase activity *in vitro* is stimulated by nucleosomal monoubiquitylation at several positions (Figure 3.1), notably those in the "stimulatory patch" on the nucleosome axial surface and at a radial site (Chatterjee et al., 2010; McGinty et al., 2008; Wu et al., 2011). This reveals extensive plasticity in the ubiquitin-mediated stimulation mechanism of Dot1L. Using H2AssUb nucleosomes I tested whether this positional-plasticity of stimulation extended to H2AK119. The *in vivo* abundance of H2AK119ub (5-15% of H2A)(Goldknopf and Busch, 1977; West and Bonner, 1980) and its nucleosomal location, nearly as far away from the stimulatory patch as possible (Figure 3.1A), made it an interesting test case for Dot1L stimulation.

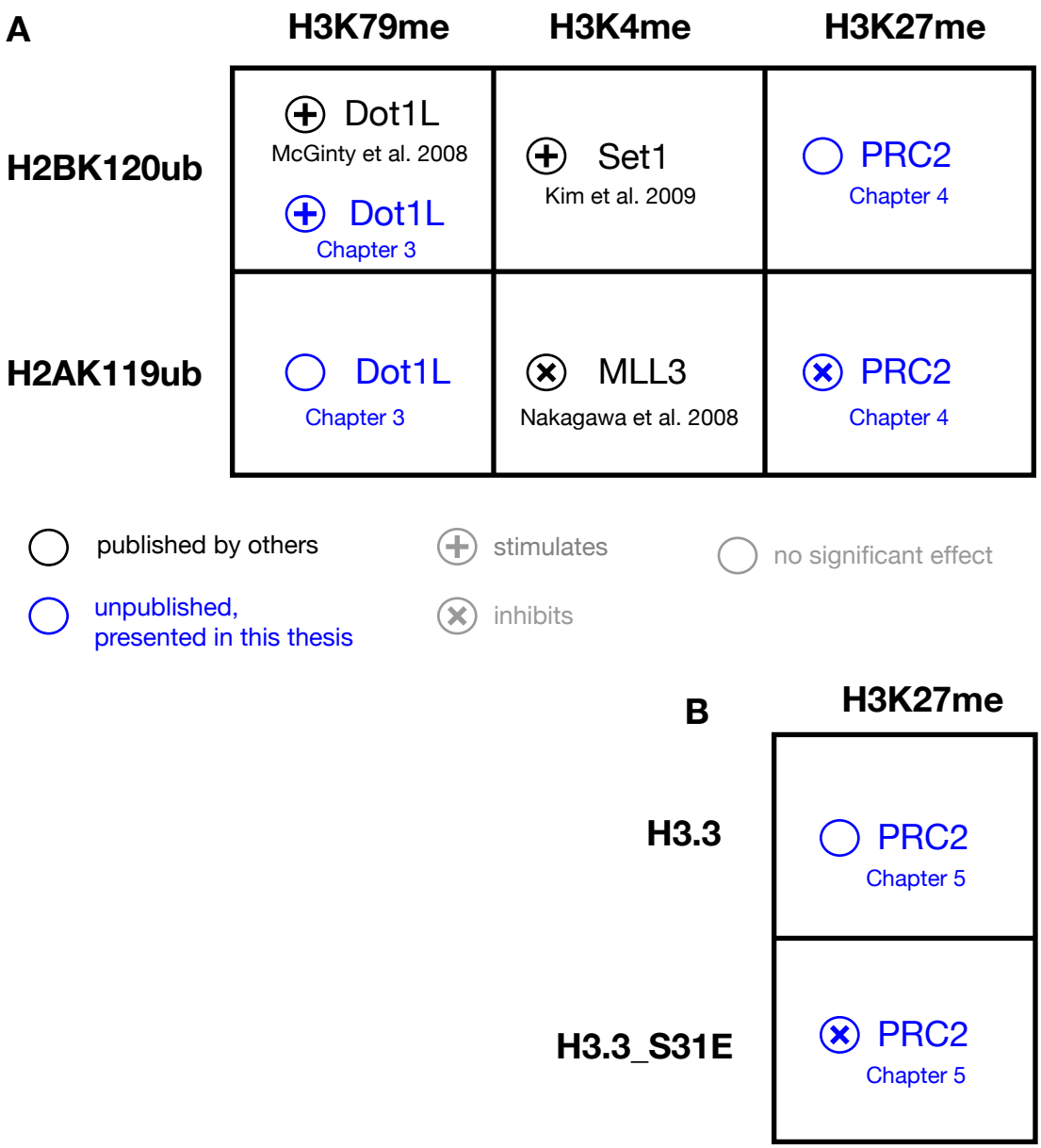

Figure 6.1 Summary of direct enzymatic crosstalk experiments (Chapters 3-5).
The results of enzymatic crosstalk studies between designer nucleosome substrates and MTases for H3K79, H3K4, and H3K27 are depicted in grid form. Text in black represents results obtained and published by others. Text in blue represents as of yet unpublished results presented in this thesis. Text inside the boxes indicates the relevant MTase, citation or thesis chapter, and type of crosstalk, if any, relative to activity on unmodified nucleosomes. A) the results of crosstalk experiments with MTases for H3K79, H3K4, and H3K27 (top) utilizing monoubiquitylated nucleosomes on H2BK120 or H2AK119 (left) as presented in Chapters 3-4. B) the results of crosstalk experiments with MTases for H3K27 (top) utilizing nucleosomes assembled with either the H3 variant H3.3 or H3.3 containing serine to glutamate substitution at position 31(left) as presented in Chapters 5.

Experiments presented in Chapter 3 did not reveal any crosstalk between H2Aub and Dot1L, suggesting that H2AK119ub is unlikely to be able to substitute for H2BK120ub in Dot1L stimulation *in vivo*, nor is it likely to repress Dot1L activity on nucleosomes doubly modified by H2Aub and H2Bub, as may exist near DNA double strand breaks (Bekker-Jensen and Mailand, 2011). An important unanswered question regarding Dot1L regulation is how ubiquitylation at a variety of sites, but not at H2AK119, is able to stimulate MTase activity.

In Chapter 4 I turned my attention to another MTase, PRC2, to test whether crosstalk between histone ubiquitylation and histone methylation extends to a critical MTase for repression of developmentally regulated genes (Margueron and Reinberg, 2011). In particular, I was interested in whether the antagonistic crosstalk between H2Aub and H2Bub on methylation of H3K4 (strongly linked to active transcription) is mirrored in antagonistic crosstalk on PRC2-mediated methylation of H3K27 (strongly linked with transcriptional repression).

H2Aub is typically understood to cooperate with PRC2-mediated H3K27 methylation in transcriptional repression. Therefore I hypothesized that H2Aub may stimulate PRC2 activity on H3K27, analogously to H2Bub stimulation of Set1 methylation of H3K4. However, I found that H2Aub produces a modest, but reproducible, inhibition of PRC2 activity *in vitro* (Figure 4.5). One more trivial explanation for this finding might be that the relatively close proximity of H2AK119ub to H3K27 in the nucleosome (Figure 1.3) may simply sterically hinder PRC2 methyltransferase activity. While this possibility cannot be ruled out by my studies, recently published data from several groups suggest that the widely-accepted link

between H2Aub and transcriptional repression may not be so straightforward (Eskeland et al., 2010; Richly et al., 2010; Scheuermann et al., 2010).

Eskeland and colleagues showed that the H2A E3 ligase activity of Ring1B is dispensable for transcriptional repression of Polycomb target genes and for long-range chromatin compaction of Hox gene clusters *in vivo* (Eskeland et al., 2010). In light of our *in vitro* results, it would be of interest to know whether cells with catalytically null Ring1B have attenuated or otherwise misregulated activation of Hox genes during differentiation.

Scheuermann and colleagues identified a novel Polycomb repressive complex in *Drosophila* with H2A deubiquitinase activity, PR-DUB (Scheuermann et al., 2010). Interestingly, they found that H2A deubiquitinase activity is required for proper transcriptional repression of Polycomb target genes *in vivo*. Further, repression of Polycomb target genes is even more severely compromised if dRing, E3 ligase for H2Aub, and PR-DUB are simultaneously depleted. Therefore, at least in *Drosophila*, complexes with directly opposing enzymatic activities on H2A synergistically regulate transcriptional repression. These results suggest that H2Aub in different genomic locations may have opposite influences on transcription or that dynamic cycles of H2A ubiquitylation and deubiquitylation may be required for proper gene repression. I look forward to studies that will investigate how the spatial, temporal and kinetic control of H2Aub turnover on chromatin contributes to gene regulation. Such studies would greatly inform future *in vitro* studies using designer chromatin that more closely mimic the dynamism of histone ubiquitylation *in vivo*.

Lastly, Richly and colleagues identified ZRF1 as an H2Aub binding protein involved in differentiation-dependent transcriptional activation of Polycomb target genes (Richly et al., 2010). If reduced PRC2 activity on PcG-repressed gene is an important early step in pushing the chromatin state towards one more permissive to transcription, then my *in vitro* crosstalk data may provide another layer of mechanistic explanation for H2Aub involvement in transcriptional de-repression.

Next, using "nearly native" H2Bub(G76A) nucleosomes, PRC2 was shown to be equally active on unmodified and H2Bub mononucleosomes, hinting that crosstalk between H2Bub and MTases may be limited to those that are involved in active transcription, such as Set1 and Dot1L. The molecular basis of this selectivity is completely unknown at this point but of great interest.

The crosstalk studies presented in this thesis were limited to Dot1L and PRC2 MTases, but a great strength of the "nearly native" chemically defined ubiquitylation method is their suitability for crosstalk studies with other enzymes that require reducing agents, either directly for their catalytic activity, or indirectly for the proper structure/architecture of their catalytic complex. In particular, I have an interest in how H2Aub and H2Bub may crosstalk with chromatin remodeling enzymes. Additionally, reconstituted chromatin containing "nearly native" H2Aub and H2Bub could also be used as bait to discover new crosstalk relationships and even new enzymatic activities on chromatin. For example, nuclear extract fractions could be screened for enzymatic activities (such as SAM or Acetyl CoA incorporation, for methylation and acetylation activities, respectively) that are specific for, or modulated by, nucleosome substrates containing H2Aub, H2Bub. This kind of enzymatic screen could open up new avenues to

pursue in investigations of histone ubiquitylation function. Of course, similar screening approaches to identify novel activities and crosstalk pathways could also be pursued with other types of designer chromatin as well.

In Chapter 5, crosstalk studies with PRC2 were extended to designer nucleosomes containing either canonical histone H3.2, the variant histone H3.3, or genetically encoded H3 phosphoserine mimetics. These studies were done in collaboration with Dr. Laura Banaszynski, a post-doctoral fellow in the Allis lab, who has been studying the function of H3.3 in lineage specification during embryonic stem cell differentiation. In the absence of H3.3, she observed that transcription of a subset of developmentally regulated genes is upregulated, accompanied by reduced PcG occupancy and reduced H3K27me3 at the promoters of these genes (unpublished). Her data suggest that at least for some genes, H3.3 is important for PcG-mediated transcriptional repression, perhaps at the level of crosstalk with PRC2. However, *in vitro* PRC2 MTase activity on H3.3 nucleosomes was found to be only slightly higher than on H3.2 nucleosomes, suggesting that intrinsic differences between mononucleosomes containing canonical versus variant histone H3 are unlikely to explain the gene expression differences she observed *in vivo*.

Interestingly, H3.3 is enriched in parts of the genome that experience higher than average nucleosome turnover including cis-regulatory elements such as PcG binding sites (Jin and Felsenfeld, 2006; Mito et al., 2007). This property of H3.3-enriched chromatin cannot be mimicked using my designer mononucleosomes. Perhaps, in some yet unknown way, the biophysical characteristics of some cis-regulatory element chromatin facilitate PcG-association and PRC2-mediated methylation of H3K27. If so, then upregulation of these developmentally regulated genes may be due not to the lack of H3.3

per se, but rather due to the changes in chromatin structure and dynamics that result from lacking H3.3-specific nucleosome turnover.

In addition to their differential genomic localization (Ahmad and Henikoff, 2002; Goldberg et al., 2010; Jin and Felsenfeld, 2006; Mito et al., 2005), and *in vivo* turnover properties (Mito et al., 2007), H3.3 differs from canonical H3.2/1 in having a serine at position 31 rather than an alanine (Figure 5.1). Interestingly, H3.3S31phos was identified in mitotically arrested cells (Hake et al., 2005), but very little is known about the function of this histone variant-specific PTM in mitosis or in any other cellular process. However, the proximity of S31 to H3K27 hints that phosphorylation at this position may participate in crosstalk with PRC2-mediated methylation of the nearby H3K27. Given that phosphorylation on H3S10 and H3S28 disrupts binding of effector proteins to the adjacent trimethylated lysine (H3K9me3 and H3K27me3, respectively) (Fischle et al., 2005; Gehani et al., 2010; Lau and Cheung, 2011), we hypothesized that PRC2 activity on H3K27 may be inhibited by phosphorylation on S31.

To begin to follow this hypothesis, designer nucleosomes were assembled with H3.3 or H3.3 carrying a substitution of glutamic acid at position 31 (H3.3_S31E) to serve as a phosphoserine mimetic. These mononucleosomes were compared as substrates for PRC2-mediated methylation of H3K27, the results of which are summarized in Figure 6.1B. PRC2 was found to be only about 60% as active on H3.3_S31E mononucleosomes as compared to WT H3.3 mononucleosomes.

The crystal structures of Eed in complex with trimethylated H3 peptides give few, if any, clues as to whether glutamic acid at position 31 would directly disrupt PRC2 binding to the N-tail of H3 (Margueron et al., 2009), and not enough is known about the

mechanism of H3K27me3-mediated allosteric stimulation of Ezh2 to infer whether glutamic acid (or phosphorylation) at position 31 in H3.3 might affect this aspect of PRC2 MTase regulation. Future studies will address these issues.

Future studies will address whether the observed *in vitro* inhibition of PRC2 by a phosphoserine mimetic at position 31 extends to phosphorylated H3.3S31 and whether this *in vitro* crosstalk identified will be validated *in vivo* as a novel, H3.3 specific methyl/phos switch.

6.3 Concluding remarks

When starting from observations made *in vivo*, the compositional and structural complexity of endogenous chromatin can make it difficult to assign mechanistic function to a particular variable. Therefore, the ability to generate substrates for chromatin-mediated processes that have reduced complexity can be a powerful tool. Throughout the text I have highlighted several success stories of the designer chromatin approach.

However, the reductionist strength of designer chromatin can also be a weakness. This thesis made use of designer mononucleosomes, and others have successfully generated designer nucleosome arrays, but even with arrays it is difficult to mimic the dynamic remodeling present in endogenous chromatin. Particularly relevant to this thesis, cycling of ubiquitylation on H2A and H2B through the action of ubiquitin ligases (E2/E3s) and deubiquitylating enzymes (DUBs) is important for transcriptional regulation (Daniel et al., 2004; Fleming et al., 2008; Henry et al., 2003; Pavri et al., 2006; Scheuermann et al., 2010; Wyce et al., 2007). This dynamism would be hard to mimic using designer chromatin, at least with the tools currently available. Furthermore,

preparing designer chromatin reagents is often a significant investment on the part of a researcher, and therefore it is an approach that should be undertaken with prudence and with a constant eye on *in vivo* evidence for the particular hypothesis to be tested *in vitro*.

Additionally, better descriptive knowledge of the chromatin states that exist *in vivo* would be very valuable in informing the most worthwhile experiments to pursue *in vitro*. For example, which histone PTMs, histone variants, or chromatin-associated proteins are specifically enriched in H2Aub and H2Bub-containing chromatin *in vivo*, and which are depleted? This kind of knowledge would be a good starting point for subsequent studies of H2Aub and H2Bub function, including future direct enzymatic crosstalk studies with designer chromatin.

In conclusion, the studies presented in this thesis contribute towards efforts to predict crosstalk relationships between pre-existing modifications on nucleosome substrates and enzymes. Increased understanding of crosstalk relationships will further the long-term goal to understand how histone PTMs and other sources of structural complexity in chromatin are coordinately regulated to generate meaningful combinations at physiologically appropriate genomic locations, and eventually to understand how these combinations of chromatin structural features are "read" by the cell.

METHODS

Recombinant human histone expression and purification

Recombinant human histones were expressed and purified essentially according to Ruthenburg et al., 2011 (Ruthenburg et al., 2011). Briefly, N-terminal hexahistidine tagged human H3.2_C110A, H4, H2A.a4, H2A.a4_K119C H2B.k, and H2B.k_K120C were expressed in BL21(DE3) *E. coli* and solubilized from inclusion bodies with 6M guanidinium chloride and 500 mM NaCl. After denaturing Ni-NTA (QIAGEN) purification, histones were dialyzed into cleavage buffer: 10 mM MOPS pH 7, 500 mM NaCl, 10% glycerol, 0.5 mM EDTA, 5 mM beta-mercaptoethanol (b-ME). Hexahistidine tags were cleaved off by addition of TEV (for H3.2, H4, H2A) or Precision protease (for H2B), and tagless histones were purified by denaturing Ni-NTA subtractive-purification. For long-term storage of purified histones the denatured flow through was desalted over PD-10 columns in 100-200 mM trimethylammonium acetate (TMAA) pH 5.0 before lyophilization.

The integrity of the eventual disulfide bond between H2AK119C, H2BK120C and ubiquitin-aminoethanethiol (Ub-aminoethanethiol) is extremely sensitive to reducing agents. Note that many other published protocols using His-tagged recombinant histones employ TEV and/or Precision cleavage during octamer assembly. However, because these proteases require reducing conditions for activity, they are not compatible with octamer assemblies including disulfide-mediated ubiquitylated histones. Careful removal by extensive dialysis and/or reverse-phase HPLC purification of any residual reducing agents from all histone preps (not only H2AK119C and H2BK120C) is crucial. Additionally, the use of β-ME in the purification and cleavage steps results in the

formation of β-ME-H2AK119C or β-ME-H2BK120C adducts, which were reduced with 20 mM Tris(2-carboxyethyl)phosphine) (TCEP) at pH 8.5 and RP-HPLC purified before use in H2AssUb or H2BssUb ligation reactions.

H2AssUb and H2BssUb preparation

Disulfide-directed ubiquitylation of histones H2A and H2B was carried out essentially according to Chatterjee *et al*., 2010. The most notable alteration to the published protocol was the use of 2,2'-dithiobis(5-nitropyridine) (DTNP) to protect/activate the sulfhydryl on the Ub-aminoethanethiol adduct rather than protect/activate the sulfhydryl of the cysteine at position 119 in H2A or at position 120 in H2B.

As described in Chatterjee et al., full length ubiquitin was expressed in *E. coli* BL21(DE3) as a GyrA intein-chitin binding domain (CBD) fusion protein. Soluble ubiquitin fusion protein was purified on chitin resin, and ubiquitin cleaved off the resin with 50 mM cystamine-dihydrochloride, 50 mM TCEP at pH 7.5. Ubiquitin with the desired C-terminal aminoethanethiol linker was further purified by C18 RP-HPLC over a 25-60% B gradient: gradient: (A) 0.1% trifluoroacetic acid (TFA) in water, (B) 90% actetonitrile, 0.1% TFA in water.

To protect/activate the C-terminal sulfhydryl of purified Ub-aminoethanethiol, an asymmetric disulfide with DTNP was generated. In a typical reaction, approximately 5 mg of DTNP dissolved in 1.5 mL acetic acid was mixed with approximately 3 mg of Ub-aminoethanethiol dissolved in 0.5 mL water. The reaction was allowed to proceed, shielded from light, for 18-24 hours at 25° C. As the DTNP reacts with Ub-

aminoethanethiol, 2-thio-5-nitropyridine (TNP) is released, which has a bright yellow color. After incubation, the now neon yellow colored solution, was dialyzed in a Slide-A-Lyzer, 3.5kDa MWCO (Pierce) against water to precipitate unreacted DTNP. The desired Ub-aminoethanethiol-5-nitro-2-pyridinesulfenyl (Ub-aminoethanethiol-pNpys) product was then purified by semi-preparative C18 RP-HPLC over a 30-50% B gradient.

Purified Ub-aminoethanethiol-pNpys was mixed at approximately 3:1 molar ratio with histone (either H2AK119C or H2BK120C) in a small volume of 6 M guanidine-HCl, 1 M HEPES, at pH 6.9. As the histone cysteine forms a disulfide bond with Ub-aminoethanethiol, TNP is again released. Within minutes the solution becomes neon yellow. After 10 minutes the reaction was stopped with 0.1% TFA. H2AssUb and H2BssUb formed in this reaction were purified by semi-preparative C18 RP-HPLC, using a 35-65% B gradient.

*xl*H2Bub(G76A) preparation

"Nearly native" *xl*H2Bub(G76A) histone and octamers were prepared by Dr. Rob McGinty as previously described (McGinty et al., 2008).

Dimer, tetramer, and octamer preparation from human histones

For this study, four types of human histone dimers were assembled: H2A/H2B, H2AssUb/H2B, H2A/H2BssUb, H2AssUb/H2BssUb. In equal molar amounts, purified histones were combined at approximately 2 mg/mL in denaturing buffer [50 mM MOPS pH 7, 6 M guanidine-HCl, 20% glycerol, 5 mM EDTA] and dialyzed overnight into refolding buffer [10 mM MOPS pH 7, 500 mM NaCl, 10% glycerol, 0.5 mM EDTA]

using dialysis buttons from Hampton Research. To remove insoluble material, samples were spun at 16,100 x *g* for 30 min at 4 degrees.

For the human octamers used in this study, only unmodified H3/H4 tetramers were needed. Consequently, these were assembled and purified on a large scale, allowing all human octamers prepared to contain the same source of H3. These H3/H4 tetramers were assembled as described above for H2A/H2B dimers, and purified by size exclusion chromatography. Briefly, after clearing the tetramer assembly with a 30 min spin at 16,100 x *g*, tetramers were concentrated to 10-15 mg/mL with Amicon Ultra centrifugal concentrators (Millipore). Size exclusion chromatography was performed on an ÄKTA FPLC with a HiLoad 16/600 Superdex 200 column (GE Healthcare) in refolding buffer. Fractions from the peak corresponding to H3/H4 tetramers were pooled and stored at -20 degrees in 50% glycerol.

Unmodified, H2AssUb, H2BssUb, and H2AssUb/H2BssUb octamers were assembled by mixing purified tetramers and dimers in refolding buffer and dialyzing them into high salt buffer [10 mM MOPS pH 7, 2 M NaCl, 10% glycerol]. Because tetramers are difficult to purify away from octamers using Superdex 200 columns, octamer assemblies were set up with a slight excess of dimer relative to tetramer (e.g. 2.2 moles H2A/H2B dimer : 1 mole H3/H4 tetramer). After clearing octamer assemblies with a 30 min spin at 16,100 x *g*, they were concentrated to 5-10 mg/mL and purified by size exclusion on a Superdex 200 10/300 GL (GE Healthcare) in high salt buffer. Pooled octamer fractions were stored at -20 degrees in 50% glycerol.

Nucleosome positioning sequence preparation and purification

DNA fragments for mononucleosome assemblies were prepared by EcoRV restriction digest of 32x153bp tandem repeats of the 601-positioning sequence(Lowary and Widom, 1998) cloned into pUC19 (a kind gift from Kyle Chiang). After checking by agarose gel electrophoresis that the digest was complete (only 153bp fragments and ~3kb plasmid backbone fragment), 153bp DNA fragments were purified by plasmid backbone precipitation in 500 mM NaCl with 7.5% polyethylene glycol (PEG-6000) on ice for several hours. The soluble DNA fragments were then further purified away from EcoRV protein with several rounds of Phenol/Chloroform extraction and finally ethanol precipitated. Starting with 1 mg of plasmid DNA, the expected yield of purified 153bp 601-positioning sequence is about 400 μg (4.25 nmoles).

Mononucleosome preparation

Gradient dialysis was used to assemble mononucleosomes from octamers and positioning sequence DNA. Approximately equal molar amounts of purified octamers and 153bp DNA were brought to 0.7 mg/mL DNA in high salt buffer (see octamer preparation method). Starting in 1 volume high salt buffer, a peristaltic pump was used to add zero salt buffer [10 mM Tris pH 7.5, 1 mM EDTA] drop-wise over ~24 hours to a final volume of 10 volumes. Completed assemblies were cleared with a spin at 16,100 x *g* and visualized on a native 5% polyacrylamide gel, stained with ethidium bromide. Because the precise octamer to DNA ratio is crucial to obtain assemblies with little or no free 153bp DNA and efficient incorporation of octamers into nucleosomes, small scale

trial assemblies were performed with each batch of purified octamer to determine the optimal measured octamer : DNA ratio.

Endogenous nucleosome purification from HeLa cells

Native nucleosomes were solubilized from HeLa cells with micrococcal nuclease (MNase) and purified by ultracentrifugation on sucrose gradients, essentially as previously described (Fang et al., 2004). Briefly, 4-5L of HeLa S3 cells were grown in spinner culture at ~ 1.5 x 10^6 cells/mL. Cell pellets were washed with PBS and resuspended at ~ 2.5 x 10^7 cells/mL in N1 buffer [10 mM MES, 5 mM $MgCl_2$, 1 mM $CaCl_2$, 15 mM NaCl, 60 mM KCl, 0.25M sucrose, 0.5% Triton X-100, 0.5 mM DTT, pH 7.5] supplemented with 0.1 mM PMSF, 0.5 mM sodium metabisulfite, and 0.5 mM benzamidine-HCl. In this buffer, gentle douncing is sufficient to lyse cells, and pelleted nuclei were washed once with N1 before being resuspended at ~ 8 x 10^8 starting cells/mL in buffer N2 [10 mM PIPES, 5 mM $MgCl_2$, 1 mM $CaCl_2$, pH 6.5] supplemented with 0.1 mM PMSF, 0.5 mM sodium metabisulfite, and 0.5 mM benzamidine-HCl. While leaving the bulk nuclei on ice, a small aliquot (~ 500 μL) was used for trail MNase digests, with the appropriate digestion time determined by 1% agarose gel electrophoresis of MNase solubilized DNA.

After determining digestion conditions, the bulk nuclei were warmed to 37 degrees, and $CaCl_2$ was raised to 5 mM. Digestion at 37 degrees was started by adding ~ 1U Worthington MNase per 10μL nuclei suspension and stopped by adding EDTA to 20mM. Solublized chromatin (S1) was separated from insoluble and nuclear debris by a 10 min spin at 3,000 x g. To solubilize very long chromatin fragments (S2), pellets were

vortexed in 1 pellet volume [1 mM EDTA, 0.2 mM PMSF], rested on ice for 15 min, and then cleared with a 15 min spin at 12,000 x g. S1 and S2 were pooled and NaCl was brought to 750 mM by adding 5 M dropwise. This elevated salt concentration strips most chromatin-associated proteins off nucleosomes, including H1.

32 mL sucrose gradients in NG buffer [10 mM Tris-Cl, 1 mM EDTA, 750 mM NaCl, 0.3 mM PMSF] were prepared in polyallomer tubes with a binary gradient mixing machine, using 5% sucrose/NG and 30% sucrose/NG solutions. After carefully applying ~ 3 mL of the MNase soluble sample on top of each gradient, fractionation was performed by ultracentrifugation for 16 hours at 26,000 rpm in a SW28 rotor. 1 mL fractions were taken from the top of each gradient. Fractions containing minimal non-histone proteins were pooled. If mononucleosomes were desired, a fraction of this pool was dialyzed out of EDTA and digested again with MNase, although this time with ~ 1/10 as much enzyme. All nucleosome pools were further purified by an addition passage over 5-30% sucrose gradients. Final pooling decisions were based on DNA fragment sizes as assessed by 1% agarose gel electrophoresis and EtBr staining. Final fraction pools were concentrated (Amicon Ultra) to ~ 200 ng DNA/μL, dialysed into HSB [10 mM Tris pH 7.5, 10 mM NaCl, 1 mM EDTA, 10% glycerol, 0.2 mM PMSF], and stored at -80 degrees.

Dot1L methyltransferase assays

Flag-hDot1L was purified from a baculovirus expression system as previously described (McGinty et al., 2009a; McGinty et al., 2008). In each methyltransferase assay, 4.1 pmoles of mononucleosomes, 0.14 pmoles of Flag-hDot1L and 15 pmoles ^{3}H-SAM

(1 μCi ^{3}H) were combined in 12 mL at 20mM Tris pH 8.0, 10 mM NaCl, 5 mM $MgCl_2$, 1 mM EDTA. Reactions were allowed to proceed for 75 min at 30 degrees and activity was assessed by fluorography and/or scintillation counting. For fluorography, a fraction of each reaction samples was run on 4-20% Tris-Glycine SDS-PAGE gels. Note that NuPAGE precast gels from Invitrogen reduce the disulfide bond between ubiquitin and histone H2AK119C and H2BK120C, and therefore are not appropriate for however, precast gradient TGX gels from Bio-Rad do not. The gel was Coomassie stained, amplified with Amersham fluorographic reagent, vacuum dried and exposed to film for 12 hours -5 days. For scintillation counting, a fraction of each reaction spotted onto Whatman p81 filter paper, air-dried, washed 3x10 min in 100 mM $NaHCO_3$ and then quickly in acetone. Washed and air-dried filter papers were immersed in Scintillation cocktail (Perkin-Elmer) and scintillation counted.

PRC2 methyltransferase assays

Recombinant PRC2 complex [Ezh2, Flag-Eed3, Suz12, RbAP48] was purified using a baculovirus expression system as previously described(Cao and Zhang, 2004). In a typical methyltransferase assay, 200 ng nucleosomal DNA, 20 ng Ezh2 in PRC2 complex, 15 pmoles ^{3}H-SAM (1 mCi ^{3}H) were combined in 12 mL reactions at 20mM Tris pH 8.0, 10 mM NaCl, 2.5 mM $MgCl_2$, 1 mM EDTA, 0.5 mM DTT. Reactions were carried out at 30 degrees and activity was assessed by fluorography and/or scintillation counting as described for Dot1L methyltransferase assays above.

In vitro enzymatic ubiquitylation of H2A

Recombinant Ring1B-6xHis and GST-Bmi1 were co-expressed in *E. coli* and tandem-affinity purified. In a typical *in vitro* ubiquitylation reaction, 600 ng nucleosomal DNA, 600 ng Ring1B/Bmi1 complex, 1 ug ubiquitin (BostonBiochem), 50 nM 6xHis-UBE1 (BostonBiochem), 3 μM UbcH5c (BostonBiochem), and 4 mM ATP-Mg (Sigma) were combined in a 20 μL reactions in 20mM Tris pH 8.0, 10 mM NaCl, 2 mM $MgCl_2$, 1 mM EDTA, 0.5 mM DTT. Reactions were carried out at 37 degrees for 45-60 minutes, stopped with Laemmli sample buffer. Ubiquitylation activity was assessed by western blotting.

Mass Spectrometry analysis of *in vitro* enzymatic ubiquitylation reactions

Mass Spectrometry analysis was performed by Joe Fernandez, The Rockefeller University Proteomics Resource Center.

Antibodies

The following antibodies were used in this study: anti-H2A (Millipore, # 07-146), anti-H2B (Proteintech, ptglab.com, rabbit polyclonal raised against full-length *Xenopus* laevis histone H2B), anti-H2AK119ub (Nakagawa et al., 2008 (Nakagawa et al., 2008)), anti-H2BK120ub (Cell Signaling Technology, #5546).

REFERENCES

Ahmad, K., and Henikoff, S. (2002). The histone variant H3.3 marks active chromatin by replication-independent nucleosome assembly. Mol Cell *9*, 1191-1200.

Al-Hakim, A., Escribano-Diaz, C., Landry, M.C., O'Donnell, L., Panier, S., Szilard, R.K., and Durocher, D. (2010). The ubiquitous role of ubiquitin in the DNA damage response. DNA repair *9*, 1229-1240.

Allfrey, V.G., Faulkner, R., and Mirsky, A.E. (1964). Acetylation and Methylation of Histones and Their Possible Role in the Regulation of Rna Synthesis. Proc Natl Acad Sci U S A *51*, 786-794.

Allis, C.D., Glover, C.V., Bowen, J.K., and Gorovsky, M.A. (1980). Histone variants specific to the transcriptionally active, amitotically dividing macronucleus of the unicellular eucaryote, Tetrahymena thermophila. Cell *20*, 609-617.

Allis, C.D., Jenuwein, T., and Reinberg, D. (2007). Epigenetics (Cold Spring Harbor, N.Y.: Cold Spring Harbor Laboratory Press).

Allis, C.D., and Muir, T.W. (2011). Spreading chromatin into chemical biology. Chembiochem *12*, 264-279.

Altaf, M., Utley, R.T., Lacoste, N., Tan, S., Briggs, S.D., and Cote, J. (2007). Interplay of chromatin modifiers on a short basic patch of histone H4 tail defines the boundary of telomeric heterochromatin. Mol Cell *28*, 1002-1014.

Armache, K.J., Garlick, J.D., Canzio, D., Narlikar, G.J., and Kingston, R.E. (2011). Structural basis of silencing: Sir3 BAH domain in complex with a nucleosome at 3.0 A resolution. Science *334*, 977-982.

Baek, S.H. (2011). When signaling kinases meet histones and histone modifiers in the nucleus. Mol Cell *42*, 274-284.

Banaszynski, L.A., Allis, C.D., and Lewis, P.W. (2010). Histone variants in metazoan development. Dev Cell *19*, 662-674.

Bannister, A.J., Zegerman, P., Partridge, J.F., Miska, E.A., Thomas, J.O., Allshire, R.C., and Kouzarides, T. (2001). Selective recognition of methylated lysine 9 on histone H3 by the HP1 chromo domain. Nature *410*, 120-124.

Barsoum, J., and Varshavsky, A. (1985). Preferential localization of variant nucleosomes near the 5'-end of the mouse dihydrofolate reductase gene. J Biol Chem *260*, 7688-7697.

Batta, K., Zhang, Z., Yen, K., Goffman, D.B., and Pugh, B.F. (2011). Genome-wide function of H2B ubiquitylation in promoter and genic regions. Genes Dev *25*, 2254-2265.

Bekker-Jensen, S., and Mailand, N. (2011). The ubiquitin- and SUMO-dependent signaling response to DNA double-strand breaks. FEBS Lett.

Ben-Saadon, R., Zaaroor, D., Ziv, T., and Ciechanover, A. (2006). The polycomb protein Ring1B generates self atypical mixed ubiquitin chains required for its in vitro histone H2A ligase activity. Mol Cell *24*, 701-711.

Berger, S.L. (2010). Cell signaling and transcriptional regulation via histone phosphorylation. Cold Spring Harb Symp Quant Biol *75*, 23-26.

Bernstein, B.E., Kamal, M., Lindblad-Toh, K., Bekiranov, S., Bailey, D.K., Huebert, D.J., McMahon, S., Karlsson, E.K., Kulbokas, E.J., 3rd, Gingeras, T.R.*, et al*. (2005). Genomic maps and comparative analysis of histone modifications in human and mouse. Cell *120*, 169-181.

Bernstein, E., Duncan, E.M., Masui, O., Gil, J., Heard, E., and Allis, C.D. (2006). Mouse polycomb proteins bind differentially to methylated histone H3 and RNA and are enriched in facultative heterochromatin. Mol Cell Biol *26*, 2560-2569.

Birve, A., Sengupta, A.K., Beuchle, D., Larsson, J., Kennison, J.A., Rasmuson-Lestander, A., and Muller, J. (2001). Su(z)12, a novel Drosophila Polycomb group gene that is conserved in vertebrates and plants. Development *128*, 3371-3379.

Blaschke, U.K., Silberstein, J., and Muir, T.W. (2000). Protein engineering by expressed protein ligation. Methods Enzymol *328*, 478-496.

Bohm, L., Briand, G., Sautiere, P., and Crane-Robinson, C. (1982). Proteolytic digestion studies of chromatin core-histone structure. Identification of limit peptides from histone H2B. Eur J Biochem *123*, 299-303.

Bohm, L., Crane-Robinson, C., and Sautiere, P. (1980). Proteolytic digestion studies of chromatin core-histone structure. Identification of a limit peptide of histone H2A. Eur J Biochem *106*, 525-530.

Boyer, L.A., Latek, R.R., and Peterson, C.L. (2004). The SANT domain: a unique histone-tail-binding module? Nature reviews Molecular cell biology *5*, 158-163.

Boyer, L.A., Plath, K., Zeitlinger, J., Brambrink, T., Medeiros, L.A., Lee, T.I., Levine, S.S., Wernig, M., Tajonar, A., Ray, M.K., *et al*. (2006). Polycomb complexes repress developmental regulators in murine embryonic stem cells. Nature *441*, 349-353.

Briggs, S.D., Xiao, T., Sun, Z.W., Caldwell, J.A., Shabanowitz, J., Hunt, D.F., Allis, C.D., and Strahl, B.D. (2002). Gene silencing: trans-histone regulatory pathway in chromatin. Nature *418*, 498.

Cao, R., Tsukada, Y., and Zhang, Y. (2005). Role of Bmi-1 and Ring1A in H2A ubiquitylation and Hox gene silencing. Mol Cell *20*, 845-854.

Cao, R., Wang, L., Wang, H., Xia, L., Erdjument-Bromage, H., Tempst, P., Jones, R.S., and Zhang, Y. (2002). Role of histone H3 lysine 27 methylation in Polycomb-group silencing. Science *298*, 1039-1043.

Cao, R., and Zhang, Y. (2004). SUZ12 is required for both the histone methyltransferase activity and the silencing function of the EED-EZH2 complex. Mol Cell *15*, 57-67.

Chandrasekharan, M.B., Huang, F., and Sun, Z.W. (2009). Ubiquitination of histone H2B regulates chromatin dynamics by enhancing nucleosome stability. Proc Natl Acad Sci U S A *106*, 16686-16691.

Chatterjee, C., McGinty, R.K., Fierz, B., and Muir, T.W. (2010). Disulfide-directed histone ubiquitylation reveals plasticity in hDot1L activation. Nat Chem Biol *6*, 267-269.

Chatterjee, C., and Muir, T.W. (2010). Chemical approaches for studying histone modifications. J Biol Chem *285*, 11045-11050.

Chen, Z.J., and Sun, L.J. (2009). Nonproteolytic functions of ubiquitin in cell signaling. Mol Cell *33*, 275-286.

Chodaparambil, J.V., Barbera, A.J., Lu, X., Kaye, K.M., Hansen, J.C., and Luger, K. (2007). A charged and contoured surface on the nucleosome regulates chromatin compaction. Nature structural & molecular biology *14*, 1105-1107.

Czermin, B., Melfi, R., McCabe, D., Seitz, V., Imhof, A., and Pirrotta, V. (2002). Drosophila enhancer of Zeste/ESC complexes have a histone H3 methyltransferase activity that marks chromosomal Polycomb sites. Cell *111*, 185-196.

Daniel, J.A., Torok, M.S., Sun, Z.W., Schieltz, D., Allis, C.D., Yates, J.R., 3rd, and Grant, P.A. (2004). Deubiquitination of histone H2B by a yeast acetyltransferase complex regulates transcription. J Biol Chem *279*, 1867-1871.

Davey, C.A., Sargent, D.F., Luger, K., Maeder, A.W., and Richmond, T.J. (2002). Solvent mediated interactions in the structure of the nucleosome core particle at 1.9 a resolution. J Mol Biol *319*, 1097-1113.

Dawson, B.A., Herman, T., Haas, A.L., and Lough, J. (1991). Affinity isolation of active murine erythroleukemia cell chromatin: uniform distribution of ubiquitinated histone H2A between active and inactive fractions. J Cell Biochem *46*, 166-173.

de Napoles, M., Mermoud, J.E., Wakao, R., Tang, Y.A., Endoh, M., Appanah, R., Nesterova, T.B., Silva, J., Otte, A.P., Vidal, M.*, et al*. (2004). Polycomb group proteins Ring1A/B link ubiquitylation of histone H2A to heritable gene silencing and X inactivation. Dev Cell *7*, 663-676.

Deshaies, R.J., and Joazeiro, C.A. (2009). RING domain E3 ubiquitin ligases. Annual review of biochemistry *78*, 399-434.

Dorigo, B., Schalch, T., Bystricky, K., and Richmond, T.J. (2003). Chromatin fiber folding: requirement for the histone H4 N-terminal tail. J Mol Biol *327*, 85-96.

Dover, J., Schneider, J., Tawiah-Boateng, M.A., Wood, A., Dean, K., Johnston, M., and Shilatifard, A. (2002). Methylation of histone H3 by COMPASS requires ubiquitination of histone H2B by Rad6. J Biol Chem *277*, 28368-28371.

Eissenberg, J.C., Morris, G.D., Reuter, G., and Hartnett, T. (1992). The heterochromatin-associated protein HP-1 is an essential protein in Drosophila with dosage-dependent effects on position-effect variegation. Genetics *131*, 345-352.

Eskeland, R., Leeb, M., Grimes, G.R., Kress, C., Boyle, S., Sproul, D., Gilbert, N., Fan, Y., Skoultchi, A.I., Wutz, A., *et al*. (2010). Ring1B compacts chromatin structure and represses gene expression independent of histone ubiquitination. Mol Cell *38*, 452-464.

Fang, J., Wang, H., and Zhang, Y. (2004). Purification of histone methyltransferases from HeLa cells. Methods Enzymol *377*, 213-226.

Feng, Q., Wang, H., Ng, H.H., Erdjument-Bromage, H., Tempst, P., Struhl, K., and Zhang, Y. (2002). Methylation of H3-lysine 79 is mediated by a new family of HMTases without a SET domain. Curr Biol *12*, 1052-1058.

Feng, Y., Yang, Y., Ortega, M.M., Copeland, J.N., Zhang, M., Jacob, J.B., Fields, T.A., Vivian, J.L., and Fields, P.E. (2010). Early mammalian erythropoiesis requires the Dot1L methyltransferase. Blood *116*, 4483-4491.

Fierz, B., Chatterjee, C., McGinty, R.K., Bar-Dagan, M., Raleigh, D.P., and Muir, T.W. (2011). Histone H2B ubiquitylation disrupts local and higher-order chromatin compaction. Nat Chem Biol *7*, 113-119.

Fischle, W., Tseng, B.S., Dormann, H.L., Ueberheide, B.M., Garcia, B.A., Shabanowitz, J., Hunt, D.F., Funabiki, H., and Allis, C.D. (2005). Regulation of HP1-chromatin binding by histone H3 methylation and phosphorylation. Nature *438*, 1116-1122.

Fischle, W., Wang, Y., and Allis, C.D. (2003). Binary switches and modification cassettes in histone biology and beyond. Nature *425*, 475-479.

Flavell, R.R., Kothari, P., Bar-Dagan, M., Synan, M., Vallabhajosula, S., Friedman, J.M., Muir, T.W., and Ceccarini, G. (2008). Site-specific (18)F-labeling of the protein hormone leptin using a general two-step ligation procedure. Journal of the American Chemical Society *130*, 9106-9112.

Flavell, R.R., and Muir, T.W. (2009). Expressed protein ligation (EPL) in the study of signal transduction, ion conduction, and chromatin biology. Accounts of chemical research *42*, 107-116.

Fleming, A.B., Kao, C.F., Hillyer, C., Pikaart, M., and Osley, M.A. (2008). H2B ubiquitylation plays a role in nucleosome dynamics during transcription elongation. Mol Cell *31*, 57-66.

Gamble, M.J., and Kraus, W.L. (2010). Multiple facets of the unique histone variant macroH2A: from genomics to cell biology. Cell Cycle *9*, 2568-2574.

Garcia, B.A., Hake, S.B., Diaz, R.L., Kauer, M., Morris, S.A., Recht, J., Shabanowitz, J., Mishra, N., Strahl, B.D., Allis, C.D., *et al*. (2007). Organismal differences in post-translational modifications in histones H3 and H4. J Biol Chem *282*, 7641-7655.

Gehani, S.S., Agrawal-Singh, S., Dietrich, N., Christophersen, N.S., Helin, K., and Hansen, K. (2010). Polycomb group protein displacement and gene activation through MSK-dependent H3K27me3S28 phosphorylation. Mol Cell *39*, 886-900.

Goldberg, A.D., Banaszynski, L.A., Noh, K.M., Lewis, P.W., Elsaesser, S.J., Stadler, S., Dewell, S., Law, M., Guo, X., Li, X., *et al*. (2010). Distinct factors control histone variant H3.3 localization at specific genomic regions. Cell *140*, 678-691.

Goldknopf, I.L., and Busch, H. (1977). Isopeptide linkage between nonhistone and histone 2A polypeptides of chromosomal conjugate-protein A24. Proc Natl Acad Sci U S A *74*, 864-868.

Haase, C., Rohde, H., and Seitz, O. (2008). Native chemical ligation at valine. Angew Chem Int Ed Engl *47*, 6807-6810.

Hake, S.B., Garcia, B.A., Kauer, M., Baker, S.P., Shabanowitz, J., Hunt, D.F., and Allis, C.D. (2005). Serine 31 phosphorylation of histone variant H3.3 is specific to regions bordering centromeres in metaphase chromosomes. Proc Natl Acad Sci U S A *102*, 6344-6349.

Han, Z., Xing, X., Hu, M., Zhang, Y., Liu, P., and Chai, J. (2007). Structural basis of EZH2 recognition by EED. Structure *15*, 1306-1315.

Hansen, J.C. (2002). Conformational dynamics of the chromatin fiber in solution: determinants, mechanisms, and functions. Annual review of biophysics and biomolecular structure *31*, 361-392.

He, S., Bauman, D., Davis, J.S., Loyola, A., Nishioka, K., Gronlund, J.L., Reinberg, D., Meng, F., Kelleher, N., and McCafferty, D.G. (2003). Facile synthesis of site-specifically acetylated and methylated histone proteins: reagents for evaluation of the histone code hypothesis. Proc Natl Acad Sci U S A *100*, 12033-12038.

Heard, E. (2004). Recent advances in X-chromosome inactivation. Current opinion in cell biology *16*, 247-255.

Hennig, L., and Derkacheva, M. (2009). Diversity of Polycomb group complexes in plants: same rules, different players? Trends in genetics : TIG *25*, 414-423.

Henry, K.W., Wyce, A., Lo, W.S., Duggan, L.J., Emre, N.C., Kao, C.F., Pillus, L., Shilatifard, A., Osley, M.A., and Berger, S.L. (2003). Transcriptional activation via sequential histone H2B ubiquitylation and deubiquitylation, mediated by SAGA-associated Ubp8. Genes Dev *17*, 2648-2663.

Huang, S.Y., Barnard, M.B., Xu, M., Matsui, S., Rose, S.M., and Garrard, W.T. (1986). The active immunoglobulin kappa chain gene is packaged by non-ubiquitin-conjugated nucleosomes. Proc Natl Acad Sci U S A *83*, 3738-3742.

Hunt, L.T., and Dayhoff, M.O. (1977). Amino-terminal sequence identity of ubiquitin and the nonhistone component of nuclear protein A24. Biochemical and biophysical research communications *74*, 650-655.

Ikeda, F., and Dikic, I. (2008). Atypical ubiquitin chains: new molecular signals. 'Protein Modifications: Beyond the Usual Suspects' review series. EMBO reports *9*, 536-542.

Jacobs, S.A., and Khorasanizadeh, S. (2002). Structure of HP1 chromodomain bound to a lysine 9-methylated histone H3 tail. Science *295*, 2080-2083.

Jacobs, S.A., Taverna, S.D., Zhang, Y., Briggs, S.D., Li, J., Eissenberg, J.C., Allis, C.D., and Khorasanizadeh, S. (2001). Specificity of the HP1 chromo domain for the methylated N-terminus of histone H3. Embo J *20*, 5232-5241.

Jason, L.J., Moore, S.C., Ausio, J., and Lindsey, G. (2001). Magnesium-dependent association and folding of oligonucleosomes reconstituted with ubiquitinated H2A. J Biol Chem *276*, 14597-14601.

Jin, C., and Felsenfeld, G. (2006). Distribution of histone H3.3 in hematopoietic cell lineages. Proc Natl Acad Sci U S A *103*, 574-579.

Jones, B., Su, H., Bhat, A., Lei, H., Bajko, J., Hevi, S., Baltus, G.A., Kadam, S., Zhai, H., Valdez, R.*, et al*. (2008). The histone H3K79 methyltransferase Dot1L is essential for mammalian development and heterochromatin structure. PLoS Genet *4*, e1000190.

Joo, H.Y., Zhai, L., Yang, C., Nie, S., Erdjument-Bromage, H., Tempst, P., Chang, C., and Wang, H. (2007). Regulation of cell cycle progression and gene expression by H2A deubiquitination. Nature *449*, 1068-1072.

Kallin, E.M., Cao, R., Jothi, R., Xia, K., Cui, K., Zhao, K., and Zhang, Y. (2009). Genome-wide uH2A localization analysis highlights Bmi1-dependent deposition of the mark at repressed genes. PLoS Genet *5*, e1000506.

Kennison, J.A. (1995). The Polycomb and trithorax group proteins of Drosophila: trans-regulators of homeotic gene function. Annual review of genetics *29*, 289-303.

Ketel, C.S., Andersen, E.F., Vargas, M.L., Suh, J., Strome, S., and Simon, J.A. (2005). Subunit contributions to histone methyltransferase activities of fly and worm polycomb group complexes. Mol Cell Biol *25*, 6857-6868.

Kharchenko, P.V., Alekseyenko, A.A., Schwartz, Y.B., Minoda, A., Riddle, N.C., Ernst, J., Sabo, P.J., Larschan, E., Gorchakov, A.A., Gu, T., *et al*. (2011). Comprehensive analysis of the chromatin landscape in Drosophila melanogaster. Nature *471*, 480-485.

Kim, J., Guermah, M., McGinty, R.K., Lee, J.S., Tang, Z., Milne, T.A., Shilatifard, A., Muir, T.W., and Roeder, R.G. (2009). RAD6-Mediated transcription-coupled H2B ubiquitylation directly stimulates H3K4 methylation in human cells. Cell *137*, 459-471.

Kim, J., Hake, S.B., and Roeder, R.G. (2005). The human homolog of yeast BRE1 functions as a transcriptional coactivator through direct activator interactions. Mol Cell *20*, 759-770.

Kim, J., and Roeder, R.G. (2009). Direct Bre1-Paf1 complex interactions and RING finger-independent Bre1-Rad6 interactions mediate histone H2B ubiquitylation in yeast. J Biol Chem *284*, 20582-20592.

Klein, R.R., and Houtz, R.L. (1995). Cloning and developmental expression of pea ribulose-1,5-bisphosphate carboxylase/oxygenase large subunit N-methyltransferase. Plant molecular biology *27*, 249-261.

Kornberg, R.D. (1974). Chromatin structure: a repeating unit of histones and DNA. Science *184*, 868-871.

Kouskouti, A., and Talianidis, I. (2005). Histone modifications defining active genes persist after transcriptional and mitotic inactivation. Embo J *24*, 347-357.

Krogan, N.J., Dover, J., Wood, A., Schneider, J., Heidt, J., Boateng, M.A., Dean, K., Ryan, O.W., Golshani, A., Johnston, M., *et al*. (2003). The Paf1 complex is required for histone H3 methylation by COMPASS and Dot1p: linking transcriptional elongation to histone methylation. Mol Cell *11*, 721-729.

Kuzmichev, A., Nishioka, K., Erdjument-Bromage, H., Tempst, P., and Reinberg, D. (2002). Histone methyltransferase activity associated with a human multiprotein complex containing the Enhancer of Zeste protein. Genes Dev *16*, 2893-2905.

Lachner, M., O'Carroll, D., Rea, S., Mechtler, K., and Jenuwein, T. (2001). Methylation of histone H3 lysine 9 creates a binding site for HP1 proteins. Nature *410*, 116-120.

Lacoste, N., Utley, R.T., Hunter, J.M., Poirier, G.G., and Cote, J. (2002). Disruptor of telomeric silencing-1 is a chromatin-specific histone H3 methyltransferase. J Biol Chem *277*, 30421-30424.

Lau, P.N., and Cheung, P. (2011). Histone code pathway involving H3 S28 phosphorylation and K27 acetylation activates transcription and antagonizes polycomb silencing. Proc Natl Acad Sci U S A *108*, 2801-2806.

Levinger, L., and Varshavsky, A. (1982). Selective arrangement of ubiquitinated and D1 protein-containing nucleosomes within the Drosophila genome. Cell *28*, 375-385.

Li, Z., Cao, R., Wang, M., Myers, M.P., Zhang, Y., and Xu, R.M. (2006). Structure of a Bmi-1-Ring1B polycomb group ubiquitin ligase complex. J Biol Chem *281*, 20643-20649.

Lorentz, A., Ostermann, K., Fleck, O., and Schmidt, H. (1994). Switching gene swi6, involved in repression of silent mating-type loci in fission yeast, encodes a homologue of chromatin-associated proteins from Drosophila and mammals. Gene *143*, 139-143.

Lowary, P.T., and Widom, J. (1998). New DNA sequence rules for high affinity binding to histone octamer and sequence-directed nucleosome positioning. J Mol Biol *276*, 19-42.

Lu, X., Simon, M.D., Chodaparambil, J.V., Hansen, J.C., Shokat, K.M., and Luger, K. (2008). The effect of H3K79 dimethylation and H4K20 trimethylation on nucleosome and chromatin structure. Nature structural & molecular biology *15*, 1122-1124.

Luger, K., Mader, A.W., Richmond, R.K., Sargent, D.F., and Richmond, T.J. (1997). Crystal structure of the nucleosome core particle at 2.8 A resolution. Nature *389*, 251-260.

Luger, K., Rechsteiner, T.J., and Richmond, T.J. (1999). Preparation of nucleosome core particle from recombinant histones. Methods Enzymol *304*, 3-19.

Margueron, R., Justin, N., Ohno, K., Sharpe, M.L., Son, J., Drury, W.J., 3rd, Voigt, P., Martin, S.R., Taylor, W.R., De Marco, V.*, et al*. (2009). Role of the polycomb protein EED in the propagation of repressive histone marks. Nature *461*, 762-767.

Margueron, R., and Reinberg, D. (2011). The Polycomb complex PRC2 and its mark in life. Nature *469*, 343-349.

McGinty, R.K., Chatterjee, C., and Muir, T.W. (2009a). Semisynthesis of ubiquitylated proteins. Methods Enzymol *462*, 225-243.

McGinty, R.K., Kim, J., Chatterjee, C., Roeder, R.G., and Muir, T.W. (2008). Chemically ubiquitylated histone H2B stimulates hDot1L-mediated intranucleosomal methylation. Nature *453*, 812-816.

McGinty, R.K., Kohn, M., Chatterjee, C., Chiang, K.P., Pratt, M.R., and Muir, T.W. (2009b). Structure-activity analysis of semisynthetic nucleosomes: mechanistic insights into the stimulation of Dot1L by ubiquitylated histone H2B. ACS Chem Biol *4*, 958-968.

Min, J., Feng, Q., Li, Z., Zhang, Y., and Xu, R.M. (2003). Structure of the catalytic domain of human DOT1L, a non-SET domain nucleosomal histone methyltransferase. Cell *112*, 711-723.

Minsky, N., and Oren, M. (2004). The RING domain of Mdm2 mediates histone ubiquitylation and transcriptional repression. Mol Cell *16*, 631-639.

Minsky, N., Shema, E., Field, Y., Schuster, M., Segal, E., and Oren, M. (2008). Monoubiquitinated H2B is associated with the transcribed region of highly expressed genes in human cells. Nat Cell Biol *10*, 483-488.

Mito, Y., Henikoff, J.G., and Henikoff, S. (2005). Genome-scale profiling of histone H3.3 replacement patterns. Nat Genet *37*, 1090-1097.

Mito, Y., Henikoff, J.G., and Henikoff, S. (2007). Histone replacement marks the boundaries of cis-regulatory domains. Science *315*, 1408-1411.

Montgomery, N.D., Yee, D., Chen, A., Kalantry, S., Chamberlain, S.J., Otte, A.P., and Magnuson, T. (2005). The murine polycomb group protein Eed is required for global histone H3 lysine-27 methylation. Curr Biol *15*, 942-947.

Mueller, R.D., Yasuda, H., Hatch, C.L., Bonner, W.M., and Bradbury, E.M. (1985). Identification of ubiquitinated histones 2A and 2B in Physarum polycephalum. Disappearance of these proteins at metaphase and reappearance at anaphase. J Biol Chem *260*, 5147-5153.

Muir, T.W., Sondhi, D., and Cole, P.A. (1998). Expressed protein ligation: a general method for protein engineering. Proc Natl Acad Sci U S A *95*, 6705-6710.

Muller, J., Hart, C.M., Francis, N.J., Vargas, M.L., Sengupta, A., Wild, B., Miller, E.L., O'Connor, M.B., Kingston, R.E., and Simon, J.A. (2002). Histone methyltransferase activity of a Drosophila Polycomb group repressor complex. Cell *111*, 197-208.

Murzina, N.V., Pei, X.Y., Zhang, W., Sparkes, M., Vicente-Garcia, J., Pratap, J.V., McLaughlin, S.H., Ben-Shahar, T.R., Verreault, A., Luisi, B.F., *et al*. (2008). Structural basis for the recognition of histone H4 by the histone-chaperone RbAp46. Structure *16*, 1077-1085.

Nakagawa, T., Kajitani, T., Togo, S., Masuko, N., Ohdan, H., Hishikawa, Y., Koji, T., Matsuyama, T., Ikura, T., Muramatsu, M., *et al*. (2008). Deubiquitylation of histone H2A activates transcriptional initiation via trans-histone cross-talk with H3K4 di- and trimethylation. Genes Dev *22*, 37-49.

Nekrasov, M., Klymenko, T., Fraterman, S., Papp, B., Oktaba, K., Kocher, T., Cohen, A., Stunnenberg, H.G., Wilm, M., and Muller, J. (2007). Pcl-PRC2 is needed to generate high levels of H3-K27 trimethylation at Polycomb target genes. Embo J *26*, 4078-4088.

Nekrasov, M., Wild, B., and Muller, J. (2005). Nucleosome binding and histone methyltransferase activity of Drosophila PRC2. EMBO reports *6*, 348-353.

Ng, H.H., Ciccone, D.N., Morshead, K.B., Oettinger, M.A., and Struhl, K. (2003a). Lysine-79 of histone H3 is hypomethylated at silenced loci in yeast and mammalian cells: a potential mechanism for position-effect variegation. Proc Natl Acad Sci U S A *100*, 1820-1825.

Ng, H.H., Dole, S., and Struhl, K. (2003b). The Rtf1 component of the Paf1 transcriptional elongation complex is required for ubiquitination of histone H2B. J Biol Chem *278*, 33625-33628.

Ng, H.H., Feng, Q., Wang, H., Erdjument-Bromage, H., Tempst, P., Zhang, Y., and Struhl, K. (2002a). Lysine methylation within the globular domain of histone H3 by Dot1 is important for telomeric silencing and Sir protein association. Genes Dev *16*, 1518-1527.

Ng, H.H., Xu, R.M., Zhang, Y., and Struhl, K. (2002b). Ubiquitination of histone H2B by Rad6 is required for efficient Dot1-mediated methylation of histone H3 lysine 79. J Biol Chem *277*, 34655-34657.

Nguyen, A.T., Xiao, B., Neppl, R.L., Kallin, E.M., Li, J., Chen, T., Wang, D.Z., Xiao, X., and Zhang, Y. (2011). DOT1L regulates dystrophin expression and is critical for cardiac function. Genes Dev *25*, 263-274.

Nickel, B.E., Allis, C.D., and Davie, J.R. (1989). Ubiquitinated histone H2B is preferentially located in transcriptionally active chromatin. Biochemistry *28*, 958-963.

Nielsen, P.R., Nietlispach, D., Mott, H.R., Callaghan, J., Bannister, A., Kouzarides, T., Murzin, A.G., Murzina, N.V., and Laue, E.D. (2002). Structure of the HP1 chromodomain bound to histone H3 methylated at lysine 9. Nature *416*, 103-107.

Okada, Y., Feng, Q., Lin, Y., Jiang, Q., Li, Y., Coffield, V.M., Su, L., Xu, G., and Zhang, Y. (2005). hDOT1L links histone methylation to leukemogenesis. Cell *121*, 167-178.

Olins, A.L., and Olins, D.E. (1974). Spheroid chromatin units (v bodies). Science *183*, 330-332.

Pasini, D., Bracken, A.P., Jensen, M.R., Lazzerini Denchi, E., and Helin, K. (2004). Suz12 is essential for mouse development and for EZH2 histone methyltransferase activity. Embo J *23*, 4061-4071.

Pavri, R., Zhu, B., Li, G., Trojer, P., Mandal, S., Shilatifard, A., and Reinberg, D. (2006). Histone H2B monoubiquitination functions cooperatively with FACT to regulate elongation by RNA polymerase II. Cell *125*, 703-717.

Pickart, C.M. (2004). Back to the future with ubiquitin. Cell *116*, 181-190.

Pina, B., and Suau, P. (1987). Changes in histones H2A and H3 variant composition in differentiating and mature rat brain cortical neurons. Developmental biology *123*, 51-58.

Qian, C., and Zhou, M.M. (2006). SET domain protein lysine methyltransferases: Structure, specificity and catalysis. Cellular and molecular life sciences : CMLS *63*, 2755-2763.

Ray-Gallet, D., Woolfe, A., Vassias, I., Pellentz, C., Lacoste, N., Puri, A., Schultz, D.C., Pchelintsev, N.A., Adams, P.D., Jansen, L.E.*, et al*. (2011). Dynamics of histone h3 deposition in vivo reveal a nucleosome gap-filling mechanism for h3.3 to maintain chromatin integrity. Mol Cell *44*, 928-941.

Rea, S., Eisenhaber, F., O'Carroll, D., Strahl, B.D., Sun, Z.W., Schmid, M., Opravil, S., Mechtler, K., Ponting, C.P., Allis, C.D.*, et al*. (2000). Regulation of chromatin structure by site-specific histone H3 methyltransferases. Nature *406*, 593-599.

Richly, H., Rocha-Viegas, L., Ribeiro, J.D., Demajo, S., Gundem, G., Lopez-Bigas, N., Nakagawa, T., Rospert, S., Ito, T., and Di Croce, L. (2010). Transcriptional activation of polycomb-repressed genes by ZRF1. Nature *468*, 1124-1128.

Robinson, P.J., An, W., Routh, A., Martino, F., Chapman, L., Roeder, R.G., and Rhodes, D. (2008). 30 nm chromatin fibre decompaction requires both H4-K16 acetylation and linker histone eviction. J Mol Biol *381*, 816-825.

Robzyk, K., Recht, J., and Osley, M.A. (2000). Rad6-dependent ubiquitination of histone H2B in yeast. Science *287*, 501-504.

Roudier, F., Ahmed, I., Berard, C., Sarazin, A., Mary-Huard, T., Cortijo, S., Bouyer, D., Caillieux, E., Duvernois-Berthet, E., Al-Shikhley, L.*, et al*. (2011). Integrative epigenomic mapping defines four main chromatin states in Arabidopsis. Embo J *30*, 1928-1938.

Ruthenburg, A.J., Li, H., Milne, T.A., Dewell, S., McGinty, R.K., Yuen, M., Ueberheide, B., Dou, Y., Muir, T.W., Patel, D.J., *et al*. (2011). Recognition of a mononucleosomal histone modification pattern by BPTF via multivalent interactions. Cell *145*, 692-706.

Santos-Rosa, H., Schneider, R., Bannister, A.J., Sherriff, J., Bernstein, B.E., Emre, N.C., Schreiber, S.L., Mellor, J., and Kouzarides, T. (2002). Active genes are tri-methylated at K4 of histone H3. Nature *419*, 407-411.

Sarma, K., Margueron, R., Ivanov, A., Pirrotta, V., and Reinberg, D. (2008). Ezh2 requires PHF1 to efficiently catalyze H3 lysine 27 trimethylation in vivo. Mol Cell Biol *28*, 2718-2731.

Sawada, K., Yang, Z., Horton, J.R., Collins, R.E., Zhang, X., and Cheng, X. (2004). Structure of the conserved core of the yeast Dot1p, a nucleosomal histone H3 lysine 79 methyltransferase. J Biol Chem *279*, 43296-43306.

Schalch, T., Duda, S., Sargent, D.F., and Richmond, T.J. (2005). X-ray structure of a tetranucleosome and its implications for the chromatin fibre. Nature *436*, 138-141.

Scheuermann, J.C., de Ayala Alonso, A.G., Oktaba, K., Ly-Hartig, N., McGinty, R.K., Fraterman, S., Wilm, M., Muir, T.W., and Muller, J. (2010). Histone H2A deubiquitinase activity of the Polycomb repressive complex PR-DUB. Nature *465*, 243-247.

Schmitges, F.W., Prusty, A.B., Faty, M., Stutzer, A., Lingaraju, G.M., Aiwazian, J., Sack, R., Hess, D., Li, L., Zhou, S., *et al*. (2011). Histone methylation by PRC2 is inhibited by active chromatin marks. Mol Cell *42*, 330-341.

Schnell, J.D., and Hicke, L. (2003). Non-traditional functions of ubiquitin and ubiquitin-binding proteins. J Biol Chem *278*, 35857-35860.

Schubeler, D., MacAlpine, D.M., Scalzo, D., Wirbelauer, C., Kooperberg, C., van Leeuwen, F., Gottschling, D.E., O'Neill, L.P., Turner, B.M., Delrow, J., *et al*. (2004). The histone modification pattern of active genes revealed through genome-wide chromatin analysis of a higher eukaryote. Genes Dev *18*, 1263-1271.

Schuettengruber, B., Chourrout, D., Vervoort, M., Leblanc, B., and Cavalli, G. (2007). Genome regulation by polycomb and trithorax proteins. Cell *128*, 735-745.

Schulze, J.M., Hentrich, T., Nakanishi, S., Gupta, A., Emberly, E., Shilatifard, A., and Kobor, M.S. (2011). Splitting the task: Ubp8 and Ubp10 deubiquitinate different cellular pools of H2BK123. Genes Dev *25*, 2242-2247.

Seale, R.L. (1981). Rapid turnover of the histone-ubiquitin conjugate, protein A24. Nucleic Acids Res *9*, 3151-3158.

Shanower, G.A., Muller, M., Blanton, J.L., Honti, V., Gyurkovics, H., and Schedl, P. (2005). Characterization of the grappa gene, the Drosophila histone H3 lysine 79 methyltransferase. Genetics *169*, 173-184.

Shema, E., Tirosh, I., Aylon, Y., Huang, J., Ye, C., Moskovits, N., Raver-Shapira, N., Minsky, N., Pirngruber, J., Tarcic, G., *et al*. (2008). The histone H2B-specific ubiquitin ligase RNF20/hBRE1 acts as a putative tumor suppressor through selective regulation of gene expression. Genes Dev *22*, 2664-2676.

Shogren-Knaak, M., Ishii, H., Sun, J.M., Pazin, M.J., Davie, J.R., and Peterson, C.L. (2006). Histone H4-K16 acetylation controls chromatin structure and protein interactions. Science *311*, 844-847.

Shogren-Knaak, M.A., and Peterson, C.L. (2004). Creating designer histones by native chemical ligation. Methods Enzymol *375*, 62-76.

Simon, M.D., Chu, F., Racki, L.R., de la Cruz, C.C., Burlingame, A.L., Panning, B., Narlikar, G.J., and Shokat, K.M. (2007). The site-specific installation of methyl-lysine analogs into recombinant histones. Cell *128*, 1003-1012.

Singer, M.S., Kahana, A., Wolf, A.J., Meisinger, L.L., Peterson, S.E., Goggin, C., Mahowald, M., and Gottschling, D.E. (1998). Identification of high-copy disruptors of telomeric silencing in Saccharomyces cerevisiae. Genetics *150*, 613-632.

Steger, D.J., Lefterova, M.I., Ying, L., Stonestrom, A.J., Schupp, M., Zhuo, D., Vakoc, A.L., Kim, J.E., Chen, J., Lazar, M.A., *et al*. (2008). DOT1L/KMT4 recruitment and H3K79 methylation are ubiquitously coupled with gene transcription in mammalian cells. Mol Cell Biol *28*, 2825-2839.

Stock, J.K., Giadrossi, S., Casanova, M., Brookes, E., Vidal, M., Koseki, H., Brockdorff, N., Fisher, A.G., and Pombo, A. (2007). Ring1-mediated ubiquitination of H2A restrains poised RNA polymerase II at bivalent genes in mouse ES cells. Nat Cell Biol *9*, 1428-1435.

Sun, Z.W., and Allis, C.D. (2002). Ubiquitination of histone H2B regulates H3 methylation and gene silencing in yeast. Nature *418*, 104-108.

Sung, S., and Amasino, R.M. (2005). Remembering winter: toward a molecular understanding of vernalization. Annual review of plant biology *56*, 491-508.

Talbert, P.B., and Henikoff, S. (2010). Histone variants--ancient wrap artists of the epigenome. Nature reviews Molecular cell biology *11*, 264-275.

Tan, M., Luo, H., Lee, S., Jin, F., Yang, J.S., Montellier, E., Buchou, T., Cheng, Z., Rousseaux, S., Rajagopal, N., *et al*. (2011). Identification of 67 histone marks and histone lysine crotonylation as a new type of histone modification. Cell *146*, 1016-1028.

Tanny, J.C., Erdjument-Bromage, H., Tempst, P., and Allis, C.D. (2007). Ubiquitylation of histone H2B controls RNA polymerase II transcription elongation independently of histone H3 methylation. Genes Dev *21*, 835-847.

Taverna, S.D., Li, H., Ruthenburg, A.J., Allis, C.D., and Patel, D.J. (2007). How chromatin-binding modules interpret histone modifications: lessons from professional pocket pickers. Nature structural & molecular biology *14*, 1025-1040.

Tschiersch, B., Hofmann, A., Krauss, V., Dorn, R., Korge, G., and Reuter, G. (1994). The protein encoded by the Drosophila position-effect variegation suppressor gene Su(var)3-9 combines domains of antagonistic regulators of homeotic gene complexes. Embo J *13*, 3822-3831.

Tse, C., Sera, T., Wolffe, A.P., and Hansen, J.C. (1998). Disruption of higher-order folding by core histone acetylation dramatically enhances transcription of nucleosomal arrays by RNA polymerase III. Mol Cell Biol *18*, 4629-4638.

Turner, S.D., Ricci, A.R., Petropoulos, H., Genereaux, J., Skerjanc, I.S., and Brandl, C.J. (2002). The E2 ubiquitin conjugase Rad6 is required for the ArgR/Mcm1 repression of ARG1 transcription. Mol Cell Biol *22*, 4011-4019.

Van Holde, K.E. (1989). Chromatin (New York: Springer-Verlag).

Van Holde, K.E., Allen, J.R., Tatchell, K., Weischet, W.O., and Lohr, D. (1980). DNA-histone interactions in nucleosomes. Biophysical journal *32*, 271-282.

van Kasteren, S.I., Kramer, H.B., Jensen, H.H., Campbell, S.J., Kirkpatrick, J., Oldham, N.J., Anthony, D.C., and Davis, B.G. (2007). Expanding the diversity of chemical protein modification allows post-translational mimicry. Nature *446*, 1105-1109.

van Leeuwen, F., Gafken, P.R., and Gottschling, D.E. (2002). Dot1p modulates silencing in yeast by methylation of the nucleosome core. Cell *109*, 745-756.

Verdaasdonk, J.S., and Bloom, K. (2011). Centromeres: unique chromatin structures that drive chromosome segregation. Nature reviews Molecular cell biology *12*, 320-332.

Villar-Garea, A., Forne, I., Vetter, I., Kremmer, E., Thomae, A., and Imhof, A. (2011). Developmental regulation of N-terminal H2B methylation in Drosophila melanogaster. Nucleic Acids Res.

Voncken, J.W., Roelen, B.A., Roefs, M., de Vries, S., Verhoeven, E., Marino, S., Deschamps, J., and van Lohuizen, M. (2003). Rnf2 (Ring1b) deficiency causes gastrulation arrest and cell cycle inhibition. Proc Natl Acad Sci U S A *100*, 2468-2473.

Walsh, C. (2006). Posttranslational modification of proteins : expanding nature's inventory (Englewood, Colo.: Roberts and Co. Publishers).

Wan, Q., and Danishefsky, S.J. (2007). Free-radical-based, specific desulfurization of cysteine: a powerful advance in the synthesis of polypeptides and glycopolypeptides. Angew Chem Int Ed Engl *46*, 9248-9252.

Wang, H., Wang, L., Erdjument-Bromage, H., Vidal, M., Tempst, P., Jones, R.S., and Zhang, Y. (2004). Role of histone H2A ubiquitination in Polycomb silencing. Nature *431*, 873-878.

Wang, Z., Zang, C., Rosenfeld, J.A., Schones, D.E., Barski, A., Cuddapah, S., Cui, K., Roh, T.Y., Peng, W., Zhang, M.Q., *et al*. (2008). Combinatorial patterns of histone acetylations and methylations in the human genome. Nat Genet *40*, 897-903.

Weake, V.M., and Workman, J.L. (2008). Histone ubiquitination: triggering gene activity. Mol Cell *29*, 653-663.

Wei, J., Zhai, L., Xu, J., and Wang, H. (2006). Role of Bmi1 in H2A ubiquitylation and Hox gene silencing. J Biol Chem *281*, 22537-22544.

West, M.H., and Bonner, W.M. (1980). Histone 2B can be modified by the attachment of ubiquitin. Nucleic Acids Res *8*, 4671-4680.

Whitcomb, S.J., Basu, A., Allis, C.D., and Bernstein, E. (2007). Polycomb Group proteins: an evolutionary perspective. Trends in genetics : TIG *23*, 494-502.

Wong, L.H., Ren, H., Williams, E., McGhie, J., Ahn, S., Sim, M., Tam, A., Earle, E., Anderson, M.A., Mann, J.*, et al*. (2009). Histone H3.3 incorporation provides a unique and functionally essential telomeric chromatin in embryonic stem cells. Genome research *19*, 404-414.

Wood, A., Schneider, J., Dover, J., Johnston, M., and Shilatifard, A. (2003). The Paf1 complex is essential for histone monoubiquitination by the Rad6-Bre1 complex, which signals for histone methylation by COMPASS and Dot1p. J Biol Chem *278*, 34739-34742.

Wu, L., Zee, B.M., Wang, Y., Garcia, B.A., and Dou, Y. (2011). The RING finger protein MSL2 in the MOF complex is an E3 ubiquitin ligase for H2B K34 and is involved in crosstalk with H3 K4 and K79 methylation. Mol Cell *43*, 132-144.

Wu, R.S., Kohn, K.W., and Bonner, W.M. (1981). Metabolism of ubiquitinated histones. J Biol Chem *256*, 5916-5920.

Wyce, A., Xiao, T., Whelan, K.A., Kosman, C., Walter, W., Eick, D., Hughes, T.R., Krogan, N.J., Strahl, B.D., and Berger, S.L. (2007). H2B ubiquitylation acts as a barrier to Ctk1 nucleosomal recruitment prior to removal by Ubp8 within a SAGA-related complex. Mol Cell *27*, 275-288.

Xiao, T., Kao, C.F., Krogan, N.J., Sun, Z.W., Greenblatt, J.F., Osley, M.A., and Strahl, B.D. (2005). Histone H2B ubiquitylation is associated with elongating RNA polymerase II. Mol Cell Biol *25*, 637-651.

Xu, C., Bian, C., Yang, W., Galka, M., Ouyang, H., Chen, C., Qiu, W., Liu, H., Jones, A.E., MacKenzie, F.*, et al*. (2010). Binding of different histone marks differentially regulates the activity and specificity of polycomb repressive complex 2 (PRC2). Proc Natl Acad Sci U S A *107*, 19266-19271.

Yamamoto, K., Sonoda, M., Inokuchi, J., Shirasawa, S., and Sasazuki, T. (2004). Polycomb group suppressor of zeste 12 links heterochromatin protein 1alpha and enhancer of zeste 2. J Biol Chem *279*, 401-406.

Yan, L.Z., and Dawson, P.E. (2001). Synthesis of peptides and proteins without cysteine residues by native chemical ligation combined with desulfurization. Journal of the American Chemical Society *123*, 526-533.

Yan, Q., Dutt, S., Xu, R., Graves, K., Juszczynski, P., Manis, J.P., and Shipp, M.A. (2009). BBAP monoubiquitylates histone H4 at lysine 91 and selectively modulates the DNA damage response. Mol Cell *36*, 110-120.

Zhang, X., Yang, Z., Khan, S.I., Horton, J.R., Tamaru, H., Selker, E.U., and Cheng, X. (2003). Structural basis for the product specificity of histone lysine methyltransferases. Mol Cell *12*, 177-185.

Zhou, W., Zhu, P., Wang, J., Pascual, G., Ohgi, K.A., Lozach, J., Glass, C.K., and Rosenfeld, M.G. (2008). Histone H2A monoubiquitination represses transcription by inhibiting RNA polymerase II transcriptional elongation. Mol Cell *29*, 69-80.

Zhu, B., Zheng, Y., Pham, A.D., Mandal, S.S., Erdjument-Bromage, H., Tempst, P., and Reinberg, D. (2005). Monoubiquitination of human histone H2B: the factors involved and their roles in HOX gene regulation. Mol Cell *20*, 601-611.